THE ROLE FOR DNA REPLICATION AND REPAIR GENES IN GERM-LINE MAINTENANCE AND TUMOR SUPPRESSION

A Dissertation

Presented to the Faculty of the Graduate School

of Cornell University

In Partial Fulfillment of the Requirements for the Degree of

Doctor of Philosophy

by

Suzanne Arlene Hartford

January 2012

THE ROLE FOR DNA REPLICATION AND REPAIR GENES IN GERM-LINE MAINTENANCE AND TUMOR SUPPRESSION

Suzanne Arlene Hartford, Ph. D.

Cornell University 2012

ABSTRACT:

Faithful DNA replication and repair of DNA damage is important for prevention of disease and birth defects. My thesis work utilized reverse and forward genetic approaches to identify novel genes involved in these processes. In one set of studies, I investigated the function of MCM9, a protein specific to multicellular eukaryotes that is related to subunits of the DNA replicative helicase. Utilizing multiple mouse disruption alleles, I have shown MCM9 is dispensable for DNA replication, however it has a role in germ-line stem cell maintenance and/or proliferation. Additionally, in the soma, *Mcm9* mutation leads to increased cancer susceptibility, particularly hepatocellular carcinoma in males. The phenotypes of MCM9 mutant mice and cells suggest that MCM9 evolved a specialized but nonessential role in DNA replication or replication-linked quality-control mechanisms. In a second set of studies, I identified a hypomorphic allele of *Fancm* in a forward genetic screen for GIN mutations in mice. *Fancm* is a member of the Fanconi Anemia complementation group and facilitates repair of lesions at the DNA replication fork. Similar to *Mcm9*, *Fancm* is required for producing a normal germ-line

stem cell pool and for tumor suppression in the soma. Together, these genetic studies underscore the importance of accurate DNA replication and repair of replication-associated damage in mammalian reproduction and cancer.

BIOGRAPHICAL SKETCH

Suzanne Arlene Hartford was born and raised in St. Albans, Maine on a dairy farm. After graduating near the top of her high school class in 1996, she went on to obtain a Bachelor of Arts Degree in Biology, with a double minor of Chemistry and Mathematics, at Saint Joseph's College of Maine in May 2000. She then went on to find employment at the Jackson Laboratory in Maine where she worked as a Research Assistant for four years in the lab of John Schimenti. Suzanne came to Cornell University to pursue her PhD in the Fall of 2004 and continued her research in the Schimenti Lab. During this time as a research assistant and at Cornell, Suzanne has co-authored 9 papers. She has also received two poster awards for presentations at the Mammalian Genome conference, once in 2006 and again in 2009, for her two research projects. Suzanne is currently researching mechanisms of genome stability and germ cell maintenance.

ACKNOWLEDGMENTS

I would like to extend a grateful thank you to John Schimenti, who took a chance on a fresh from undergrad, from a small college, quiet person to employ as a research assistant. In this position you allowed my research interests to grow and further my interests in genetics. I also want to express my gratitude to John for allowing me to continue in his laboratory as a graduate student and allowing me to see one of my projects through to publication.

I wish to acknowledge my committee members of Robert Weiss, Bik-Kwoon Tye, and Paula Cohen for helpful input to my research projects and critical review of my writing. I would like to extend a thank-you to all of the Schimenti Lab members, past and present, for all their helpful guidance through the numerous years I have been in this lab.

I'm grateful for the funding that I have received over the past few years. Funding from Reproductive Sciences and Genomics Training Program supported by National Institutes of Child Health and Human Development T32HD052471 and funding from NYSTEM.

I also want to extend thanks to my husband, Zack Burkett and my daughter Lucile, for keeping me sane and focused in the last couple of years, and for giving me their support. I express gratitude to my parents, Dana and Colleen Hartford, for first introducing me to biology and genetics on our family dairy farm. I also wish to thank my in-laws, David and Winnie Burkett for support during my dissertation writing.

TABLE OF CONTENTS

LIST OF FIGURES

LIST OF TABLES

Chapter 1: Introduction

Efficient and accurate DNA replication is crucial to the health and survival of the species. Defects in DNA replication can lead to mutations, insertions, deletions, chromosomal fragmentation, and whole chromosome amplifications or loss. Ongoing or elevated frequency of alteration of the genome leads to genomic instability (GIN), a hallmark of cancer. To find new genes involved in GIN our lab conducted an ENU mutagenesis screen in mice. This screen utilized micronuclei formation in peripheral blood as a biomarker to screen for potential GIN (1). Micronuclei (MN) arise from acentric chromosome fragments or whole chromosomes that have not been incorporated in the main nuclei following cell division (2). Since erythrocytes lack nuclei, and the expelling of the nuclei does not always include MN, flow cytometry was used to detect the change in micronuclei levels(1, 3). From this screen we expected to find genes involved in DNA repair, DNA replication, and genes in DNA cell cycle checkpoints. Three mutations were pursued: *Chaos1, Chaos3,* and *Chaos4* (Chromosomal aberrations occurring spontaneously). *Chaos1* contains a mutation in *Polq* and is involved in translesion synthesis repair of DNA, and is particularly important for somatic hypermutation (1, 4, 5). *Chaos3* contains a point mutation in a member of the DNA replicative helicase, *Mcm4* (6). *Chaos4* is an allele of *Fancm,* a member of the Fanconi Anemia complementation group which regulates DNA interstrand cross-link repair. Of these three alleles, *Chaos3* and *Chaos4* confer increased tumor susceptibility.

1.1 DNA Replication Initiation and Elongation

The Mcm gene family is composed of 8 genes, Mcm2,3,4,5,6,7, and in a subset of eukaryotes, Mcm8 and Mcm9. These genes contain a highly conserved, ~200 amino acid "MCM domain" containing Walker A and Walker B motifs, an arginine finger, and a Zinc finger motif (Figure 1-1). MCM2-7 form the replicative helicase (7–9) involved in both the initiation and the elongation of the DNA replication fork (10). The activities of these six proteins are highly controlled to prevent re-replication of DNA during a cell cycle (11). Each of the MCM2-7 proteins is essential. Null mutations in Mcm2-7 are lethal in both yeast (12, 13) and mice (14). Prior to the initiation and elongation of the replication fork the origin of replication needs to be "licensed" (Figure 1-2). A licensed origin has all the factors needed for replication to begin. First the origin is bound by the origin recognition complex (ORC) (Figure 1-2A). This is followed by binding of CDC6 and CDT1 which then proceeds to load on the MCM2-7 heterohexameric helicase (Figure 1-2B,C). This collection of proteins consist the pre-replication complex (pre-RC) and the origin is now "licensed" (Figure 1-2D)(15). In order to become active, CDC7 and CDK remove CDC6 and recruit MCM10 (Figure 1-2E). MCM10 with MCM2-7 recruits CDC45, followed by the rest of the replisome, the origin is now active (Figure 1-2F,G)(15).

MCM2-7 are present at levels exceeding what is needed to execute their direct roles in replication initiation and elongation (Figure 1-2) (16–19). Recent studies indicate that the primary reason for this excess is to license backup origins that are utilized to rescue defective origins. These back-up origins can be

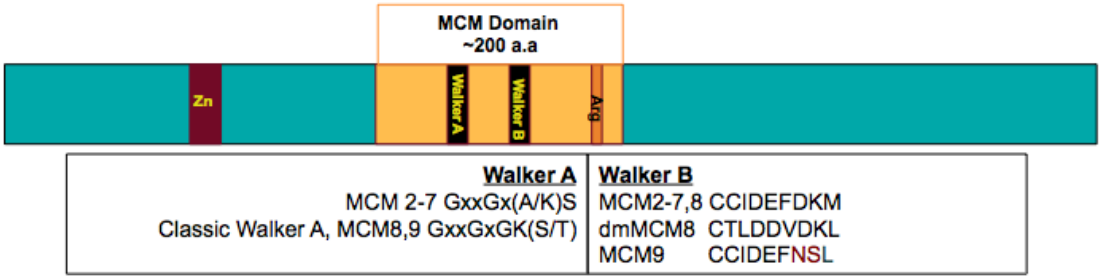

Figure 1-1: MCM gene family conserved motifs. The highly conserved 200 amino acid region seen in the MCM gene family is called the MCM domain. This domain consists of a Walker A and B motif and an Arginine finger. Outside of the MCM domain is a zinc finger. MCM8 and 9 contain a more classical form of the Walker A motif than seen in MCM2-7. The Walker B motif canonical sequence is seen in MCM2-7 and MCM8, with the exception of *Drosophila* MCM8 that contains some conserved amino acid changes. MCM9 has some non-conserved amino acid changes in the Walker B motif (red) as well as some conserved changes (blue).

Figure 1-2: Replication licensing, initiation, and elongation
A. ORC proteins bind to DNA replication origins. **B.** CDT1 and CDC6 and load onto the pre-RC. **C.** MCM8 and MCM9 may be loaded onto the pre-RC based on their interaction with CDC6 and CDT1. **D.** The MCM2-7 heterohexameric helicase is loaded onto the pre-RC and now the origin or replication is licensed. **E.** CDK and CDC7 replace CDC6 and recruit MCM10 to what will be the active origin. **F.** MCM10 recruits CDC45 which then brings in the replisome and replication is initiated, with **G.** elongation of the DNA replication fork at the active origin.

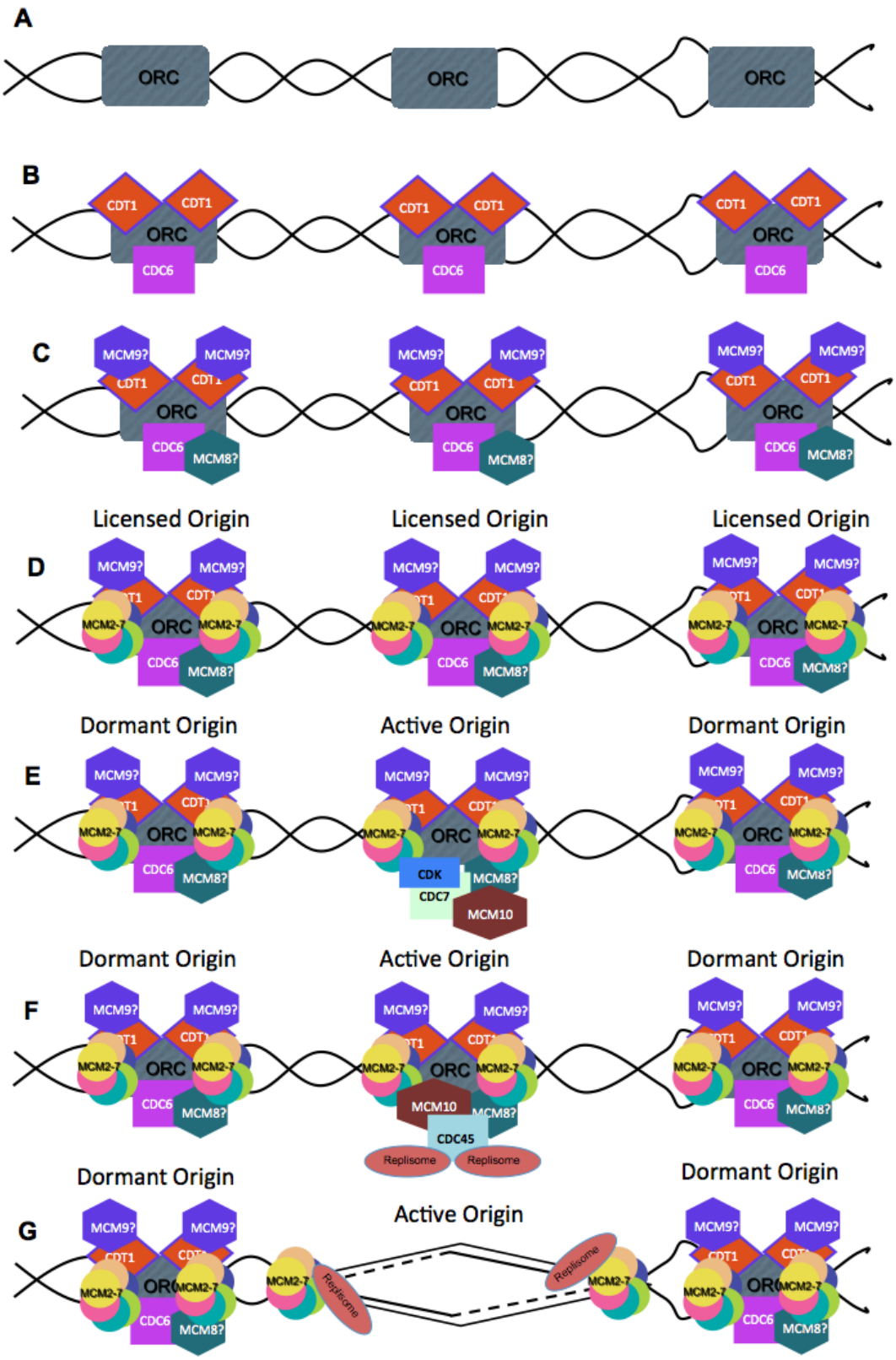
A
ORC
ORC
ORC
B
CDT1
CDT1
ORC
CDC6
C
MCM9?
CDT1
MCM8?
Licensed Origin
D
MCM2-7
E
CDK
CDC7
MCM10
Dormant Origin
Active Origin
F
CDC45
Replisome
G

activated under conditions of replication stress (20, 21). Dysfunction of, or decreases in MCMs can cause genome instability and cancer (6, 14, 22–24). The *Mcm4*^{Chaos3} mutation causes mammary adenocarcinoma formation in >80% of females in approximately 1 year in the C3Heb/Fej (C3H) background (6). In the C57BL/6J (B6) genetic background there is reduced survival and these animals are prone to histiocytic sarcomas (25, 26). Another mutant in the MCM2-7 family, (Mcm2$^{IRES\text{-}CreERT2/wild\text{-}type}$), causes a drastic decrease in MCM2 levels. These mice are prone to lymphomas and have stem/progenitor cell deficiency (23, 27).

1.2 Divergent MCMs, MCM8 and MCM9.

Mcm2-7 genes exist in all eukaryotes. However, there are two additional paralogs, *Mcm8* and *Mcm9*, which are present only in a subset of eukaryotic species. Both genes usually co-exist in genomes of that subset, except for *Drosophila* which has *Mcm8* but lacks *Mcm9* (Figure 1-3) (28, 29). Neither MCM8 nor MCM9 have been shown to directly interact with the MCM2-7 helicase. Currently, there is no definitive role for MCM8 in DNA replication, but it is thought to be involved in the recruitment of CDC6 to replication origins (Figure 1-2C) (30). MCM8 has helicase activity and may facilitate in the elongation of the replication fork (31). *Drosophila* females lacking Mcm8 (*Rec*) have high levels of chromosomal non-disjunction and reduced fertility (28). *Rec* is required for normal levels of meiotic crossing over, possibly by facilitating repair synthesis in

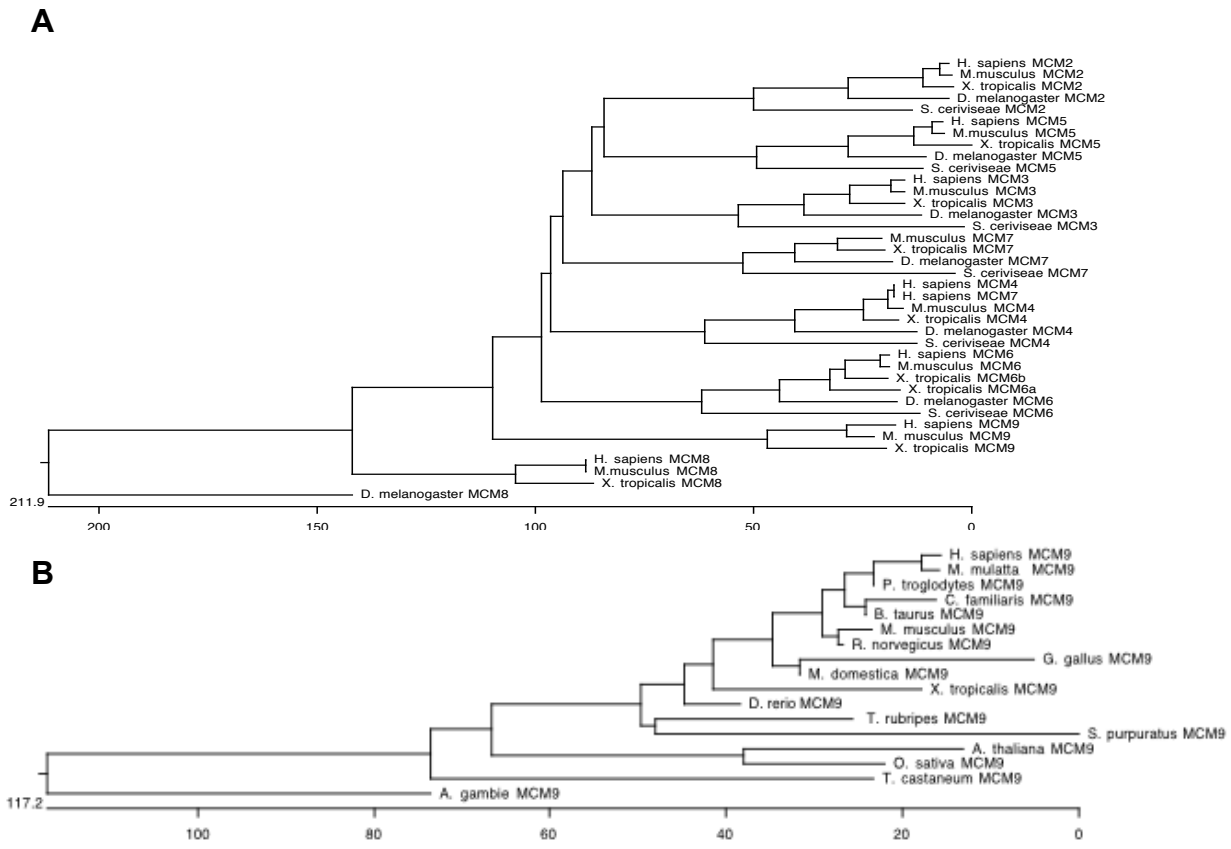

Figure 1-3: Phylogenetic tree of MCMs
A-Phylogenetic tree of MCM2,3,4,5,6,7,8,9 in *S.cerevisiae, D.melanogaster, X.tropicalis, M.musculus,* and, *H.sapiens.* Note that *D.melanogaster* only has an MCM8 that it is divergent from the other MCM8. **B-**Phylogenetic tree of the MCM9 genes seen in a subset of higher eukaryotes.

these recombination intermediates. The substantial divergence of *Drosophila* Mcm8 from orthologs in higher eukaryotes, as well as the absence of *Mcm9* in the fruit fly, led Blanton *et al*. to hypothesize that *Drosophila* MCM8 may also provide MCM9 function (28).

Mouse *Mcm9* was first described as encoding a 386 amino acid, C-terminal-truncated paralog of the MCM2-7 proteins. This truncated isoform ($MCM9^{S}$) contains a partial MCM domain lacking the Walker B motif (32). Upon further analysis, Lutzmann *et al* bioinformatically deduced that *Mcm9* actually encoded a long isoform ($MCM9^{L}$) that has both the Walker A and B motifs (33). The predicted amino acid sequence of MCM9 reveals some unusual features. The Walker A motif in MCM9 is more similar to the classical Walker A consensus than the MCM2-7 canonical sequence. The MCM9 Walker B motif is also atypical with some non-conserved amino acid changes (Figure 1-1).

From these studies information concerning the function of MCM9 is beginning to emerge. It is upregulated in mid-to-late S-phase in NIH3T3 cells suggested a possible role in the termination of DNA replication (32). It was subsequently reported that, in *Xenopus*, MCM9 interacts with CDT1 to load MCM2-7 onto replication origins. Thus, MCM9 was thought to be required for pre-RC formation and DNA replication (33). These studies showed that MCM9 is a positive regulator of CDT1 and a DNA replication co-licensor, counteracting the inhibitory effects of Geminin upon CDT1 (33). Our own lab has found that MCM9 is not essential for DNA replication, but it does have roles in germ-line stem cells and tumor suppression (chapter 2 and (34)).

1.3 Germline stem cells

Proper specification and maintenance of the germ-line stem cell is a key to maintaining the genome and vitality of the species, making germ cells the ultimate stem cell. Germ cell development starts with the initial cell specification and cell proliferation of the primordial population in the extra-embryonic tissue (Figure 1-4A) at approximately embroyonic day 7.5 (E7.5). These germ cells then migrate towards the primitive gonads while still proliferating. Between E7.5 and E11.5 the primordial germ cells undergo epigenetic reprogramming that changes methylcytosine into and unmethylated cytosine, which causes ssDNA to form and the repair is facilitated through the base excision repair pathway (BER) (35). Once the germ cells arrive at the bipotential gonads the cells will continue to proliferate until they undergo sexual differentiation. This cell proliferation happens rapidly, expanding the number of germ cells from~100 to >20,000 cells (36, 37) (Figure 1-4A). By E13.5 the male germ cells are arrested in mitosis and after birth will once again start to divide and populate the seminiferous tubules. Spermatogenesis begins in a coordinated wave for the first round of meiosis and the spermatogonial stem cells maintain the germ cell population in the male for life (Figure 1-4B). The female germ cells enter meiosis I and arrest at diplotene until the oocyte is ready to be ovulated (37). During gamete formation genome maintenance it is critical to prevent mutation, insertions, and deletions to prevent the offspring from inheriting detrimental diseases.

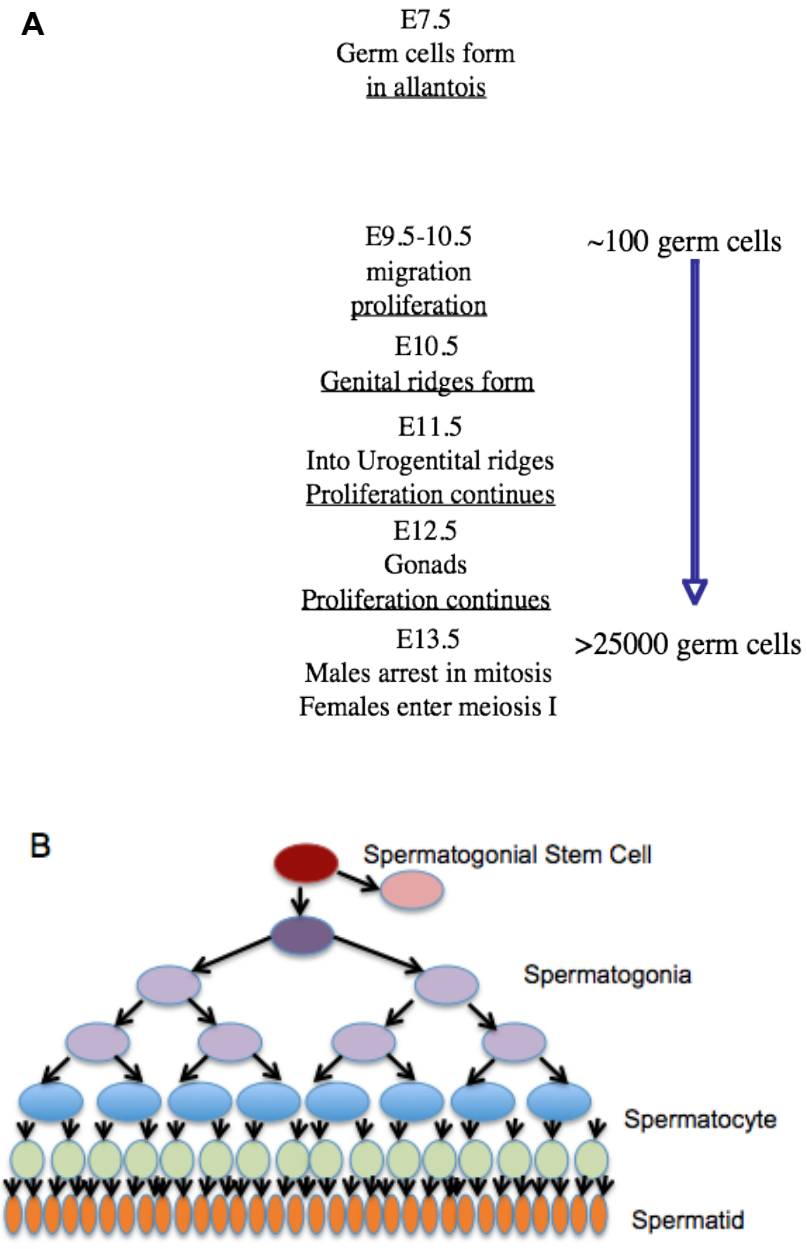

Figure 1-4 Germ cell formation and spermatogenesis
A. Germ cell formation in the embryo starts at embryonic day 7.5 (E7.5) and the initial population of germ cells is complete by E13.5. **B.** Spermatogenesis starts with the spermatogonial stem cell which either self-renews or differentiates into a spermatogonia. A number of cell divisions occur before meiosis. Then the spermatocyte goes through1 final round of replication with 2 round of division to complete meiosis and is now a spermatid.

1.4 Fanconi Anemia

Fanconi Anemia (FA) is a rare human genetic disorder characterized by bone marrow failure, developmental abnormalities, decreased fertility, and high incidence of malignancies. Cells from these patients have a high susceptibility to DNA crosslinking agents (38). DNA interstrand crosslinks (ICLs) are lesions that link two DNA strands and are cytotoxic since they interfere with both DNA replication and gene transcription. The Fanconi Anemia complementation group currently consists of 15 genes. The complementation group can be sub-divided into 3 components, the core complex, the ID group, and the repair group. The core complex consists of FANC-A,B,C,E,F,G,L, and M (Figure 1-5)(39, 40). The core complex is loaded to the site of damage partially by FANCM (41). Then the core complex acts as an E3 ubiquitin ligase with the E2 protein UBE2T to mono-ubiquitinate the ID heterodimer that consists of FANCD2 and FANCI (Figure 1-5) (42, 43). This activation of the FA pathway is done in conjunction with activation of the ATR pathway that phosphorylates a number of the FA proteins (44–46). FANCM has a role in stabilizing ATR through its interaction with HCLK, and it also participates in RPA localization to sites of ssDNA (47–51). The repair group is activated by the ID group. The repair group consists of BRCA2/FANCD1, FANCN, FANCJ, FANCO (RAD51C) and FANCP (SLX4). These proteins have roles in homologous recombination and translesion synthesis (Figure 1-5)(49–52). The overall role of the Fanconi Anemia complex is to preserve genome stability. This is accomplished through processing blocked and/or broken

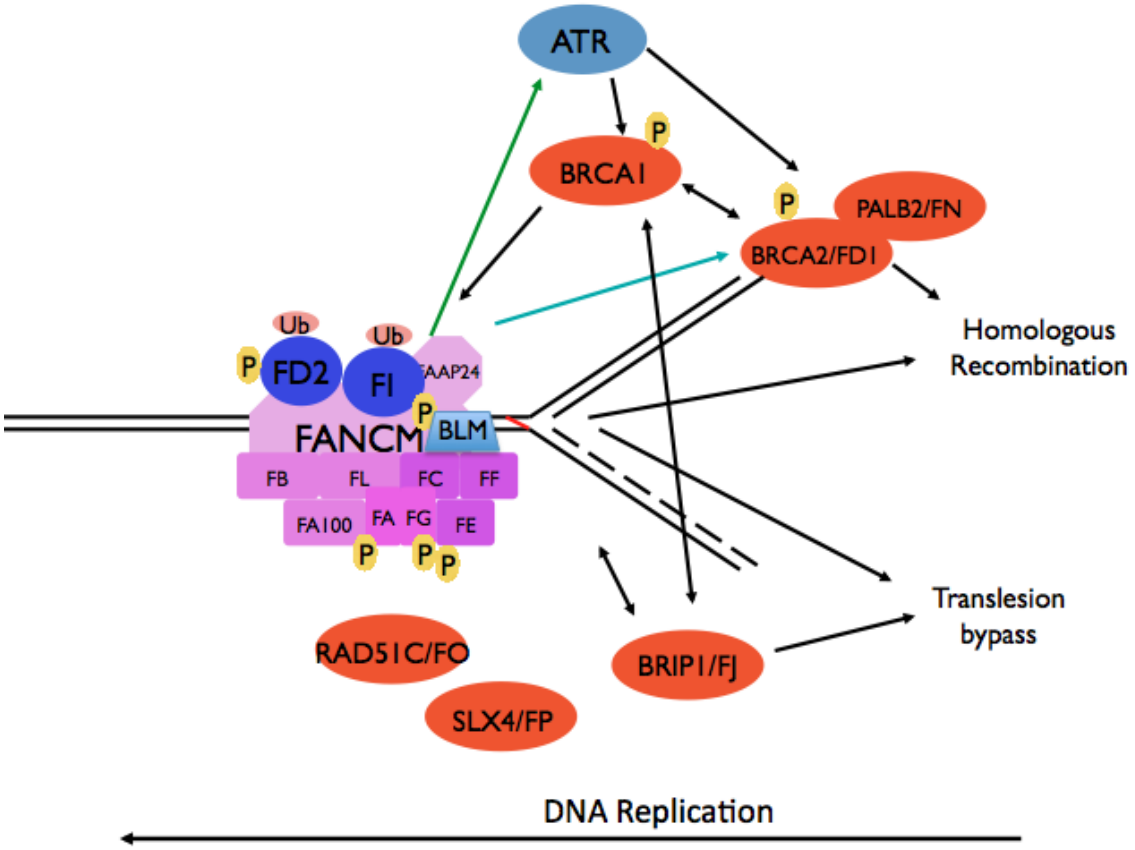

Figure 1-5 The Fanconi Anemia complementation group
FANCM is chromatin bound and acts as a sensor of DNA damage (red line seen in front of the DNA replication fork). FANCM then anchors the rest of the FA core complex (in purple) to the site of damage. The core complex acts as a E3 ligase and ubiquitinate FANCD2 and FANCI (dark blue). This then allows the repair factors (red) to perform homologous recombination or translesion bypass of the damage.

replication forks through the coordination of homologous recombination and translesion synthesis (52).

There are several knock-out (KO) mouse models of the Fanconi Anemia complementation group. They all have similar phenotypes including germ cell depletion and sensitivity to MMC, however only a subset have congenital defects and only one (FANCP/SLX4) recapitulates hematopoietic defects that are characteristic of the human disease (52). *Fancd2* and *Fancm* mouse mutants are the only ones that have been shown to have a higher incidence of cancer (53, 54). *Fancm* is unique from other FA mutants in that intercrosses of *Fancm*$^{-/-}$ animals yield a non-Mendelian ratio of female offspring. The *Fancm*$^{-/-}$ homozygous cells exhibit a high incidence of sister-chromatin exchange (SCE), and have a decreased ability to mono-ubiquitinate FANCD2 (55). *Fancm* is conserved through evolution and has homologues in yeast and archaea. Furthermore, unlike other FA gene mutations, *Fancm* cell lines also have sensitivity to UV (activates nucleotide excision repair) and camptothecin (CPT, activates double stranded break repair) (44), suggesting a role in other DNA repair pathways. All these activities suggest FANCM is functions in a closely linked DNA replication repair pathway.

1.5 Hypothesis

Both MCMs and FA have roles at the DNA replication fork. If the MCM2-7 helicase is disrupted, activation of S-phase checkpoint occurs. This allows for three main responses: stabilization of already perturbed replication forks,

inhibition of late origin firing, and co-ordination of cell cycle progression with repair events (56). Both the MCM9 mutant and mutants in FA have germ cell loss, so is it possible that germ cells are very sensitive to specific perturbations of DNA replication? Recently it has been suggested that FANCM is involved in not only sensing DNA damage, but also deciding which DNA repair pathway to choose. The signal cascade from disrupted MCM2-7 helicase progression to activation of DNA repair and recovery from cell-cycle arrest is still not clearly understood. My hypothesis is that MCM9 and FANCM both function at the DNA replication fork in a pathway that directly links perturbed DNA replication with DNA repair. In the following chapters I hope to elucidate further the potential mechanisms from disrupted DNA replication to the potential sensors, to how the repair pathway may be chosen.

1.6 References

1. Shima N et al. (2003) Phenotype-based identification of mouse chromosome instability mutants. *Genetics* 163:1031-40.
2. Nüsse M, Miller BM, Viaggi S, Grawé J (1996) Analysis of the DNA content distribution of micronuclei using flow sorting and fluorescent in situ hybridization with a centromeric DNA probe. *Mutagenesis* 11:405-13.
3. Dertinger SD, Torous DK, Tometsko KR (1996) Simple and reliable enumeration of micronucleated reticulocytes with a single-laser flow cytometer. *Mutation research* 371:283-92.
4. Shima N, Munroe RJ, Schimenti JC (2004) The mouse genomic instability mutation chaos1 is an allele of Polq that exhibits genetic interaction with Atm. *Molecular and cellular biology* 24:10381-9.
5. Zan H et al. (2005) The translesion DNA polymerase theta plays a dominant role in immunoglobulin gene somatic hypermutation. *The EMBO journal* 24:3757-69.
6. Shima N et al. (2007) A viable allele of Mcm4 causes chromosome instability and mammary adenocarcinomas in mice. *Nature genetics* 39:93-8.
7. Bochman ML, Schwacha A (2008) The Mcm2-7 complex has in vitro helicase activity. *Molecular cell* 31:287-93.
8. Labib K (2000) Uninterrupted MCM2-7 Function Required for DNA Replication Fork Progression. *Science* 288:1643-1647.

9. Moyer SE, Lewis PW, Botchan MR (2006) a candidate for the eukaryotic DNA replication fork helicase. *PNAS*.

10. Forsburg SL (2004) Eukaryotic MCM Proteins : Beyond Replication Initiation. *Society* 68:109-131.

11. Blow JJ, Dutta A (2005) Preventing re-replication of chromosomal DNA. *Nature reviews. Molecular cell biology* 6:476-86.

12. Yan H, Gibson S, Tye BK (1991) Mcm2 and Mcm3, two proteins important for ARS activity, are related in structure and function. *Genes & development* 5:944-57.

13. Forsburg SL, Sherman D a, Ottilie S, Yasuda JR, Hodson J a (1997) Mutational analysis of Cdc19p, a Schizosaccharomyces pombe MCM protein. *Genetics* 147:1025-41.

14. Chuang C-H, Wallace MD, Abratte C, Southard T, Schimenti JC (2010) Incremental genetic perturbations to MCM2-7 expression and subcellular distribution reveal exquisite sensitivity of mice to DNA replication stress. *PLoS genetics* 6.

15. Sun J, Kong D (2010) DNA replication origins, ORC/DNA interaction, and assembly of pre-replication complex in eukaryotes. *Acta biochimica et biophysica Sinica* 42:433-9.

16. Burkhart R et al. (1995) Interactions of human nuclear proteins P1Mcm3 and P1Cdc46. *European journal of biochemistry / FEBS* 228:431-8.

17. Mahbubani HM, Chong JP, Chevalier S, Thömmes P, Blow JJ (1997) Cell cycle regulation of the replication licensing system: involvement of a Cdk-dependent inhibitor. *The Journal of cell biology* 136:125-35.

18. Donovan S, Harwood J, Drury LS, Diffley JF (1997) Cdc6p-dependent loading of Mcm proteins onto pre-replicative chromatin in budding yeast. *Proceedings of the National Academy of Sciences of the United States of America* 94:5611-6.

19. Wong PG et al. (2011) Cdc45 limits replicon usage from a low density of preRCs in mammalian cells. *PloS one* 6:e17533.

20. Woodward AM et al. (2006) Excess Mcm2-7 license dormant origins of replication that can be used under conditions of replicative stress. *The Journal of cell biology* 173:673-83.

21. Ge XQ, Jackson DA, Blow JJ (2007) Dormant origins licensed by excess Mcm2-7 are required for human cells to survive replicative stress. *Genes & development* 21:3331-41.

22. Ibarra A, Schwob E, Méndez J (2008) Excess MCM proteins protect human cells from replicative stress by licensing backup origins of replication. *Proceedings of the National Academy of Sciences of the United States of America* 105:8956-61.

23. Pruitt SC, Bailey KJ, Freeland A (2007) Reduced Mcm2 expression results in severe stem/progenitor cell deficiency and cancer. *Stem cells (Dayton, Ohio)* 25:3121-32.

24. Bailis JM, Forsburg SL (2004) MCM proteins: DNA damage, mutagenesis and repair. *Current opinion in genetics & development* 14:17-21.

25. Kawabata T et al. (2011) A reduction of licensed origins reveals strain-specific replication dynamics in mice. *Mammalian genome : official journal of the International Mammalian Genome Society*.

26. Kawabata T et al. (2011) Stalled Fork Rescue via Dormant Replication Origins in Unchallenged S Phase Promotes Proper Chromosome Segregation and Tumor Suppression. *Molecular cell* 41:543-53.

27. Kunnev D et al. (2010) DNA damage response and tumorigenesis in Mcm2-deficient mice. *Oncogene* 29:3630-8.

28. Blanton HL et al. (2005) REC, Drosophila MCM8, drives formation of meiotic crossovers. *PLoS genetics* 1:e40.

29. Liu Y, Richards TA, Aves SJ (2009) Ancient diversification of eukaryotic MCM DNA replication proteins. *BMC evolutionary biology* 9:60.

30. Volkening M, Hoffmann I (2005) Involvement of human MCM8 in prereplication complex assembly by recruiting hcdc6 to chromatin. *Molecular and cellular biology* 25:1560-8.

31. Maiorano D, Cuvier O, Danis E, Méchali M (2005) MCM8 is an MCM2-7-related protein that functions as a DNA helicase during replication elongation and not initiation. *Cell* 120:315-28.

32. Yoshida K (2005) Identification of a novel cell-cycle-induced MCM family protein MCM9. *Biochemical and biophysical research communications* 331:669-74.

33. Lutzmann M, Méchali M (2008) MCM9 binds Cdt1 and is required for the assembly of prereplication complexes. *Molecular cell* 31:190-200.

34. Hartford SA et al. (2011) Minichromosome maintenance helicase paralog MCM9 is dispensible for DNA replication but functions in germ-line stem cells and tumor suppression. *Proceedings of the National Academy of Sciences of the United States of America*.

35. Hajkova P et al. (2010) Genome-wide reprogramming in the mouse germ line entails the base excision repair pathway. *Science (New York, N.Y.)* 329:78-82.

36. Felici M De et al. (2004) Experimental approaches to the study of primordial germ cell lineage and proliferation. *Human reproduction update* 10:197-206.

37. McLaren A (2003) Primordial germ cells in the mouse. *Developmental Biology* 262:1-15.

38. Kennedy RD, D'Andrea AD (2005) The Fanconi Anemia/BRCA pathway: new faces in the crowd. *Genes & development* 19:2925-40.

39. Winter JP de, Joenje H (2009) The genetic and molecular basis of Fanconi anemia. *Mutation research* 668:11-9.

40. Rego MA, Kolling FW, Howlett NG (2009) The Fanconi anemia protein interaction network: casting a wide net. *Mutation research* 668:27-41.

41. Kim JM, Kee Y, Gurtan A, D'Andrea AD (2008) Cell cycle-dependent chromatin loading of the Fanconi anemia core complex by FANCM/FAAP24. *Blood* 111:5215-22.

42. Machida YJ et al. (2006) UBE2T is the E2 in the Fanconi anemia pathway and undergoes negative autoregulation. *Molecular cell* 23:589-96.

43. Meetei AR et al. (2003) A novel ubiquitin ligase is deficient in Fanconi anemia. *Nature genetics* 35:165-70.

44. Wang W (2007) Emergence of a DNA-damage response network consisting of Fanconi anaemia and BRCA proteins. *Nature reviews. Genetics* 8:735-48.

45. Pichierri P, Rosselli F (2004) The DNA crosslink-induced S-phase checkpoint depends on ATR-CHK1 and ATR-NBS1-FANCD2 pathways. *The EMBO journal* 23:1178-87.

46. Andreassen PR, D'Andrea AD, Taniguchi T (2004) ATR couples FANCD2 monoubiquitination to the DNA-damage response. *Genes & development* 18:1958-63.

47. Ishiai M et al. (2008) FANCI phosphorylation functions as a molecular switch to turn on the Fanconi anemia pathway. *Nature structural & molecular biology* 15:1138-46.

48. Collins NB et al. (2009) ATR-dependent phosphorylation of FANCA on serine 1449 after DNA damage is important for FA pathway function. *Blood* 113:2181-90.

49. Collis SJ et al. (2008) FANCM and FAAP24 function in ATR-mediated checkpoint signaling independently of the Fanconi anemia core complex. *Molecular cell* 32:313-24.

50. Horejŝí Z, Collis SJ, Boulton SJ (2009) FANCM-FAAP24 and HCLK2: roles in ATR signalling and the Fanconi anemia pathway. *Cell cycle (Georgetown, Tex.)* 8:1133-7.

51. Huang M et al. (2010) The FANCM/FAAP24 complex is required for the DNA interstrand crosslink-induced checkpoint response. *Molecular cell* 39:259-68.

52. Crossan GP et al. (2011) Disruption of mouse Slx4, a regulator of structure-specific nucleases, phenocopies Fanconi anemia. *Nature Genetics* 43.

53. Houghtaling S et al. (2003) Epithelial cancer in Fanconi anemia complementation group D2 (Fancd2) knockout mice. *Genes & development* 17:2021-35.

54. Bakker ST et al. (2009) Fancm-deficient mice reveal unique features of Fanconi anemia complementation group M. *Human molecular genetics* 18:3484-95.

55. Bakker ST et al. (2009) Fancm-deficient mice reveal unique features of Fanconi anemia complementation group M. *Human molecular genetics* 18:3484-95.

56. Paulsen RD, Cimprich K a (2007) The ATR pathway: fine-tuning the fork. *DNA repair* 6:953-66.

CHAPTER 2:

The MCM2-7 helicase paralog MCM9 is dispensible for DNA replication but functions in germ-line stem cells and tumor suppression

Suzanne A. Hartford, Yunhai Luo, Teresa L. Southard, Irene M. Min, John T. Lis, and John C. Schimenti

Similar to article published:

Hartford SA et al. (2011) Minichromosome maintenance helicase paralog MCM9 is dispensible for DNA replication but functions in germ-line stem cells and tumor suppression. *Proceedings of the National Academy of Sciences of the United States of America*. 2011 Oct 25;108(43):17702-7. Epub 2011 Oct 10.

Author Contributions:

Yunhai Luo- Germ Cell counts and checkpoint mutant crosses
Teresa Southard- Histopathology
Irene Min and John Lis- Gro-Seq analysis
John Schimenti- Funding and help with research design

2.1 Abstract

Effective DNA replication is critical to the health and reproductive success of organisms. The six MCM2-7 proteins, which form the replicative helicase, are essential for high fidelity replication of the genome. Many eukaryotes have a divergent paralog, MCM9, which was reported to be essential for loading MCM2-7 onto replication origins in the *Xenopus* oocyte extract system. To address the *in vivo* role of mammalian MCM9, we created and analyzed the phenotypes of mice with various mutations in *Mcm9* and an intronic DNA replication-related gene *Asf1a*. Ablation of *Mcm9* was compatible with cell proliferation and mouse viability, showing that it is nonessential for MCM2-7 loading or DNA replication. *Mcm9* mutants underwent p53-independent embryonic germ cell depletion in both sexes, with males also exhibiting defective spermatogonial stem cell renewal. MCM9-deficient cells had elevated genomic instability and defective cell cycle re-entry following replication stress, and mutant animals were prone to gender-specific cancers, most notably hepatocellular carcinoma in males. The phenotypes of mutant mice and cells suggest that MCM9 evolved a specialized but non-essential role in DNA replication or replication-linked quality control mechanisms that are especially important for germ-line stem cells, also for tumor suppression and genome maintenance in the soma.

2.2 Introduction

The eukaryotic Mcm gene family consists of 8 genes, *Mcm2-7,* and in a subset of organisms, *Mcm8* and *Mcm9*. They encode a highly conserved, ~200 amino acid "MCM domain" containing Walker A and Walker B AAA+ ATPase motifs. MCM2-7 forms the DNA replicative helicase (1-3). The activities of MCM2-7 are controlled to prevent re-replication during a cell cycle (4). In both yeast and mice, each of the MCM2-7 proteins are essential despite having structural similarity (5, 6). Dysfunction of, or decreases in MCMs can cause genome instability and cancer (6-8).

Mcm8 and *Mcm9* are both present in diverse eukaryotes, although yeast lacks them and *Drosophila melanogaster* has only *Mcm8* (9, 10). *Drosophila Mcm8* is involved in meiotic recombination (9), while human MCM8 was suggested to enable recruitment of CDC6 to replication origins (11). CDC6 is needed for loading MCM2-7 onto replication origins, and formation of the pre-replication complex (pre-RC).

Mouse *Mcm9* was first described as encoding a 386 amino acid, C-terminal-truncated paralog of the MCM2-7 proteins (12). This isoform ($MCM9^{S}$) contains a partial MCM domain (see Figure 2-1) containing the Walker A-type ATPase motif, but not a Walker B domain. A larger form ($MCM9^{L}$) was predicted to contain both the Walker A and B motifs required for helicase activity in MCM2-7 (13). However, the canonical Walker A motif in MCMs is GDP[G/S]x[S/A]KS, while in MCM8 and 9 it is GDPG[L/T]GKS. The latter is more similar to the

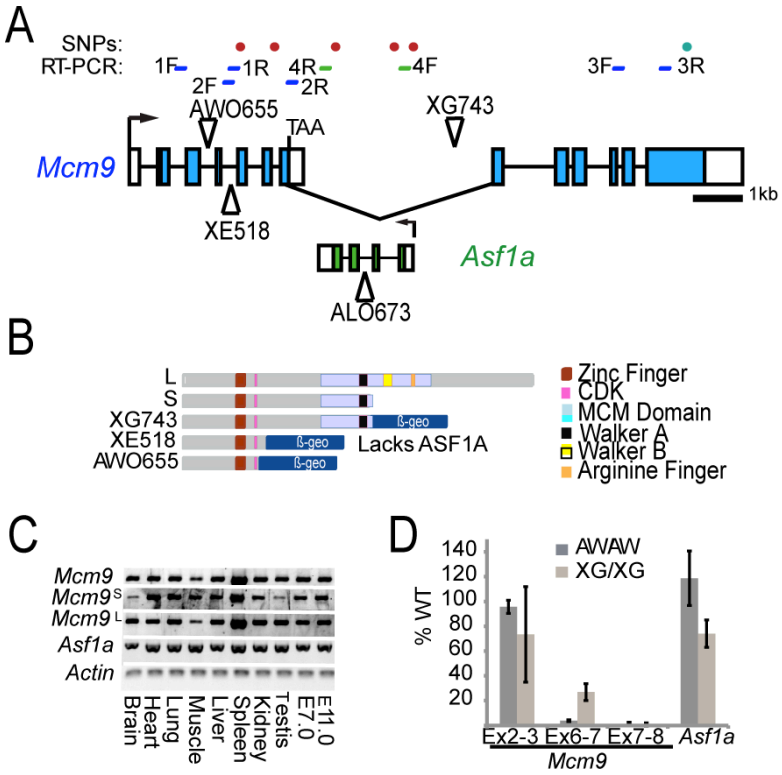

Figure 2-1. *Mcm9* locus structure and isoforms. (A) *Mcm9* has 2 isoforms: *Mcm9*^{S} and *Mcm9*^{L}. The former utilizes an alternative splice site in exon 7 that results in termination. Triangles depict the insertion sites of the gene traps. XE518 created a deletion that includes *Asf1a*. Locations of polymorphic SNPs used for measuring deletion size in the *Mcm9*^{XE518} allele are indicated. From left to right, these are: rs51772485, rs46087546, rs51382030, rs51176035, rs47659858, rs49316622. The *Asf1a* gene trap is located 640 bp downstream of exon 2. (B) MCM9 isoforms and the gene trap alleles. MCM9 contains a zinc finger, CDK site, and the MCM domain. (C) Tissue expression of *Mcm9* and *Asf1a* by semi-qRT-PCR. Primer pairs used in the top 4 panels are sets 1-4, respectively, as shown in *(A)*. (D) qRT-PCR analysis of *Mcm9* and *Asf1a* in mutant MEFs (n=3). AWO = *Mcm9*^{AWO655}; XG = *Mcm9*^{XG743}. Error bars indicate Std Dev.

canonical AAA+ ATPase consensus of GxxGxGK[S/T]. The MCM9 Walker B motif is also atypical (CCIDEFNSL compared to the more canonical motif of MCM2-7 [C/V][C/L]IDEFDKM).

The first major functional study of MCM9 reported that in *Xenopus* egg extracts, MCM9 interacts with CDT1 to load MCM2-7 onto replication origins, and also counteracts the inhibitory effects of Geminin upon CDT1 for replication licensing (14). Thus, MCM9 was deemed essential for pre-RC formation and DNA replication. Here, we report that *Mcm9* is not required for pre-RC formation or DNA replication in mice, but is important for germ-line stem cell maintenance and/or proliferation, genome stability, and cancer prevention.

2.3 Results

Structure of the *Mcm9* locus

Based on available EST and genomic sequence data, Yoshida (12) characterized mouse *Mcm9* as encoding a protein of 386 amino acids, whereas Lutzmann *et al* (13) presented bioinformatic evidence for a much longer 14 exon model encoding 1291 amino acids. The latter is essentially identical to the current RefSeq gene model NM_027830.

To corroborate these gene models, we performed RT-PCR analyses of *Mcm9* and re-examined existing mRNA and EST data. The shorter gene model, which is apparently synonymous with the 7 exon UCSC gene model uc007fbs.1 (Figure 2-2), specifies an ORF beginning within its exon 2 to encode an N terminus that

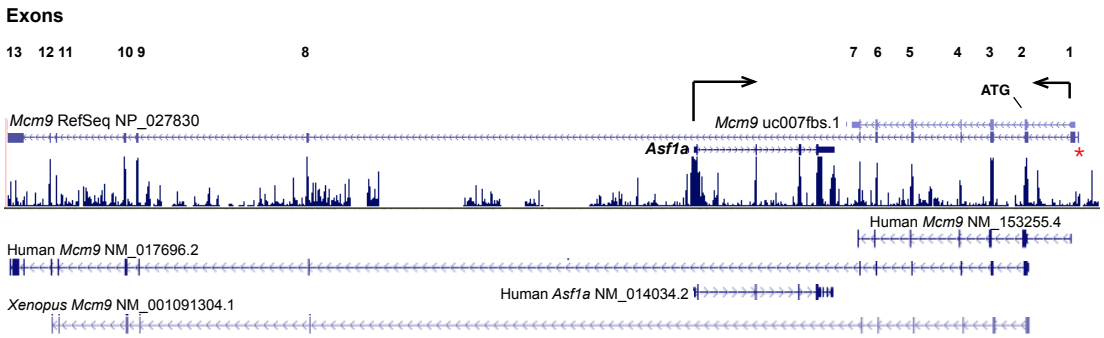

Figure 2-2. The mouse Mcm9 locus and gene models. Shown is a screen shot from the UCSC genome browser, July 2007 assembly. Two *Mcm9* gene models are shown, and are transcribed right to left as indicated. The uc007fbs.1 UCSC gene model is shorter than the RefSeq NP_027830 model, due to usage of a splice donor site internal to exon 7 that bypasses a termination codon. There is no evidence supporting the 5'-most exon in the RefSeq model, marked by a red asterisk, and despite the RefSeq prediction that the entirety of this and the next exon is protein-coding, there is no evidence of strong sequence conservation (as shown by the "30-way Multiz alignment and conservation" track graphed at the bottom of the figure) as there is for other protein coding exons throughout the gene. Furthermore, we were unable to verify an mRNA transcript containing this exon by RT-PCR. Therefore, we believe the correct gene structure has only 13 exons as indicated, and the initiation codon is within the indicated exon 2. Note that our predicted exon 1, which we assume does not encode protein, is also not conserved. The entirety of *Asf1a* lies within intron 7 and is transcribed in the direction opposite to that of *Mcm9*.

coincides with other vertebrate orthologs (Figure 2-2). The longer model predicts an additional 5' exon that begins with an initiation codon, resulting in a 150 aa N-terminal extension in the mouse protein compared to humans and other vertebrates (13). However, there is no experimental or EST evidence to support this additional 5' exon, and it is not evolutionarily conserved (Figure 2-2). Analysis of the 5' region of *Mcm9* with the First Exon Finder program concurred with the 5' end specified in uc007fbs.1. Finally, whereas we failed to generate RT-PCR products using a primer situated in the predicted exon 1 of NM_027830, amplimers were produced when the 5' primer was situated in exon 1 of uc007fbs.1 (Figure 2-2). Therefore, we conclude that the 5' structure of mouse *Mcm9* is as depicted in Figure 2-1A, in agreement with uc007fbs.1 and as originally reported (12).

Existing DNA sequence data supports the existence of two alternative C-terminal *Mcm9* mRNA isoforms, corresponding to those previously described (12,13). As depicted in Figure 2-1, the different isoforms appear to be generated by alternative usage of a splice site within exon 7. Failure to utilize this site results in the shorter isoform ($Mcm9^S$), whereas splicing to exon 8 creates the longer isoform ($Mcm9^L$). The existence of $Mcm9^S$ transcripts (equivalent to UCSC gene model uc007fbs.1) is supported by at least 3 ESTs (AK046636, AK018494, BB648447), and RT-PCR. Numerous ESTs validate the 3' structure of RefSeq NP_082106 (which we designate $Mcm9^L$). $Mcm9^L$ contains 13 exons, is 4836 bp in length, and encodes an 1134 aa protein (Figure 2-1A).

Genomic structure of the mouse *Mcm9* locus and mRNA isoforms.

Although RefSeq and published *Mcm9* gene models are available (12, 13), we performed additional bioinformatic analyses and targeted RT-PCR to derive the correct structure as shown in Figure 2-1. *Mcm9* produces two alternative C-terminal mRNA isoforms by alternative usage of a splice site within exon 7. Skipping this site results in a short isoform ($Mcm9^S$) encoding a protein of 386 amino acids. Splicing to exon 8 creates a longer isoform ($Mcm9^L$) encoding an 1134 amino acid (aa) protein (Figure 2-1A). $MCM9^s$ contains only half of the conserved MCM domain containing the Walker A motif (Figure 2-1B).

The 7th intron contains another gene, *Asf1a* (Anti-silencing function 1 homolog A) with a transcriptional orientation antisense to *Mcm9* (Figure 2-1A). ASF1a is a histone chaperone with diverse functions, including the regulation of replication fork progression under normal and replication stressed conditions (15, 16). Evidence suggests it does so by interacting with MCM2-7 via a histone H3-H4 bridge to transfer histones from dissociated nucleosomes to newly forming nucleosomes in the wake of the replication fork (15).

***Mcm9* isoforms are expressed ubiquitously in mice.**

EST data in Unigene show that *Mcm9* is expressed in many tissues, but does not distinguish between the 2 isoforms. RT-PCR analysis of $Mcm9^S$ and $Mcm9^L$ revealed expression of both in all tissues and through early development (Figure 2-1C). Levels of transcription in the gene body were assessed by analyzing GRO-Seq (Global Run-on Sequencing) data from ES cells and mouse embryonic

fibroblasts (MEFs) (17). This method determines the amount and locations of engaged RNA polymerase on a gene at the time of the assay (18). Run-on transcripts are produced across the entire *Mcm9* gene body. The expression levels of mature transcripts indicate that the amounts of each isoform produced are similar, based on the exon sequence counts of $Mcm9^{S}$ and $Mcm9^{L}$ (19) (Figure 2-3). *Asf1a* had similar amounts of engaged RNA pol II (Figure 2-3).

MCM9 is not required for DNA replication.

To determine the *in vivo* function of the MCM9 isoforms, we generated mice containing 3 different gene trap insertions within *Mcm9* (Figure 2-1A,B). We also generated a mutant allele of *Asf1a* ($Asf1a^{ALO673}$) to explore potential regulatory or functional relationships between the two genes.

The $Mcm9^{XE518}$ insertion actually caused a deletion beginning downstream of *Mcm9* exon 4, extending through the entire *Asf1a* gene, and terminating upstream of the final *Mcm9* exon (Figure 2-1A). Thus, $Mcm9^{XE518}$ is null for *Asf1a* and presumably *Mcm9*. Intercrosses of $Mcm9^{XE518/+}$ mice failed to produce newborn homozygotes ($P<<0.001$ by Chi^2; Table 2-1), indicating the allele is embryonically lethal. Timed matings revealed that $Mcm9^{XE518/XE518}$ embryos were viable at E9.5 but were smaller and developmentally arrested at a stage resembling E8.5 embryos (Figure 2-4B). These embryos contained no detectable *Asf1a* mRNA or *Mcm9* transcripts downstream of the gene trap insertion site (Figure 2-4E).

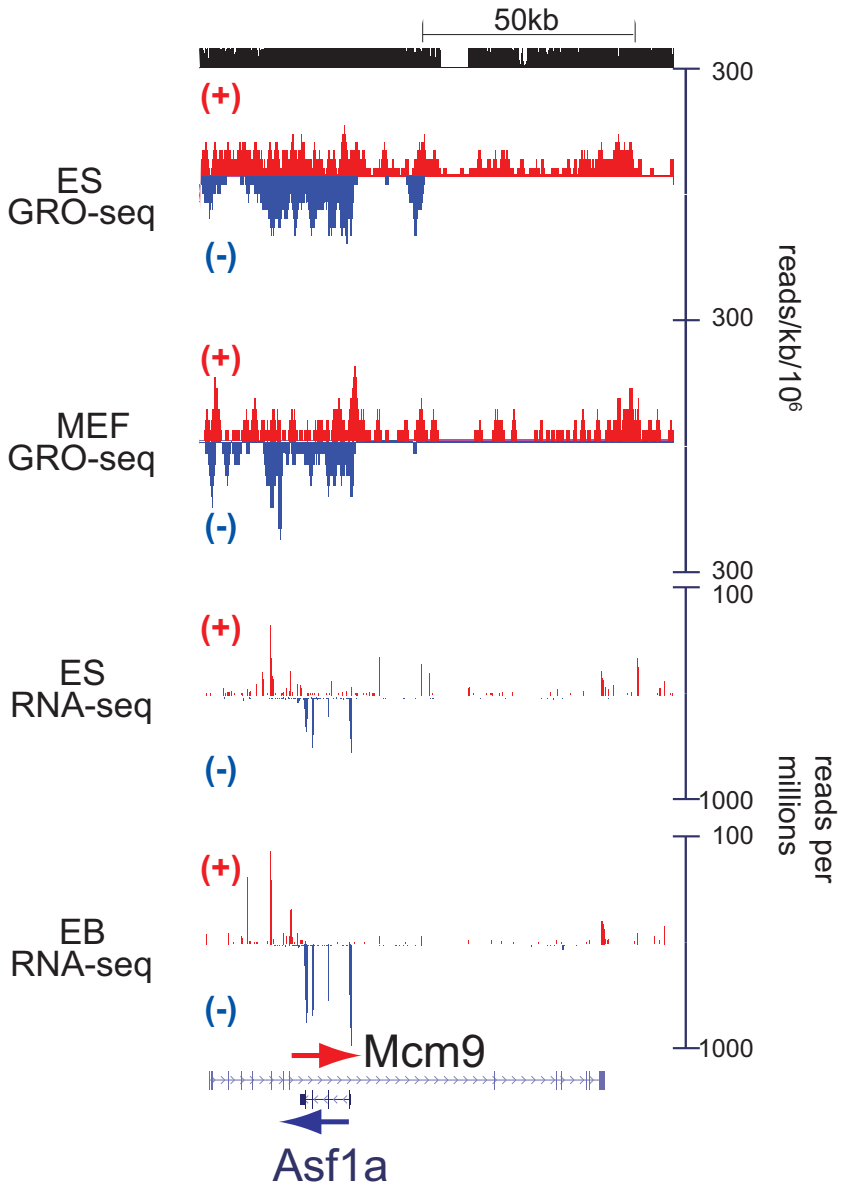

Figure 2-3. The ES and MEF GRO-seq maps of *Mcm9 and Asf1* loci compared with RNA-seq maps of ES cells and embryoid bodies. GRO-seq and RNA-seq maps are presented in a strand-specific manner, with transcripts along the top/forward (red +) and bottom/reverse (blue -) strands. Mappable regions are depicted as black bars in the top row, and RefSeq gene annotations are shown in the bottom row. Y-axes show the total sequence reads per 1 kb per one million of total uniquely mapped sequences. Note that RNA Pol II occupancy peaks downstream of the annotated UTRs; this is typical since the polymerase proceeds past the polyA site before stopping (see Core et al, Science 2008, 322:1845).

Because *Asf1a* is also disrupted in the *Mcm9*^{XE518} allele, the lethal phenotype could be due to mutation of either gene or a combination of both. To distinguish between these possibilities, we created mice bearing the *Asf1a*^{ALO673} gene-trap allele, which is predicted to truncate 129 C-terminal amino acids from the 209 aa protein. Homozygotes died at midgestation, with a phenotype similar to *Mcm9*$^{XE518/XE518}$ embryos (Figure 2-4D). The phenotype is likely due to loss of *Asf1a* alone, since normal *Mcm9* transcripts are produced in *cis* from the *Asf1a*^{ALO673} allele (Figure 2-4F). As expected, *Mcm9*^{XE518} failed to complement the lethality of *Asf1a*^{ALO673} (Figure 2-4C, Table 2-1). These data demonstrate that neither gene is required for cell division (and presumably DNA replication) during the first half of mouse gestation, a period of dramatic cell proliferation. However, these data do not reveal the developmental role of MCM9, since the lethal phenotype of *Asf1a* in the *Mcm9*^{XE518} allele obscures or precludes potential contemporaneous or subsequent roles.

Since ASF1 physically associates with MCM2-7 and facilitates nucleosome re-assembly during DNA replication and DNA repair (15, 20), processes that may overlap with MCM9, the question arises as to whether the physical arrangement of these two genes (which is conserved in mammals and chickens but apparently not zebrafish, based on current genome assemblies) is entirely coincidental. It is possible that there is a regulatory relationship between the genes, either with respect to their sharing common enhancer elements or modulators of chromatin structure, or in still more complex ways involving the complementarity of their transcripts or the interplay of the mechanics of divergent transcription complexes.

Table 2-1 *Viability of gene trap alleles*

***Mcm9*^{XE518} Intercross**			
	XE/XE	XE/+	WT
Observed	0	58	40
Expected	24.5	49	24.5
χ^2 *P* =	1.55E-08		

***Asf1a*^{ALO673} Intercross**			
	AL/AL	AL/+	WT
Observed	0	27	16
Expected	10.75	21.5	10.75
χ^2 *P* =	6.36E-04		

***Mcm9*^{XE518} *X Asf1a*^{ALO673}**				
	XE/AL	AL/+	XE/+	WT
Observed	1*	16	23	15
Expected	13.75	13.75	13.75	13.75
χ^2 *P* =	3.42E-04	* born dead		

***Mcm9*^{XG743} Intercross**			
	XG/XG	XG/+	WT
Observed	62	123	63
Expected	62	124	62
χ^2 *P* =	0.99		

***Mcm9*^{XE518} *X Mcm9*^{XG743}**				
	XE/XG	XE/+	XG/+	WT
Observed	11	9	14	16
Expected	11.25	11.25	11.25	11.25
χ^2 *P* =	0.37			

***Mcm9*^{AWO655} Intercross**			
	AW/AW	AW/+	WT
Observed	12	33	11
Expected	14	28	14
χ^2 *P* =	0.40		

***Mcm9*^{XE518} *X Mcm9*^{AWO655}**				
	XE/AW	XE/+	AW/+	WT
Observed	3	3	6	6
Expected	4.5	4.5	4.5	4.5
χ^2 *P* =	0.57			

Legend: Observed and Expected values are for liveborn pups of the indicated genotypes. Red c^2 *P* values indicate a significant loss of one or more genotypic class in any given cross. XE=*Mcm9*^{XE518}, XG=*Mcm9*^{XG743}, AW=*Mcm9*^{AWO655}, AL=*Asf1a*^{ALO673}.

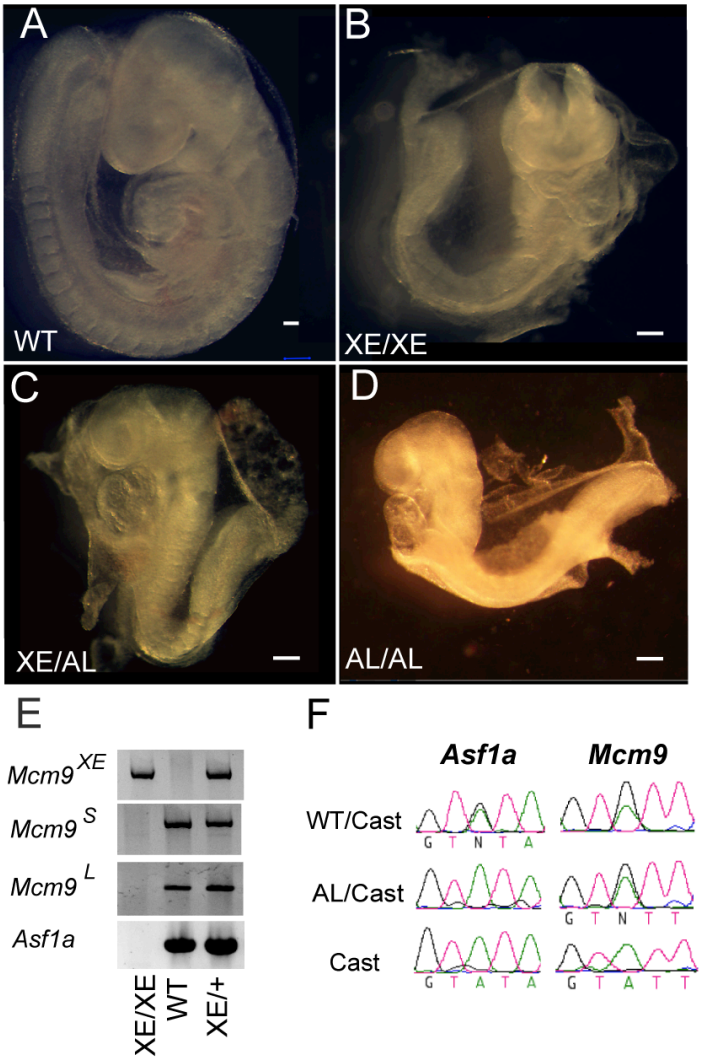

Figure 2-4. Midgestation lethality in MCM9- and ASF1A-deficient embryos. (A-D) embryonic day 9.5 embryos. (E) RT-PCR of e9.5 embryos. Primers for *Mcm9*^{S} and *Mcm9*^{L} are sets 2 and 3, respectively, from Fig. 1A. Primers (XE518WTF & XE518GTR) for *Mcm9*^{XE} are specific for the gene trap fusion transcript. (F) RT-PCR/sequencing of polymorphic coding SNPs (rs51382030 for *Asf1a*; rs51772485 for *Mcm9*). The WT allele here is C3H, which is identical to the parental 129-based gene trap chromosome. XE = *Mcm9*^{XE518} ; AL= *Asf1a*^{AL0673}. Bars = 500μM.

However, transcription of *Mcm9* through the *Asf1a* gene is not required for *Asf1a* transcription in *cis* (Figure 2-1D), and intact *Asf1a* is not needed for *Mcm9* transcription (Figure 2-4F). These results indicate that if there is indeed a regulatory relationship between the genes, it is likely to be related to sharing control sequences, identical regional chromosomal structure, or post-transcriptional processing.

Mice with severe depletion or elimination of *Mcm9* are viable.

To identify the *in vivo* roles of each *Mcm9* isoform, two other gene-trap alleles were utilized that do not ablate *Asf1a*. *Mcm9*^{XG743} is located downstream of exon 7 and *Asf1a* mRNA levels are ~75% of WT (Figure 2-1D). *Mcm9*^{XG743} is predicted to allow production of the entire MCM9^{S} polypeptide, either as a fusion to β-geo or as the endogenous protein (Figure 2-1B). A slight amount (<3%) of mRNA was detected that corresponds to splicing over the gene trap (exon 7-8 products). *Mcm9*^{S} and/or fusion transcripts were also reduced from WT levels (Figure 2-1D). These results indicate that *Mcm9*^{XG743} is severely hypomorphic or null for *Mcm9*^{L}, and potentially hypomorphic for *Mcm9*^{S}. Heterozygote intercrosses produced *Mcm9*$^{XG743/XG743}$ offspring at the expected Mendelian ratio (*P*=0.98; Supplemental Table 2-1). The *Mcm9*^{AW0655} allele, which effectively terminates transcripts upstream of the entire MCM domain (Figure 2-1A,B,D), thus appears null for *Mcm9* but leaves *Asf1a* transcription intact (Figure 2-1D). *Mcm9*$^{AWO655/AWO655}$ and *Mcm9*$^{AWO655/XE518}$ animals are completely viable (Table 2-1). Therefore, MCM9 is unnecessary for DNA replication.

MCM9 deficiency causes germ cell loss.

Despite being grossly normal, *Mcm9*^{XG743} male homozygotes had markedly smaller testes than WT littermates, a differential that was evident at puberty and widened over time (Figure 2-5A). Despite a consequent 67% decrease in epididymal sperm concentration at 12 weeks of age, these mutant males were fertile. Testis histology revealed three notable seminiferous tubules abnormalities (Figure 2-5B-D). The most striking was progressive germ cell depletion. The second was the presence of seminiferous tubule sections (~5%) lacking spermatogonia (the adult germ-line stem cells), but containing differentiated meiotic spermatocytes and/or postmeiotic spermatids (Figure 2-5D, arrows). The third class of abnormal tubule cross sections (5%) contained a cohort of spermatocytes arrested in meiosis (Figure 2-5D, inset). These abnormalities were also observed in *Mcm9*^{AWO655} male homozygotes and compound heterozygotes (Figure 2-6). Notably, mice with severe depletion of MCM2-7 are fertile and do not exhibit these germ cell loss phenotypes (Figure 2-6) (6, 8), suggesting that the germ cell effects in *Mcm9* mutants likely occur by mechanisms distinct from MCM2-7 helicase defects.

Young *Mcm9*$^{XG743/XG743}$ females were fertile but also exhibited germ cell loss. Mutant 6-12 wk ovaries had fewer total follicles, and were nearly devoid of primordial follicles. Oocytes were almost completely absent at 24 weeks (Figure 2-5E,F). Most *Mcm9*$^{AWO655/AWO655}$ females were infertile and exhibited ovarian hyperplasias and tubulostromal adenomas consistent with premature ovarian failure (see below).

Figure 2-5. *Mcm9* mutations cause germ cell depletion and loss of spermatogonial stem cells. (A,B) quantification of testis weights and histological abnormalities. * significantly different from WT, ** significant decrease in mutant testis size over time (n=10). Abbreviations in (B) for seminiferous tubule cross-sections that contain or exhibit the following: GMC=Giant multinucleated cells; MEI=Meiotic arrest; MW=missing wave of spermatogenesis; GCD=Germ cell depletion; Norm= normal. (C,D) H&E-stained histological sections of testes from 12 wk old mice of the indicated genotypes. WT= wild type; XG = $Mcm9^{XG743}$ (200X). Error bars indicate Std Dev. Seminiferous tubules marked with "*" are devoid of germ cells; those marked with "^" exhibit meiotic arrest (inset); and those indicated by arrows are depleted of spermatogonia but undergoing a final wave of spermatogenesis. Circled tubules are examples of normal spermatogenesis. (E,F) H&E-stained histological sections of ovaries from 24 wk old mice of the indicated genotypes. (G-L) Immunofluorescence of 1 dpp testes (G,H) and ovaries (200X) (J,K) of the indicated genotypes. MVH (green) stains germ cells and DAPI stains nuclei (blue). (I,L) Germ cell counts from MVH staining data at 1dpp (n=3). *Significant difference vs WT (see Methods). XG= $Mcm9^{XG743/XG743}$, p53=$Trp53^{-/-}$, p21=$Cdkn1a^{-/-}$ Error bars indicate Std Dev.

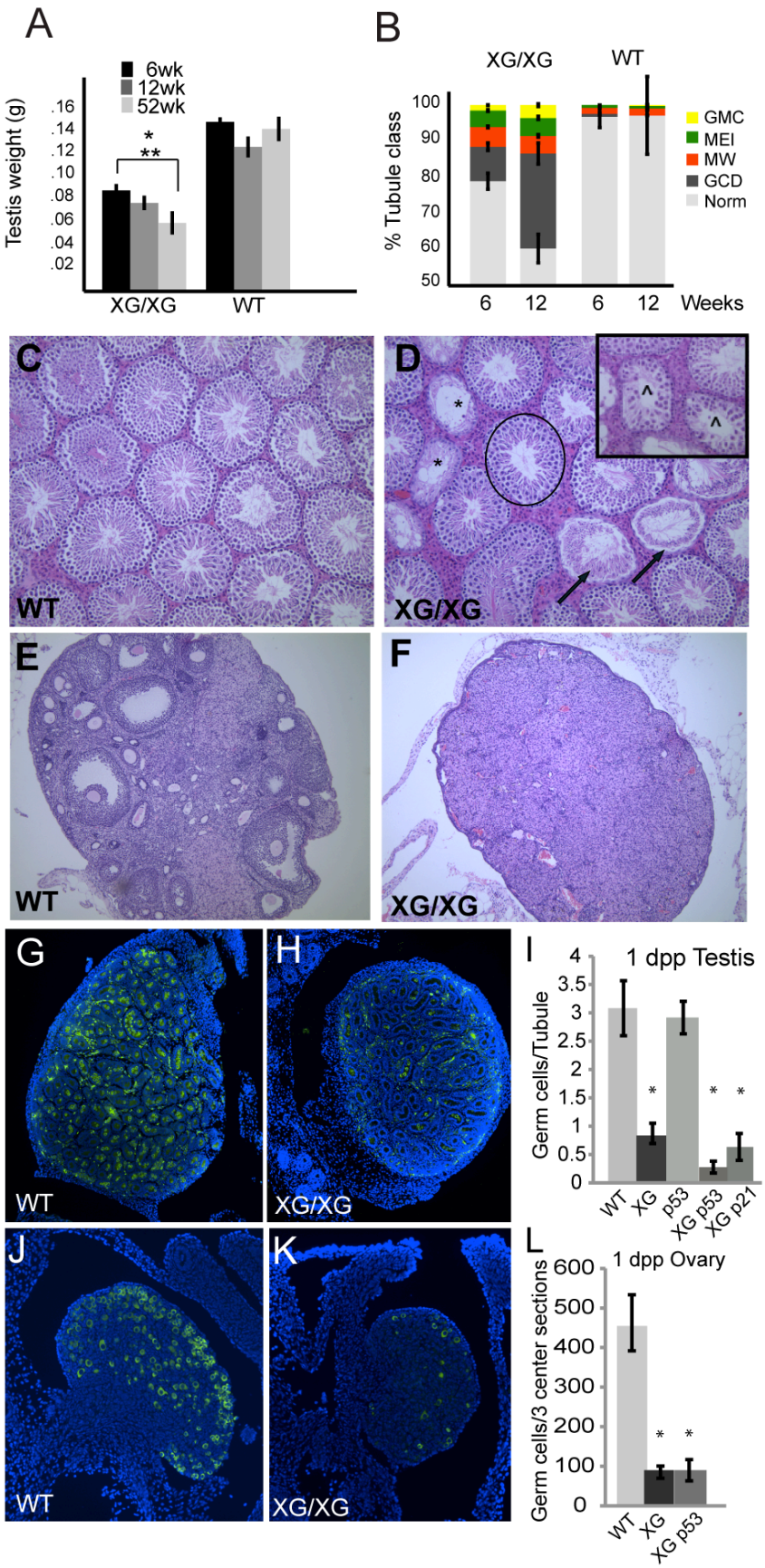
A
Testis weight (g)
.16
.14
.12
.10
.08
.06
.04
.02
6wk
12wk
52wk
*
**
XG/XG
WT
B
XG/XG
WT
% Tubule class
100
90
80
70
60
50
GMC
MEI
MW
GCD
Norm
6
12
6
12
Weeks
C
WT
D
*
*
^
^
XG/XG
E
WT
F
XG/XG
G
WT
H
XG/XG
I
1 dpp Testis
Germ cells/Tubule
4
3.5
3
2.5
2
1.5
1
0.5
0
*
*
*
WT
XG
p53
XG p53
XG p21
J
WT
K
XG/XG
L
1 dpp Ovary
Germ cells/3 center sections
600
500
400
300
200
100
0
*
*
WT
XG
XG p53

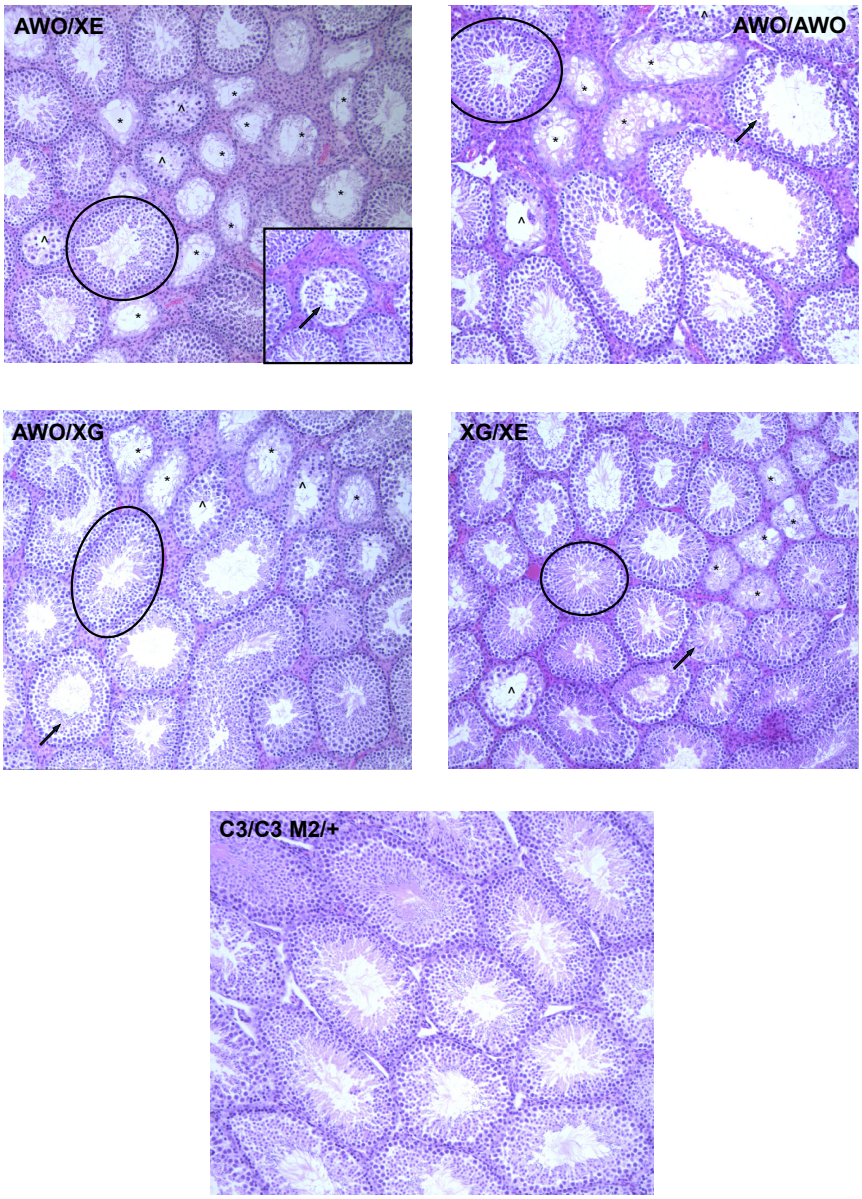

Figure 2-6. Testicular histology of various *Mcm9* allelic combinations and normal histology in a hypomorphic Mcm2-7 compound genotype. Similar to *Mcm9*^{XG743} homozygotes shown in Fig. 3, the other *Mcm9* alleles and allelic combinations show spermatogenesis and germ cell defects: germ cell depletion (*); meiotic arrest (^); terminal wave of spermatogenesis (arrow). Circled seminiferous tubules are undergoing normal spermatogenesis. Mice with severe MCM2-7 depletion have normal spermatogenesis (bottom panel). AWO=*Mcm9*^{AWO655}; XE=*Mcm9*^{XE518}; XG=*Mcm9*^{XG743}. C3/C3=*Mcm4*$^{Chaos3/Chaos3}$ M2=*Mcm2*$^{GT/+}$.

The sex-independent shortfall of germ cells in peripubertal animals is suggestive of a defect early in the germ lineage, possibly during the expansion or establishment of germ-line stem cell pools during embryonic development. To test this, 1-day-old control and *Mcm9*$^{XG743/XG743}$ gonads were serially sectioned and probed with the germ cell-specific marker MVH (mouse vasa homolog). This revealed a 72% decrease of gonocytes in nascent seminiferous tubules (Figure 2-5G-I), and 82% fewer oocytes in newborn ovaries (Figure 2-5J-L). Therefore, the shortfall in germ cells occurred during gestation. To determined if germ cell loss occurs *via* TRP53-pathway-mediated elimination, *Mcm9*$^{XG743/XG743}$ *Trp53*$^{-/-}$ and *Mcm9*$^{XG743/XG743}$ *Cdkn1a*$^{-/-}$ (*Cdk1na* = *p21*) animals were bred and their germ cell numbers were scored at 1dpp. There was no rescue of germ cell depletion in either of these compound mutants (Figure 2-5I,L). Curiously, TRP53 deficiency actually further decreased the numbers of germ cells in *Mcm9*$^{XG743/XG743}$ newborn males but not females (Figure 2-5I,L).

MCM9 deficiency does not impact MCM2-7 chromatin loading, has minimal impact on genome stability, but predisposes to cancer.

Mutations reducing MCM2-7 levels cause genomic instability and cancer susceptibility in mice (7, 8) as a consequence of decreased pre-RC formation (6, 21, 22). Since it was reported that MCM9 is essential for MCM2-7 loading onto replication origins and thus pre-RC formation in *Xenopus* oocyte extracts (14), we tested whether MCM9 depletion impacts MCM2-7 chromatin loading in

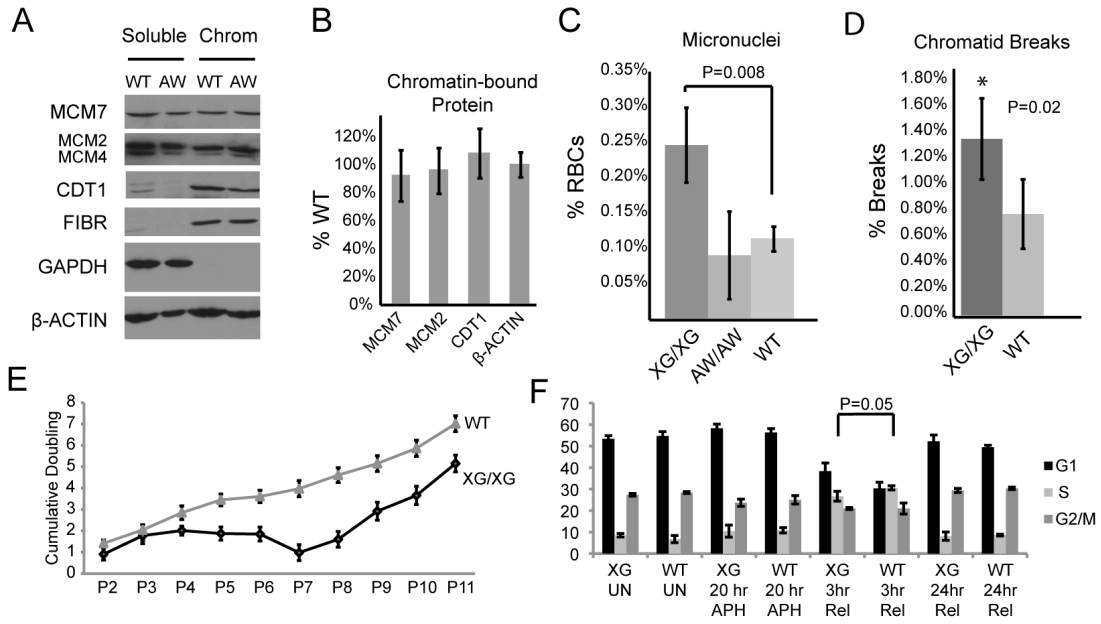

Figure 2-7. Loss of MCM9 does not alter MCM2-7 or CDT1 levels, however leads to mild genomic instability and cell cycle defects under replication stress.

(A) Western blots of mutant and WT MEFS showing detergent soluble vs. chromatin bound levels of indicated proteins. (B) Quantification of data in "A." (C) Micronucleus levels in erythrocytes. (D) Chromatid breaks in mutant MEFS. (E) *Mcm9* mutant MEFs undergo premature senescence. Y axis values were taken every 3 days upon passage. (F) Mutant MEFs exhibit a delay in cell cycle entry following Aphidicolin-induced replication stress. Primary data are in Fig. S3. MEFs were serum-starved to synchronize at G0/G1, serum was then added, then measurements were taken. AW = $Mcm9^{AWO655}$; XG = $Mcm9^{XG743}$. The P value is based on t-testing. "UN" = measurements 20 hrs after serum addition, but untreated with APH; "20 hr APH" = same as previous, but with APH treatment; "3hr Rel" or "24hr Rel" = same as previous, but 3 hrs or 24 hrs after APH was removed from media (n=3). Error bars indicate Std Dev.

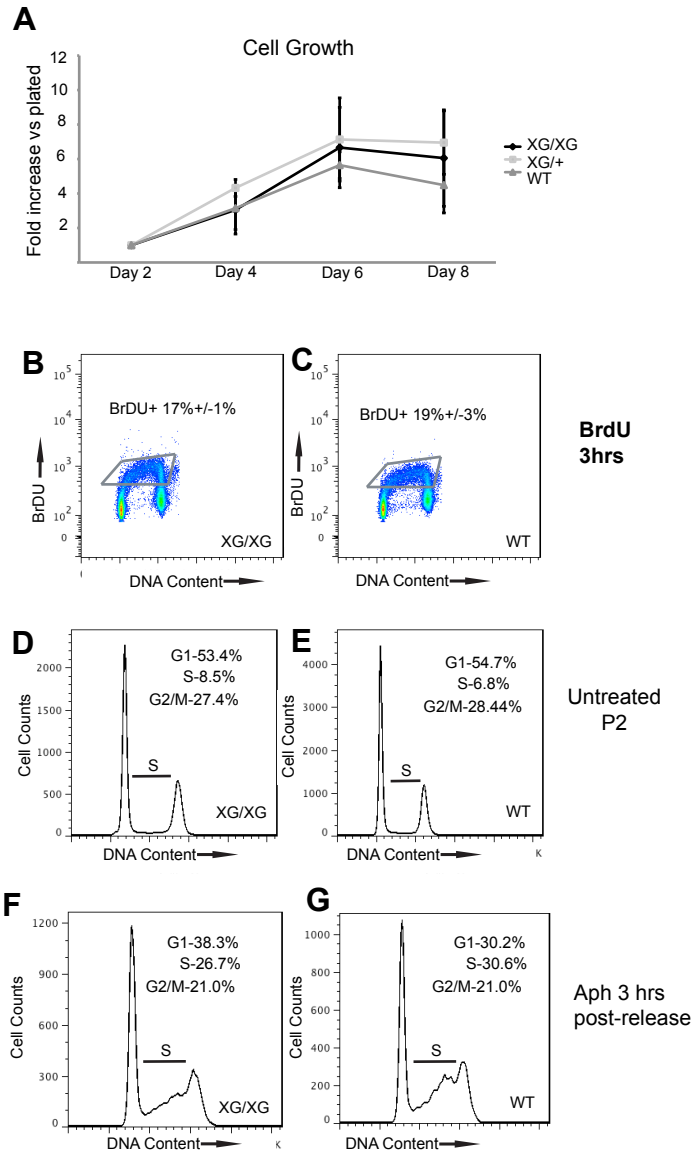

Figure 2-8. Sensitivity of MCM9-deficient MEFs to replication stress. (A) Untreated mutant MEFs proliferate normally in unsynchronized cultures. (B,C) BrdU incorporation in unsynchronized MEF cultures. (D,E) Cell cycle profiles of MEFs analyzed by flow cytometry. DNA was stained with Hoescht. These data were plotted in Fig. 4G of text. (F,G). Cell cycle profiles of MEFs arrested in G1 by serum starvation, then treated with aphidicolin (Aph) for 3 hours, followed by addition of serum (”post-release”)(N=3 for each experiment).

Mcm9 $^{AWO655/AWO655}$ MEFs. No difference in chromatin-bound MCM2, MCM4, and MCM7 was observed (Figure 2-7A,B). Furthermore, in contrast to *Xenopus* oocyte extracts immunodepleted for MCM9, no decrease of CDT1 was observed in mutant MEFs (Figure 2-7A,B).

To test for somatic chromosome instability (CIN), we measured peripheral blood micronucleus levels, an indicator of CIN that is elevated in *Mcm2-7* deficient mice (6, 8). Relative to WT, micronucleus levels were marginally higher in *Mcm9*$^{XG743/XG743}$ but not *Mcm9*$^{AWO655/AWO655}$ mice (Figure 2-7C). We also observed a 1.6 fold increase in metaphase chromatid breaks in *Mcm9*$^{XG743/XG743}$ MEFs (Figure 2-7D).

Although *Mcm9* disruption had no apparent impact on MCM2-7 homeostasis in MEFs and only slightly increased chromosomal instability, we aged *Mcm9* homozygotes, compound heterozygotes, and control siblings to assess potential long-term health consequences. All mutant males developed tumors by 1 year of age (vs. 32-33% of heterozygote and WT controls; Table 2-2). The most remarkable difference compared to controls was in the incidence of hepatocellular carcinoma (HCC; 8/13 mutants vs 0/28 controls). Furthermore, 8/8 affected animals had multiple HCCs (Table 2-3). MCM9-deficient females were prone to ovarian tumors (10/22 vs 0/12 in controls) by 1 year of age (Table 2).

Table 2-2. *Tumor incidence in MCM9-deficient mice*

MALES Genotype	Age (wks)	#	N	HCC	HA	Oth	Tumor Free
WT	40-55	9	≥N5	0	2	1	67%
Mcm9$^{GT/+}$	40-55	19	≥N4	0	6	1	68%
Mcm9$^{GT/GT}$	40-55	13	≥N4	8	4	1	0%

FEMALES Genotype	Age (wks)	#	N	OvT	OvH	Oth	Tumor Free
Controls	31-66	12	≥N2	0	1	1	92%
Mcm9$^{GT/GT}$	32-56	7	≥N2	4	2**	1	29%
Mcm9$^{GT/GT}$	9-25	15	<N3	6	3	2	47%

N = # of backcross generations into strain C3H; HCC=hepatocellular carcinoma; HA=hepatocellular adenoma; Oth=other tumors; OvT=ovarian tumor; OvH=ovarian hyperplasia; WT=Wild-type; GT=*Mcm9*^{XE518}, *Mcm9*^{XG743}, or *Mcm9*^{AWO655}. **OvH in contralateral ovary to tumor. In females, "Controls" include both heterozygotes and WT animals. Data on all individuals are presented in Table S3.

Table 2-3. Histopathology of Mcm9 mutant alleles

Animal Number	Geno	Age (wks)	Sex	Tumors	Tumor size (mm)	Pathology	N# C3H
Male Control							
16100, 16197, 18414, 18416, 18417, 18418	WT	52-53	M	0			N5, N10
16802	WT	52	M	1-Liver	6	Hepatocellular adenoma	N6
17877	WT	55	M	1-Pancreas	2	Islet Cell Adenoma	N7
18415	WT	52	M	1-Liver	7	Hepatocellular adenoma	N10
17364, 17365, 17368, 19192, 19193, 19195	XE/+	52-55	M	0			N5, N10
19194	XE/+	52	M	1-Liver	18	Hepatocellular adenoma and enlarged spleen with lymphoid hyperplasia	N10
17099	XE/+	52	M	1-Liver, 1-Lung	6 and 1	Hepatocellular adenoma and hepatic lipidosis; Lymphoid hyperplasia in thymus (possible lymphoma); pulmonary adenoma	N5
15639, 15640	XG/+	40	M	0			N4
16801,17359, 17360, 17367	XG/+	52-55	M	0			N6
17875	XG/+	55	M	0		Lipidosis, Ito cell hyperplasia of the liver, reactive cervical lymph node	N7
16101	XG/+	52	M	1-Liver	small	Hepatocellular adenoma	N5
16198	XG/+	53	M	1-Liver	21	poor histological section	N5
16196	XG/+	53	M	1-Liver	22	Hepatocellular adenoma	N5
17874	XG/+	55	M	1-Liver	16	Hepatocellular adenoma with hepatocyte disorganization, vacuolation, lipidosis	N7
Male *Mcm9*$^{GT/GT}$							
17097	XG/XE	52	M	Mult Liver	27	Hepatocellular adenoma with vacuolar change	N5
17098	XG/XE	52	M	3-Liver	15, 4, and 1	Hepatocellular adenoma with vacuolar change	N5
17366	XG/XE	55	M	4-Liver	24,12, 7, and 2	Hepatocellular Carcinoma	N5
16798	XG/XG	52	M	3-Liver	22, 12, and 4	Hepatocellular Carcinoma	N6
16103	XG/XG	52	M	3-Liver	18, 9, and 5	Hepatocellular Carcinoma	N5

17361	XG/XG	56	M	3-Liver	19, 5, and 5	Hepatocellular Carcinoma	N6
17876	XG/XG	55	M	2-Liver	22 and 16	Hepatocellular Carcinoma	N7
16102	XG/XG	52	M	3-Liver	19, 14, and 5	Hepatocellular Carcinoma	N5
16099	XG/XG	52	M	3-Liver	24, 18, and 5	Hepatocellular Carcinoma,	N5
16800	XG/XG	52	M	Mult. sm. liver	1 to 2 mm	Hepatocholantiocellular Carcinoma	N6
15641	XG/XG	40	M	2-Liver	15 and 3	Hepatocellular adenoma and thrombus	N4
16195	XG/XG	53	M	2-Liver, 1-Lung	15, 9, and 2	Hepatocellular adenoma with vacuolar change, Lung Adenoma, cardiac muscle in pulmonary arteries	N5
16799	XG/XG	52	M	1-Testis	3	Interstitial cell tumor of the testis	N6
Female Control							
13116	WT	45	F			Large follicular cyst	N9
17250	WT	54	F				F2
17251	WT	54	F				F2
18352	WT	56	F			Unilateral atrophy/involution of the ovary	N7
17863	WT	66	F				N11
11549	XE/+	41	F				N5
13882	XG/+	31	F				N4
21247	XG/+	32	F			Enlarged spleen with lymphoid hyperplasia	N10
18356	XG/+	52	F			Papillary cyst with hyperplasia and mineralization	N7
18359	XG/+	52	F			Hepatic lipidosis, Cutaneous fibropapilloma	N7
18351	XG/+	56	F			Small follicular cyst, Adenomyosis of the uterus	N7
10840	XG/+	57	F	1-Lung	1.5	Lung Carcinoma, Mild lipidosis, hepatitis, necrosis of the liver	N2
Female *Mcm9*$^{GT/GT}$ 32-56wks							
21246	XG/XG	32	F			Mild multifocal hepatic lipidosis, mild multifocal infiltrats of lymphocytes in the pancreas	N10
20543	XG/XG	43	F	1-Mammary	9	Mammary adenocarcinoma, mild lymphoplasmacytic metritis	N10
16110	XG/XG	44	F	1-Ovary		Cystadenoma and tubulostromal hyperplasia	N2
16111	XG/XG	44	F	1-Ovary		Papillary cystadenoma and tubulostromal hyperplasia	N2
18357	XG/XG	52	F			polycystic ovaries	N7
18358	XG/XG	52	F	1-Ovary		Benign mixed sex cord tumor	N7
18353	XG/XG	56	F	1-Ovary	9	Granulosa cell tumor, epithelial metaplasia	N7
Female *Mcm9*$^{GT/GT}$ 9-25wks							
21371	XG/XE	11	F			Tubulostromal hyperplasia, Lymphoid hyperplasia, Enlarged	F3

						lymph nodes (reactive?)	
21373	XG/XE	11	F				F3
21374	XG/XE	11	F			Enlarged lymph nodes (reactive?)	F3
21237	XG/XE	14	F	1-Ovary	Large	Ovarian teratoma and enlarged spleen with lymphoid hyperplasia	F3
21681	XG/XE	17	F			Focal tubulostromal hyperplasia, Enlarged lymph node (reactive?)	F3
21754	AW/XG	12	F	Lymphoma		Lymphoma and enlarged spleen with lymphoid hyperplasia	N2
21235	AW/XG	14	F	1-Ovary		Tubulostromal ovarian adenoma	F3
21238	AW/XG	14	F				F3
21682	AW/XG	17	F	1-Ovary, Lymphoma	11	Ovarian teratoma, Lymphoma, and enlarged spleen with lymphoid hperplasia; mixed inflammatory cells in mesentery	F3
21680	AW/XG	17	F				F3
21683	AW/XG	17	F	Possible Lymphoma		Enlarged lymph node (possible lymphoma)	F3
21105	AW/XG	25	F	1-Ovary		Tubulostromal ovarian adenoma	F2
21455	AW/AW	9	F			Tubulostromal hyperplasia,Neutrophilic peribronchial infiltrates in lung	F2
21362	AW/AW	13	F	1-Ovary		Tubulostromal ovarian adenoma, Enlarged pancreatic lymph node (reactive?)	F2
21364	AW/AW	13	F	1-Ovary		Tubulostromal ovarian adenoma	F2

Legend. XE=*Mcm9*^{XE518}, XG=*Mcm9*^{XG743}, AW=*Mcm9*^{AWO655}. N# C3H = Backcross generation into C3HeB/FeJ[a].

MCM9 deficiency does not perturb the cell cycle, but does delay cell cycle re-entry following replication stress.

To determine if *Mcm9* deficiency alters the cell cycle as does depletion of MCM2-7 (8, 23), *Mcm9*$^{XG743/XG743}$ primary MEFs (made from C3H congenic embryos) were evaluated under normal or replication stressed conditions. Continuous cultures of early passage cells were no different than WT with respect to proliferation, BrdU incorporation, and cell cycle profile (Figure 2-8A-E). However, the mutant cultures underwent senescence prematurely (by passage 5), ultimately producing immortalized survivors (Figure 2-7E). When *Mcm9*$^{XG743/XG743}$ and WT MEFs were synchronized at G0/G1 by serum starvation, then released (by serum addition) in the presence of aphidicolin (APH), APH-treated (but not untreated) mutant cells exhibited a delay in progression from G0/G1 through S-phase (Figure 2-7F; Figure 2-8G). These results confirm that MCM9 is dispensable for unperturbed DNA replication in mouse cells, but its absence accelerates senescence and confers susceptibility to DNA replication stress.

2.4 Discussion

Mcm9 encodes at least 2 isoforms, however the collection of mutant alleles reported here shows that neither is necessary for pre-RC formation or DNA replication in mice or mouse cells. This result was surprising, given a report that MCM9 is essential for loading MCM2-7 and thus formation of pre-RCs and DNA replication in a *Xenopus* egg extract system (14). In this widely-used model,

sperm DNA added to the extract gets converted into chromatin, and a single round of replication ensues in a putatively physiological manner. That study found that MCM9 binds to chromatin in an ORC-dependent manner, and by virtue of interacting directly with the essential helicase loading factor CDT1, enables MCM2-7 assembly into pre-RCs. Evaluation of MCM9's role was determined by immunodepletion, and supplementation of immunodepleted extracts with *in vitro*-produced *Mcm9* mRNA partially rescued MCM2-7 loading and the block in DNA replication.

We can offer theories on these contradictory data. First, amphibians and mammals may differ in the need for MCM9 in DNA replication, such that whereas it is essential in *Xenopus*, it has acquired a more specialized (e.g., germ-line stem cells), but non-essential role in mammals. In this regard, it should not be overlooked that the *Xenopus* oocyte is a specialized cell. Many eukaryotes lack *Mcm9* (and *Mcm8*) which supports the idea that MCM9 evolved to have a specialized role, rather than an essential one for DNA replication in some species. Second, the *Xenopus* egg extract system may not be entirely accurate in recapitulating all aspects of DNA replication and its regulation. Third, it is possible that, despite rigorous controls (14), that the MCM9 immunodepletion had an unknown, deleterious effect upon pre-RC formation. Furthermore, since CDT1 interacts directly with MCM2-7 *in vivo* (24), MCM9 would not be required to mediate the essential CDT1:MCM2-7 interaction needed for loading. Whatever the reason for the disparity in results, the present study underscores the

importance of *in vivo* genetic ablation studies to reveal the true physiological role of genes in the context of a whole animal.

Although *Mcm9* is ubiquitously expressed, its ablation appears to affect only a subset of tissues in the mouse under normal laboratory conditions. There were two major phenotypes: germ cell depletion and cancer susceptibility. The observed germ cell loss appears to occur at two stages. The shortfall observed at birth must have its roots in: a) the specification or proliferation of the primordial germ cell (PGC) lineage; b) migration of the PGCs to the genital ridges and primitive gonads; or c) proliferation within the primitive gonads. This germ cell proliferation happens rapidly, expanding the number from ~100 to >20,000 (25). Alternatively, PGCs may get depleted due to a failure in maintenance after migration to the primitive gonads. The second stage of loss is specific to males, where there appears to be a defect in spermatogonial self-renewal during adulthood. How MCM9 deficiency causes these defects is not clear. Although MCM9 is related to the MCM2-7 replicative helicase proteins, we do not believe that overall DNA replication *per se* is impaired, since severely hypomorphic MCM2-7 mutations do not have germ cell defects. Rather, we conjecture that given the observed phenotypes of cancer susceptibility, GIN, and replication stress sensitivity, that MCM9 deficiency causes a subtle defect in repair of replication-induced damage to which rapidly proliferating germ-line stem cells are especially sensitive. If true, this might trigger cell death as a means to prevent transmission of a compromised genome to offspring. However, like DNA damage- or replication stress-induced apoptosis of ES cells (26), such death

would have to occur *via* a TRP53 –independent pathway as indicated by our genetic studies. Alternatively, the progressive loss of spermatogonial stem cells in adult male *Mcm9* mutants points to stem cell maintenance or proliferation defects. Future experiments will be geared towards identifying the stages at which germ cells are being lost during development, and what cell cycle and/or damage checkpoint pathways might be activated to cause their elimination or failure to proliferate.

Interestingly, *Mcm9* mutant mice were susceptible to distinct sex-specific cancers. Males were highly prone to hepatocellular carcinomas (HCC). In humans, HCC is more common in males than females (27). The majority of HCC mouse models are driven by viral induction, drug treatments, deregulated oncogenes, or a combination of these (28, 29). We are aware of only one germ-line mutation (*Abcb4/Mdr2)* that causes a high incidence of HCC formation with <1 year latency (30). Therefore, the *Mcm9* mutants may provide a useful model for genetic susceptibility to HCC. Mutant females were prone to ovarian tumors, although these may be related to germ cell depletion and premature ovarian failure (31). In conclusion, MCM9 depletion drives neoplasia by a mechanism that does not seem to involve a major increase in chromosome instability or disrupted loading of MCM2-7 onto pre-RCs. However, the delayed ability of mutant MEFs to re-enter the cell cycle following Aph treatment suggests that certain cell types may have a sensitivity to replication stress, and this may play a role in the cancer susceptibilities.

2.5 Materials and Methods

Mice. Gene trap-bearing ES cell lines (from 129 substrains) ware obtained from BayGenomics (XG743 and XE518) and The Sanger Institute (AWO655 and ALO673). Chimeras were generated by microinjection of the ES cells into C57BL/6J blastocysts using standard procedures. Following germ-line transmission, alleles were backcrossed into C3HeB/FeJ^{a} ("C3H"). Exact insertion sites of gene trap vectors were determined by "primer walking" as described (6, 8). Genotyping of was performed either by PCR amplification of the neo gene within the vector, by insertion-specific assay, or utilizing polymorphic flanking microsatellite markers *D10Mit20* and *D10Mit194* that are polymorphic between 129 and C3H (Table S1).

Histology and immunohistochemistry. For basic histology, tissues were fixed in 4% paraformaldehyde overnight, paraffin embedded, sectioned, and stained with hematoxylin and eosin (H&E). For germ cell counts, 10μM sections of 1 day old gonads were immunostained as described (32). Antibodies: Rabbit anti-DDX4/MVH (Abcam ab13840, 1:250); goat anti-rabbit Alexa 488 conjugate (Molecular Probes A11008, 1:1000). Germ cells were counted in three sections from the midportion of each gonad and averaged. The data were analyzed using one-way ANOVA with Bonferroni correction (Prism software package). The resulting *P* values were used to determine significance ($P<0.05$).

RT-PCR and cDNA analysis. Semi-quantitative PCR analysis of various mouse tissues (Fig. 1c) was performed on the Mouse Multiple Tissue cDNA panel from Clontech (636745). Real-time RT-PCR was performed as described (6, 8). Oligonucleotide primers are listed in Supplemental Table S1.

MEF growth studies. MEF growth analyses and metaphase spreads were performed as described (33). For senescence assays, cells were counted every 3 days and replated at $5X10^5$. All MEFs were derived from C3HeB/FeJ congenic (N10) embryos and were primary cultures.

Micronucleus assays. These were performed essentially as described (34).

Isolation of protein fractions. For Western analyses of chromatin bound vs non-chromatin-bound proteins, we used a Triton-100 detergent fractionation protocol. Briefly, MEFs were trypsinized, washed twice in cold PBS, resuspended by vortexing in 1ml TX-NE (320 mM sucrose, 7.5 mM $MgCl_2$, 10 mM HEPES, 1% Triton X-100, plus protease inhibitor), and incubated on ice for 30 min. Nuclei were pelleted (1200 RPM, 3 min) and the supernatant, containing proteins of cell membrane, cytosolic, and free forms of MCMs, was designated as the detergent “soluble” fraction (23, 35). The nuclear pellet was resuspended in 0.5ml RIPA, liberating the chromatin fraction containing nuclear scaffold proteins, DNA, and chromatin binding forms of MCMs. Antibodies used were as follows. MCM2: ab31159 (Abcam); MCM7: ab2360 (Abcam); Beta-actin: A1978 (Sigma); Fibrillarin: ab5821 (Abcam), CDT1: 06-1295 (Millipore), GAPDH: 6C5 (Advanced Immunochemical).

Acknowledgements This work was supported by grants from the NY Stem Cell Foundation (JS), and the NIH (T32 HD052471 training slot to SAH). We thank R. Munroe for ES cell microinjections, and C. Chuang and M. Wallace for providing tissue samples.

2.6 References

1. Bochman ML & Schwacha A (2008) The Mcm2-7 complex has in vitro helicase activity. *Mol Cell* 31:287-293.
2. Labib K, Tercero JA, & Diffley JF (2000) Uninterrupted MCM2-7 function required for DNA replication fork progression. *Science* 288:1643-1647.
3. Moyer SE, Lewis PW, & Botchan MR (2006) Isolation of the Cdc45/Mcm2-7/GINS (CMG) complex, a candidate for the eukaryotic DNA replication fork helicase. *PNAS* 103:10236-10241.
4. Blow JJ & Dutta A (2005) Preventing re-replication of chromosomal DNA. *Nature Reviews* 6:476-486.
5. Tye BK (1999) MCM proteins in DNA replication. *Ann Rev Biochem* 68:649-686.
6. Chuang CH, Wallace MD, Abratte C, Southard T, & Schimenti JC (2010) Incremental genetic perturbations to MCM2-7 expression and subcellular distribution reveal exquisite sensitivity of mice to DNA replication stress. *PLoS Genetics* 6 e1001110.
7. Pruitt SC, Bailey KJ, & Freeland A (2007) Reduced Mcm2 expression results in severe stem/progenitor cell deficiency and cancer. *Stem Cells* 25:3121-3132.
8. Shima N*, et al.* (2007) A viable allele of Mcm4 causes chromosome instability and mammary adenocarcinomas in mice. *Nature Genetics* 39:93-98.

9. Blanton HL*, et al.* (2005) REC, Drosophila MCM8, drives formation of meiotic crossovers. *PLoS Genetics* 1:e40.
10. Liu Y, Richards TA, & Aves SJ (2009) Ancient diversification of eukaryotic MCM DNA replication proteins. *BMC Evol Biol* 9:60.
11. Volkening M & Hoffmann I (2005) Involvement of human MCM8 in prereplication complex assembly by recruiting hcdc6 to chromatin. *Mol Cell Biol* 25:1560-1568.
12. Yoshida K (2005) Identification of a novel cell-cycle-induced MCM family protein MCM9. *Biochem Biophys Res Commun* 331:669-674.
13. Lutzmann M, Maiorano D, & Mechali M (2005) Identification of full genes and proteins of MCM9, a novel, vertebrate-specific member of the MCM2-8 protein family. *Gene* 362:51-56.
14. Lutzmann M & Mechali M (2008) MCM9 binds Cdt1 and is required for the assembly of prereplication complexes. *Mol Cell* 31:190-200.
15. Groth A*, et al.* (2007) Regulation of replication fork progression through histone supply and demand. *Science* 318:1928-1931.
16. Groth A*, et al.* (2005) Human Asf1 regulates the flow of S phase histones during replicational stress. *Mol Cell* 17:301-311.
17. Min IM*, et al.* (2011) Regulating RNA polymerase pausing and transcription elongation in embryonic stem cells. *Genes Devel* 25:742-754.
18. Core LJ, Waterfall JJ, & Lis JT (2008) Nascent RNA sequencing reveals widespread pausing and divergent initiation at human promoters. *Science* 322:1845-1848.

19. Cloonan N*, et al.* (2008) Stem cell transcriptome profiling via massive-scale mRNA sequencing. *Nature Methods* 5:613-619.
20. Mousson F, Ochsenbein F, & Mann C (2007) The histone chaperone Asf1 at the crossroads of chromatin and DNA checkpoint pathways. *Chromosoma* 116:79-93.
21. Kunnev D*, et al.* (2010) DNA damage response and tumorigenesis in Mcm2-deficient mice. *Oncogene* 29:3630-3638.
22. Kawabata T*, et al.* (2011) Stalled Fork Rescue via Dormant Replication Origins in Unchallenged S Phase Promotes Proper Chromosome Segregation and Tumor Suppression. *Molecular Cell* 41:543-553.
23. Ibarra A, Schwob E, & Mendez J (2008) Excess MCM proteins protect human cells from replicative stress by licensing backup origins of replication. *PNAS* 105:8956-8961.
24. Zhang J*, et al.* (2010) The interacting domains of hCdt1 and hMcm6 involved in the chromatin loading of the MCM complex in human cells. *Cell Cycle* 9:4848-4857.
25. McLaren A (2003) Primordial germ cells in the mouse. *Dev Biol* 262:1-15.
26. Aladjem MI*, et al.* (1998) ES cells do not activate p53-dependent stress responses and undergo p53- independent apoptosis in response to DNA damage. *Curr Biol* 8:145-155.
27. El-Serag HB (2004) Hepatocellular carcinoma: recent trends in the United States. *Gastroenterology* 127(5 Suppl 1):S27-34.

28. Heindryckx F, Colle I, & Van VH (2009) Experimental mouse models for hepatocellular carcinoma research. *Int J Exp Path* 90:367-386.
29. Fausto N & Campbell JS (2010) Mouse models of hepatocellular carcinoma. *Sem Liver Disease* 30:87-98.
30. Mauad TH*, et al.* (1994) Mice with homozygous disruption of the mdr2 P-glycoprotein gene. A novel animal model for studies of nonsuppurative inflammatory cholangitis and hepatocarcinogenesis. *The American journal of pathology* 145:1237-1245.
31. Vanderhyden BC, Shaw TJ, & Ethier JF (2003) Animal models of ovarian cancer. *Reprod Biol Endocrinol* 1:67.
32. Reinholdt L, Munroe RJ, Kamdar S, & Schimenti J (2006) The mouse *gcd2* mutation causes primordial germ cell depletion. *Mech Devel* 123:559-569.
33. Shima N, Munroe RJ, & Schimenti JC (2004) The mouse genomic instability mutation chaos1 is an allele of Polq that exhibits genetic interaction with Atm. *Mol Cell Biol* 24:10381-10389.
34. Reinholdt L, Ashley T, Schimenti J, & Shima N (2004) Forward genetic screens for meiotic and mitotic recombination-defective mutants in mice. *Methods Mol Biol* 262:87-107.
35. Frisa PS & Jacobberger JW (2010) Cytometry of chromatin bound Mcm6 and PCNA identifies two states in G1 that are separated functionally by the G1 restriction point. *BMC Cell Biol* 11:26.

APPENDIX I

2.7 Additional MCM9 data

To investigate further into the testicular phenotype that we observed 5% of the seminiferous tubules contained cells that were in meiotic arrest, we performed meiotic surface spreads. Using antibodies against γ-H2AX and RAD51 on pachetene spermatocytes there was a persistence of both at 38% and 31% respectively (Figure A1-1A-F). This indicates there is still unrepaired DNA damage in these cells. However this does not correspond to the 5% of tubules arrested in meiosis, so a subset of these cells must eventually go on to repair the damage and complete meiosis or undergo apoptosis. To quantify the apoptosis levels in *Mcm9*$^{XG743/XG743}$ animals, TUNEL assays were performed. We observed a 1.6 fold increase in TUNEL positive cells in the mutant over the control testes (Figure A1-1G-I). This is only a slight but significant increase over WT with the spread of TUNEL positive cells in the interior of the tubule and not near the basal lamina where the stem cells reside. This indicates that the cells that are being lost are not the stem cells population.

Since there appears to be a spermatogonial stem cell defect, we wanted to see if the stem cell loss could extend to other populations. So we tested the induced pluripotent stem cell (iPS) induction potential of the *Mcm9*$^{XG743/XG743}$ MEFS. The mutant cell lines were significantly induced at a lower rate by metric of colony formation than the wild-type lines ($p<0.001$ TTEST) (Figure A1-2).

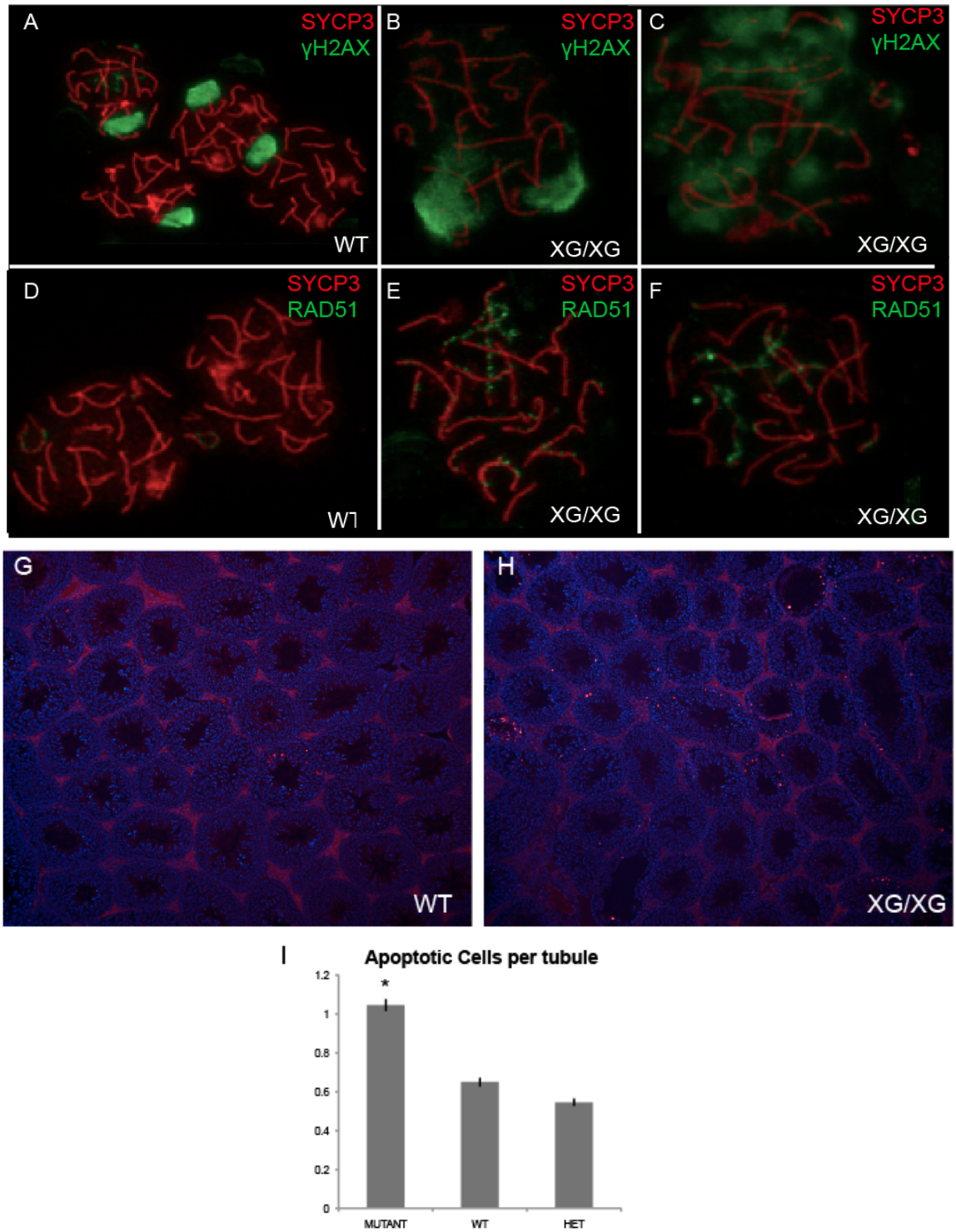

Figure A2-1 Persistent double strand breaks in MCM9 mutant Spermatocytes and increased apoptosis in seminiferous tubules.

Surface spread spermatocyte nuclei were immunostained with SYCP3 for the central element in red (A-F) and γ-H2AX (A-C) and RAD51 in green (D-F). (G-I) There is an increase in TUNEL positive cells in the MCM9 mutant testes (H,I). TUNEL (RED) counterstained with DAPI.

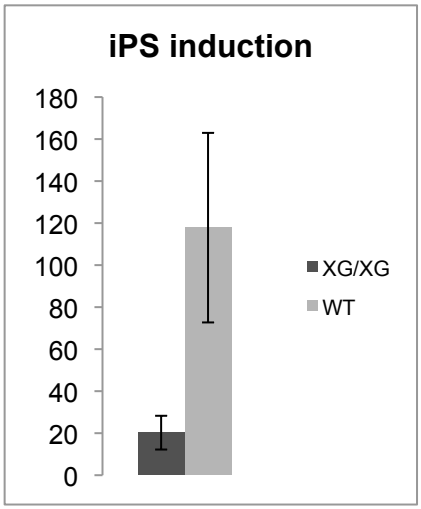

Figure A2-2 Decreased iPS effenciency in MCM9 mutant cells.
The number of colonies formed by *Mcm9*$^{XG/XG}$ cell lines were significantly decreased from wild-type.

These results indicate that while spermatogenesis is occurring in these mice, the set of problems that we have observed is not due to just one defect. There is only a slight increase in apoptosis occurring, however 1/3 of the pachytene cells contain persistent DNA damage. This suggests that the damage may be getting repair, or that the damaged cells are being removed by other methods not involved in apoptosis. There may be an over-proliferation of the early spermatogonial stem cell that could lead to premature senescence or terminal differentiation.

The decrease transformation of MEFs into iPS cells may be due to the inability of *Mcm9*$^{XG743/XG743}$ to maintain stem cell properties. This decrease may also be due to the cell cycle of the MEFs, such that the stress casued by the viral induction interferes with the cell cycle in a way that MCM9 is needed, and this leads to fewer cells that can be transformed.

Geminin is the negative interactor of CDT1. One of geminin's other roles is involved in differentiation. Geminin in the testes is only expressed in differentiated cells. Leading to a hypothesis that Mcm9 may be a "stemness" factor at least in the testes. Not only does geminin have a role in suppressing CDT1 to prevent formation of a pre-RC during DNA replication, geminin has roles in balancing DNA replication with differentiation(1)

METHODS:

Meiotic spreads were performed as described(2). The primary antibodies used were as follows: mouse anti-SCP3 (1:500; Abcam); rabbit anti-RAD51 (1:250, this polyclonal antibody recognizes both RAD51 and DMC1; Oncogene Research Products); rabbit anti-γH2AX (1:500; Upstate Biotechnology).

For immunohistochemistry, the sections were deparaffinized and dehydrated through Xylene/Ethanol/PBS gradients. Slides were subjected to antigen retrieval by boiling at 95o C for 40 minutes in 10mM Tris-sodium citrate/PBS (pH=6.0) with 0.05% Tween 20. Mouse monoclonal anti-PCNA antibody (clone PC10; Sigma; diluted 1:200), and conterstained with DAPI.

Induced pluripotent stem cells were made as previously described (3).

References:

1. Yoshida K (2007) Geminin organizes the molecular platform to balance cellular proliferation and differentiation. *Frontiers in bioscience : a journal and virtual library* 12:2984-92.
2. Reinholdt L, Ashley T, Schimenti J, Shima N (2004) Forward genetic screens for meiotic and mitotic recombination-defective mutants in mice. *Methods in molecular biology (Clifton, N.J.)* 262:87-107.
3. Chuang C-H, Wallace MD, Abratte C, Southard T, Schimenti JC (2010) Incremental genetic perturbations to MCM2-7 expression and subcellular distribution reveal exquisite sensitivity of mice to DNA replication stress. *PLoS genetics* 6.

CHAPTER 3:

Fancm separation of function mouse alleles dissect the roles of the translocase and endonuclease domains.

Suzanne A. Hartford, Yunhai Luo, Ruizhu Zeng, Gabriel Balmus, Teresa L. Southard, Naoko Shima, John C. Schimenti

Author Contributions:

Yunhai Luo- Germ Cell counts and checkpoint mutant crosses
Ruizhu Zeng and Gabriel Balmus- Sequencing
Teresa Southard- Histopathology
Naoko Shima- Research design
John Schimenti-Funding and Research Design

3.1 Abstract

Fanconi Anemia (FA) is a rare human genetic disorder characterized by bone marrow failure, developmental abnormalities, decreased fertility, and high incidence of malignancies. The FA complementation group has roles in resolution of DNA interstrand crosslinks. The role of FANCM in FA crosslink repair is as part of the damage sensor and loads the FA core complex to the site of the DNA interstrand crosslink. FANCM also participates in the S-phase checkpoint through signaling with ATR, and FANCM has FA complex-independent roles in DNA damage repair. Our lab conducted an ENU mutagenesis screen for animals with elevated genomic damage in peripheral blood. From this screen we recovered an allele, *chaos4*, which contains a point mutation in a highly conserved amino acid within the helicase domain of FANCM. We also created a gene-trap allele that removes the endonuclease domain of FANCM. Phenotypic analysis revealed that these mutants share some phenotypes with each other and the published null *Fancm* mouse. There are also a number of phenotypes unique to each of these mutant mice. Subsets of these mutants have germ cell depletion and a G2/M delay in primary MEFs. Meanwhile none of our *Fancm* mutant cells are sensitive to MMC. These data suggest that these different alleles may allow for separation of function analyses of the translocase and endonuclease domains of FANCM.

3.2 Introduction

The Fanconi Anemia complementation group currently consists of 15 genes. The complementation group can be sub-divided into 3 components, the core complex, the ID group, and the repair group. The core complex consists of FANC-A,B,C,E,F,G,L, and M (1, 2). The core complex is loaded onto the site of DNA damage partially by FANCM (3). Then the core complex acts as an E3 ubiquitin ligase with the E2 protein UBE2T to mono-ubiquitinate the ID heterodimer that consists of FANCD2 and FANCI (4, 5). The mono-ubiquitination of FANCD2 and FANCI then allows for the activation of the repair group constisting of BRCA2/FANCD1, FANCN, FANCJ, FANCO (RAD51C) and possibly FANCP (SLX4). These proteins have roles in homologous recombination and translesion synthesis (6–9). This activation of the FA pathway is in conjunction with activation of the ATR pathway which phosphorylates a number of the FA proteins (10–12). FANCM has a role in stabilizing ATR through its interaction with HCLK, and it also participates in RPA localization to sites of ssDNA (6–8, 13, 14). The overall role of the Fanconi Anemia complex is to preserve genome stability. This is accomplished through processing blocked and/or broken replication forks through the coordination of homologous recombination and translesion synthesis. (9).

There are several knock-out (KO) mouse models of the Fanconi Anemia complementation group. They all have similar phenotypes including germ cell depletion and sensitivity to MMC, however only a subset have congenital defects, and only one (FANCP/SLX4) recapitulates hematopoietic defects that are

characteristic of the human disease (9, 15). *Fancd2* mouse mutants have been shown to exhibit a higher incidence of cancer (15). The *Fancm* deletion mouse exhibits germ cell depletion, sensitivity to MMC, and a high incidence of cancers. In contrast to other FA mutants is that intercrosses of *Fancm*$^{-/-}$ animals yield a non-Mendelian ratio of female offspring. Homozygous *Fancm*$^{-/-}$ cells exhibit a high incidence of sister-chromatid exchange (SCE), and a decreased ability to mono-ubiquitinate FANCD2 (16). As a core complex member, FANCM unique from the other FA core members as it is conserved through evolution as it has homologues in yeast and archaea. Furthermore, unlike other FA gene mutations, *Fancm* cell lines also have sensitivity to UV (activates nucleotide excision repair) and camptothecin (CPT, activates double stranded break repair) (10). This all suggests that FANCM has roles in DNA repair pathways in addition to interstrand crosslink repair.

FANCM has 2 conserved domains: a helicase/translocase domain and an endonuclease domain, but neither of these have any known helicase or endonuclease activity (17). Additionally, FANCM contains three known protein binding motifs, MM1, MM2, and MHF (18–20). The biochemical roles of these domains and motifs are the subject of ongoing investigations. The overall role of FANCM appears to be binding chromatin and localizing the FA core complex to the site of DNA damage. However, FANCM can facilitate holliday junctions (HJ) branch migration, and possess fork reversal activity that may facilitate template switching during lesion bypass (21–23). FANCM has been shown to be involved in D-loop dissociation, and has translocase activity to allow movement along

DNA (21, 24, 25). FANCM interacts with ATR through HCLK (which stabilizes ATR). This interaction suggests that FANCM may be part of the S-phase checkpoint (6, 7, 26). Most of these functions mentioned above are facilitated through the helicase/translocase domain of the protein with some overlap with the endonuclease domain.

The C-terminal endonuclease domain of FANCM is needed for its interaction with its binding partner FAAP24 (which also has an endonuclease domain). Both are required, at least partially, for interaction with the FA core complex. Both the interaction with FAAP24 and the endonuclease domain are needed for resistance to CPT, but not for resistance to MMC, cisplatin or mono-ubiquitination of FANCD2. FAAP24 does increase FANCM binding specificity to certain DNA structures (3, 6, 7, 27).

The FANCM histone fold motif (MHF) binds to MHF1 (CENP-S) and MHF2 (CENP-X). The binding to these proteins localizes FANCM to the chromatin and possibly to the centromere. This interaction is also important for FANCD2 mono-ubiquitination and foci formation, as well as resistance to MMC and CPT(18, 19). Two other binding motifs are FANCM Motif 1 and 2 (MM1, MM2) which are important in tethering the FA core complex members and the HR repair complex of BLM respectively (20).

Recently FANCM has been shown to have some functional redundancy with the MutS homologues which are important for mismatch repair (28). All of these activities of FANCM suggest that it is involved in multiple DNA repair

processes, from sensing DNA damage to choice and recruitment of repair pathways to actually facilitating the repair itself.

Given the importance of FANCM for the functioning of the FA core complex, and the roles of FANCM in DNA repair, these studies are aimed at understanding FANCM functions in various cellular contexts. We accomplish this through the use of two mutant alleles of *Fancm* that have hypomorphic function with respect to the different domains of FANCM.

3.3 Results

Identification of *Chaos4,* an allele of *Fancm,* from a screen for mutations causing genomic instability (GIN):

Chromosomal aberrations occurring spontaneously 4 (*Chaos4)* arose from an ENU mutagenesis screen for mouse mutations causing GIN (29). The screen used elevated micronuclei (MN) in peripheral blood as a marker for GIN. *Chaos4* mutant animals had a 0.43% micronucleus level, representing an approximately 3 fold increase over the WT (0.14%; Figure 3-1A). Using the SNP mapping service from the Beier Lab (30), we localized the mutation to a 44Mb region on mouse chromosome 12. Microsatellite markers further reduced the region to a 14Mb region between *D12Mit285* and *D12Mit71*. Using elevated micronuclei as

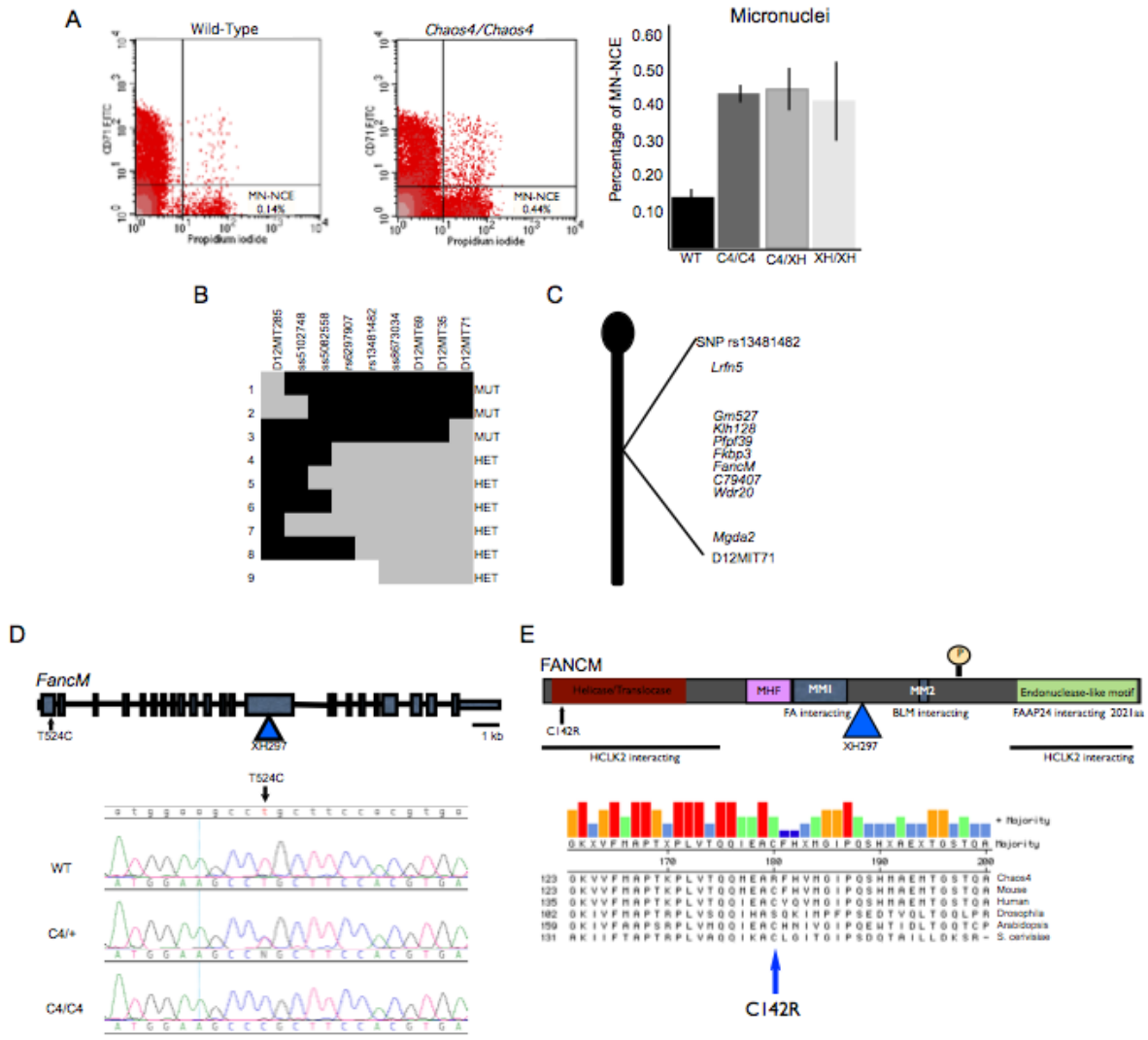

Figure 3-1 Chaos4 is an allele of *Fancm.*
A. Representative flow cytometric plots of Wild-Type (left) and *Fancm*$^{C4/C4}$ (right). Micronucleated erythrocytes are the population positive for propidium iodide (lower right quadrant). On the far right are total quantification of MN in wild-type (WT), *Fancm*$^{C4/C4}$ (C4/C4), *Fancm*$^{C4/XH}$ (C4/XH), and *Fancm*$^{XH/XH}$ (XH/XH) mutant alleles. **B**. The critical recombinant animals with black=B6, grey=B6/C3H, white=C3H. **C.** Genes on mouse chromosome 12 within the critical recombinant region. **D.** *Fancm* showing location of T524C point mutation in first exon (arrow), insertion of the XH297Genetrap in the 14th exon (blue triangle). Below is the Sanger sequence trace of wild-type (WT), *Fancm*$^{C4/+}$ (C4/+), and *Fancm*$^{C4/C4}$ (C4/C4). **E.** FANCM showing location of the C142R a.a. change in the helicase/translocase domain (arrow) and insertion of the gene-trap (blue triangle). Below shows the conservation of the amino acid.

the phenotype, recombination mapping was pursued and 956 meioses were scored. Nine critical recombinants narrowed the region to 9 Mb between RS13481482 and D12MIT71 (Figure 3-1B) containing 9 RefSeq annotated genes (Figure 3-1C). *Fancm* was a strong candidate, as it is part of the Fanconi Anemia complementation group known to be important in DNA crosslink repair. DNA Sanger sequencing revealed a T524C transition in *Chaos4* (Figure 3-1D). This point mutation leads to a non-synonomous cysteine to an arginine (C142A) change in a highly conserved amino acid in the helicase domain (Figure 3-1E).

To test if *Chaos4* is indeed an allele of *Fancm,* we created mice carrying a gene-trap in *Fancm* from BayGenomics. The XH297 ($Fancm^{XH}$) gene-trap insertion is located distal to the helicase domain but upstream of the endonuclease domain (Figure 3-1D,E). Homozygous gene-trap animals have elevated MN (Figure 3-1A). Compound heterozygotes ($Fancm^{C4/HX}$) they did not complement by analysis of micronuclei levels (Figure 3-1A). Therefore, *Chaos4* ($Fancm^{C4}$) is an allele of *Fancm.*

Sex skewing and subviability associated with the $Fancm^{XH}$ mice.

The published knock-out allele of *Fancm* is associated with a decreased number of females born from heterozygous intercrosses (16). While the $Fancm^{C4/C4}$ and $Fancm^{C4/XH}$ mice had expected numbers of animals born (χ^2 p-value of 0.48 and 0.36 respectively), the $Fancm^{XH/XH}$ mice have a significant decreased number of female pups and an elevated number of male pups (χ^2 p-value of 0.047). More

Table 3-1 *Viability of* mice with indicated *Fancm alleles*

	Male		Female		Combined		
	Obs	Exp	Obs	Exp	Obs	Exp	N10
C4/C4	40	44	52	44	92	88	
C4/+	81	88	84	88	165	175	
WT	49	44	44	44	93	88	
χ^2 p-value	0.48		0.43		0.56		

	Male		Female		Combined		
	Obs	Exp	Obs	Exp	Obs	Exp	<N5
XH/XH	**12**	8	**5**	8	17	16	
XH/+	10	16	15	16	25	33	
WT	12	8	11	8	**23**	16	
χ^2 p-value	0.05		0.31		0.10		

	Male		Female		Combined		
	Obs	Exp	Obs	Exp	Obs	Exp	<N5
C4/XH	2	3	4	3	6	6	
C4/+	1	3	2	3	3	6	
XH/+	5	3	3	3	8	6	
WT	4	3	4	3	8	6	
χ^2 p-value	0.36		0.83		0.44		

Obs=Observed, Exp=Expected, C4=*FancM*^{Chaos4}, XH=*FancM*^{XH297}, N= number of generations into the C3Heb/FejA strain background. χ^2 p-value is significant below 0.05.

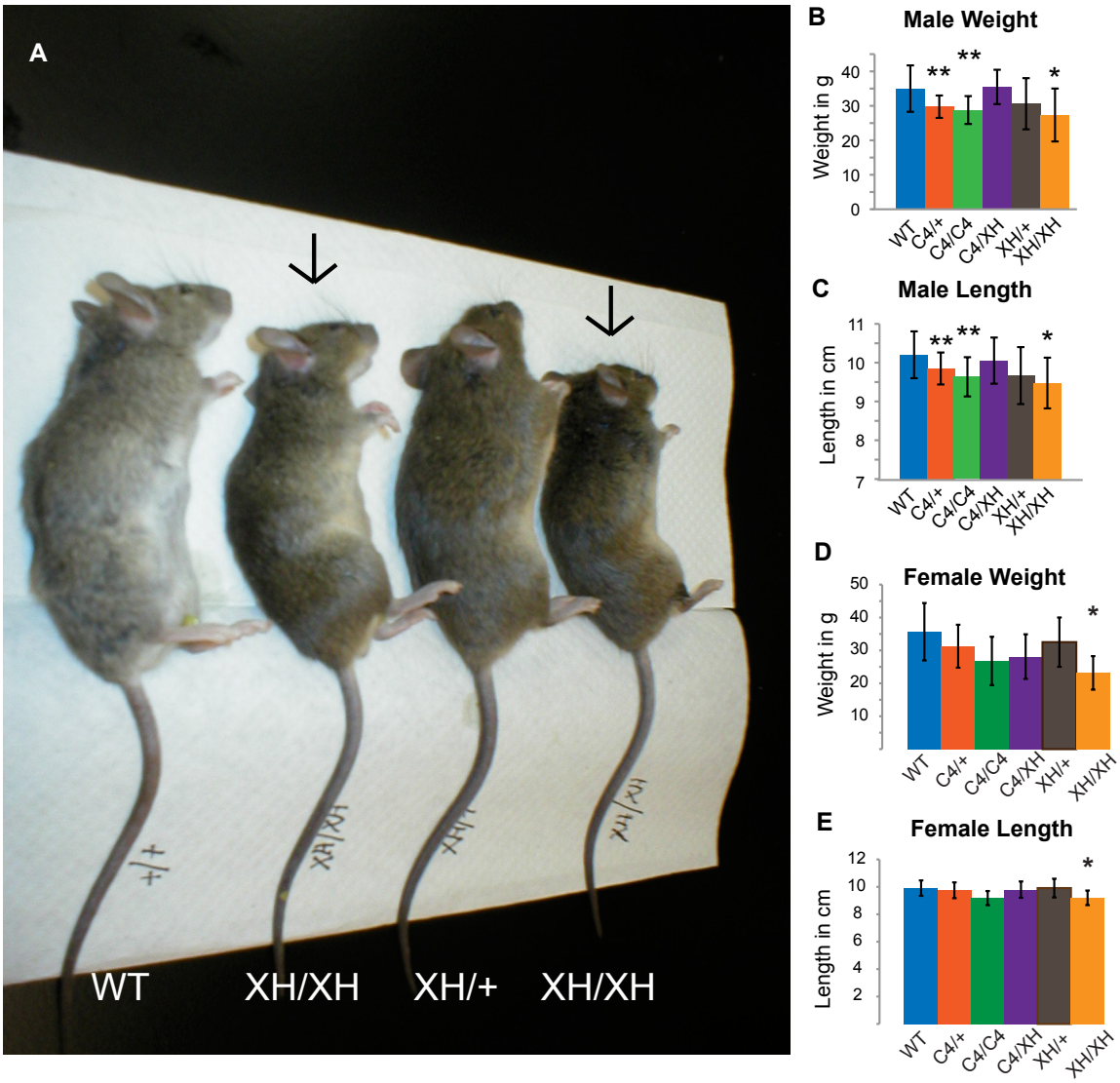

Figure 3-2. Decreased body size in *Fancm*$^{XH/XH}$ mice.
A. Male littermates of a *Fancm*$^{XH/+}$ intercross at 24 weeks. Arrows point to *Fancm*$^{XH/XH}$ animals that were noticeably smaller. **B-E** Weights and body lengths separated by male (**B,C)** and female **(D,E)** n=>10, combined weights and lengths after 12wks of age is shown**.** * is significant ($p<0.05$ TTEST) throughout the animals lifespan, and decrease in body size ** is significant only after 1 yr of age. Wild-type (WT), *Fancm*$^{C4/C4}$ (C4/C4), *Fancm*$^{C4/XH}$ (C4/XH), and *Fancm*$^{XH/XH}$ (XH/XH) mutants.

Fancm$^{XH/XH}$ animals need to be evaluated to see when in gestation the loss/gain is occurring (Table 3-1).

Body size differences are more prominent in the *Fancm*$^{XH/XH}$ mice than the other *Fancm* mutants.

While there were no overt or visible phenotypes seen in these mice, it was observed that the *Fancm*$^{XH/XH}$ males animals had a lower body weight and shorter body length as early as 12 wks. These differences compared to WT animals persisted throughout their lifetimes (TTEST p=0.006 and 0.002 respectively) (Figure 3-2A-C). Similar to the males, the *Fancm*$^{XH/XH}$ females had a significant decrease in body weight and length (p=0.03 TTEST and p=0.02 TTEST respectively) (Figure 3-2D,E). The *Fancm*$^{C4/+}$ and *Fancm*$^{C4/C4}$ males did have a decrease in body weight and length once they were >1yr of age (TTEST *Fancm*$^{C4/+}$ p=0.0001 and 0.002, *Fancm*$^{C4/C4}$ p<<0.0001 for both) (Figure 3-2B,C), however compound heterozygotes had neither of these defects (TTEST p=0.89 and 0.39 respectively) (Figure 3-2B,C). The *Fancm*$^{C4/C4}$ females also had a suggestive decrease in body length (P=0.08 TTEST) (Figure 3-2D,E). There was no disparity in body weight or body length published in the *Fancm*^{KO} allele(16).

Germ cell depletion occurs in the *Fancm*$^{C4/C4}$ mice, but not the *Fancm*$^{C4/XH}$ or *Fancm*$^{XH/XH}$ mutant mice.

Since all of the Fanconi Anemia mouse models as well as the *Fancm*^{KO} have germ cell depletion, these mice were evaluated for germ cell loss. The only

Figure 3-3 Decrease in testis size in *Fancm*$^{C4/C4}$
A-D Testes section (10X) of 12 wk old males of indicated genotypes. **C-D** examples of phenotypes seen in all males of mutant genotype. **E-G** Testes section of males >1yr of age showing meiotic arrest and testicular degeneration in *Fancm*$^{C4/C4}$ males. ^ Giant multinucleated cells, * Meiotic arrested tubule. # Terminally differentiated spermatogenesis. **H-I** Quantification of testes weight and sperm count, * significant difference $p<0.05$ by TTEST was seen in the *Fancm*$^{C4/C4}$ males. Wild-type (WT), *Fancm*$^{C4/C4}$ (C4/C4), *Fancm*$^{C4/XH}$ (C4/XH), and *Fancm*$^{XH/XH}$ (XH/XH) mutant alleles. n>10.

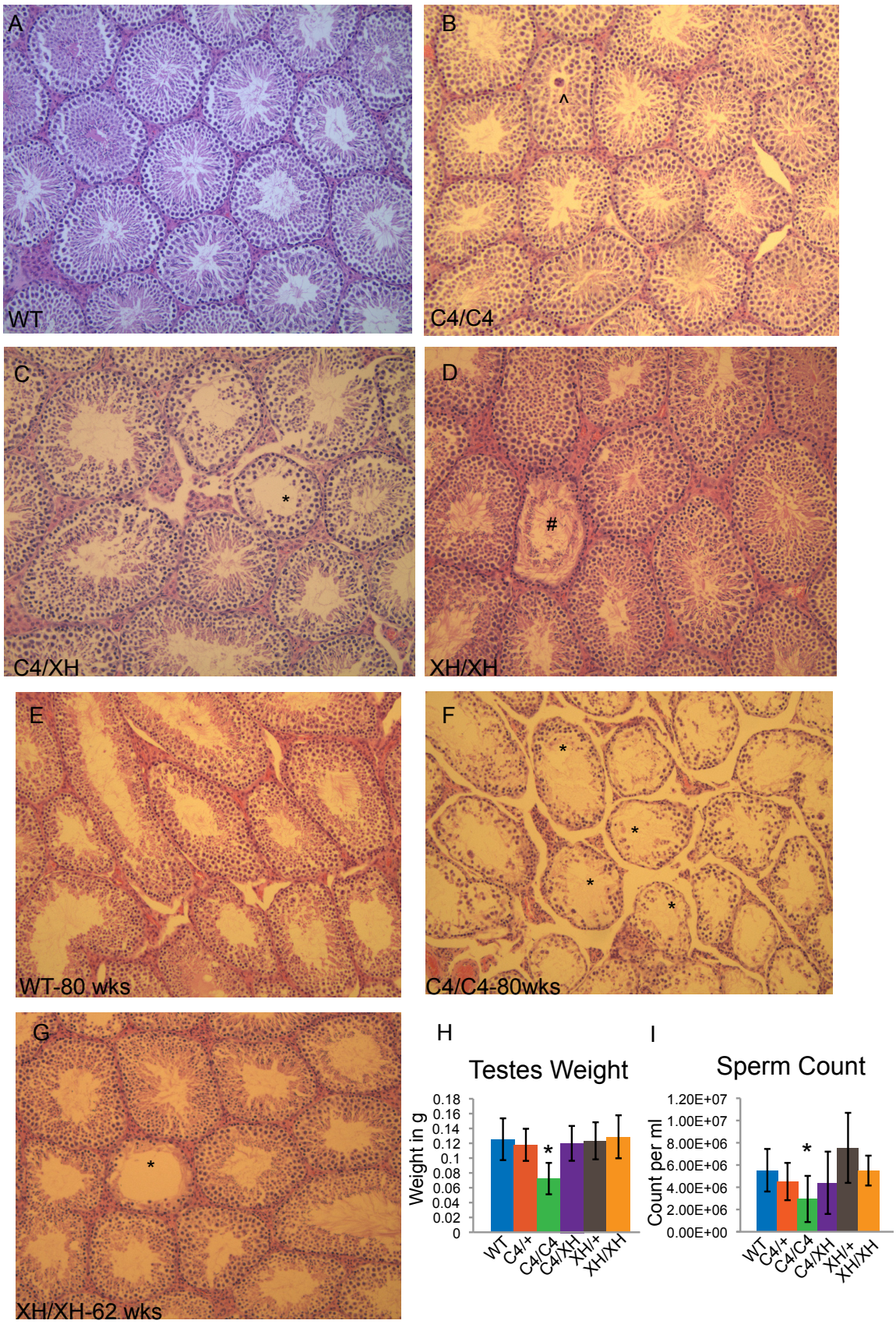
A
WT
B
^
C4/C4
C
*
C4/XH
D
#
XH/XH
E
WT-80 wks
F
*
*
*
*
C4/C4-80wks
G
*
XH/XH-62 wks
H
Testes Weight
Weight in g
0.18
0.16
0.14
0.12
0.1
0.08
0.06
0.04
0.02
0
*
WT
C4/+
C4/C4
C4/XH
XH/+
XH/XH
I
Sperm Count
Count per ml
1.20E+07
1.00E+07
8.00E+06
6.00E+06
4.00E+06
2.00E+06
0.00E+00
*
WT
C4/+
C4/C4
C4/XH
XH/+
XH/XH

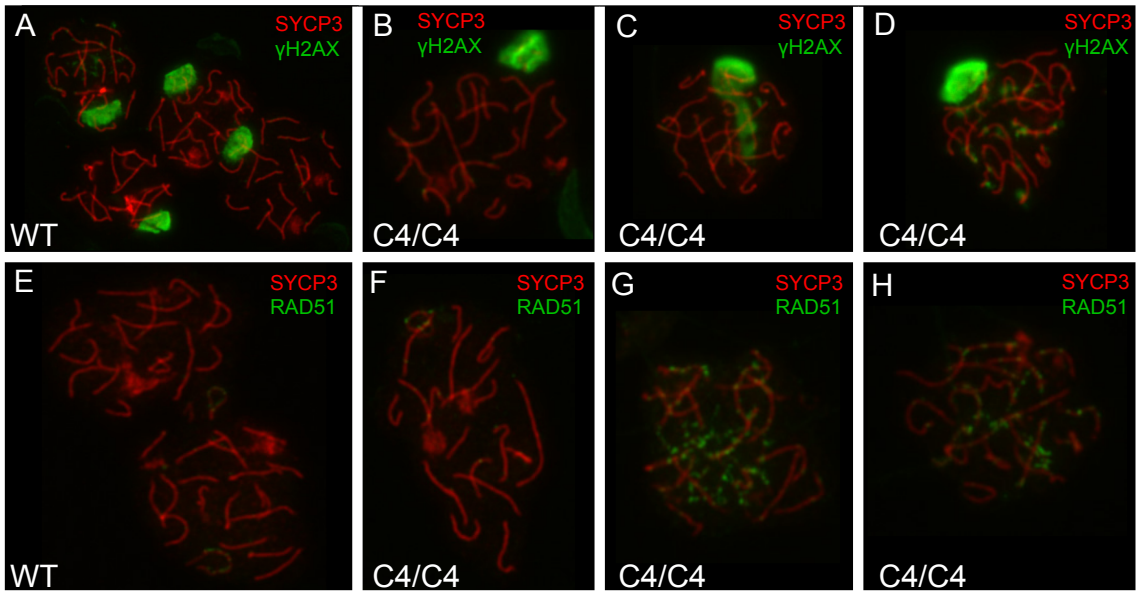

Figure 3-4 Meiotic spreads showing unrepaired DNA damage in *Fancm*$^{C4/C4}$ spermatocyte nuclei.
Surface meiotic spreads of spermatocyte nuclei were immunostained with SYCP3 for the central element in red (**A-H**) and γ-H2AX (**A-D**) and RAD51 in green (**E-H**). **A,E** WT examples of normal distribution of γ-H2AX and RAD51 in meiotic spreads at pachynema/diplonema at the XY sex body. **B, F** shows normal localization in *Fancm*$^{C4/C4}$ mutants, however in a subset of spreads there is abnormal localization showing either unpaired chromosomes (**C)**, or unrepaired/persistent DNA breaks **(D,G,H).**

genotype that was associated with a significant decrease in testes weight and sperm count was *Fancm*$^{C4/C4}$ ($p<<0.0001$ and $p=0.01$ respectively by TTEST) (Figure 3-3H-I). Histology sections revealed several abnormalities within testes of young, not inbred, *Fancm*$^{C4/C4}$ males, namely germ cell depletion (GCD) (not shown). However as they became more inbred into the C3Heb/FejA genetic background, this phenotype was lost. In testis cross-sections of inbred *Fancm*$^{C4/C4}$ mice, there were giant multinucleated cells (GMC), tubules that appears to be missing a wave of spermatogenesis, and tubules that appear to be stalled in meiosis with no postmeiotic cell types (Figure 3-3B). While animals bearing the *Fancm*$^{XH/XH}$ and *Fancm*$^{C4/XH}$ genotypes had most of these phenotypes except for the GCD that was observed in less inbred mice (Figure 3-3C,D). Interestingly, as the *Fancm*$^{C4/C4}$ males aged, the majority of the tubules appears to be arrested in meiosis and undergoing testicular degeneration. However, in the testes of *Fancm*$^{XH/XH}$ males normal spermatogenesis remains intact (Figure 3-3E-G).

The potential meiotic arrest seen in a subset of tubules was further explored in 10wk old *Fancm*$^{C4/C4}$ males by analyzing surface-spread preparations of meiotic chromosomes. Staining with γH2AX (indicator of DSBs and unpaired chromosomes) and SYCP3 (a marker of axial elements of meiotic chromosomes) revealed persistent γH2AX staining with mispaired/unpaired chromosomes in 42% of the spreads analyzed (Figure 3-4A-D). This correlates with 27% of nuclei having persistent RAD51 (localizes to DSBs) foci (Figure 3-4E-H), which

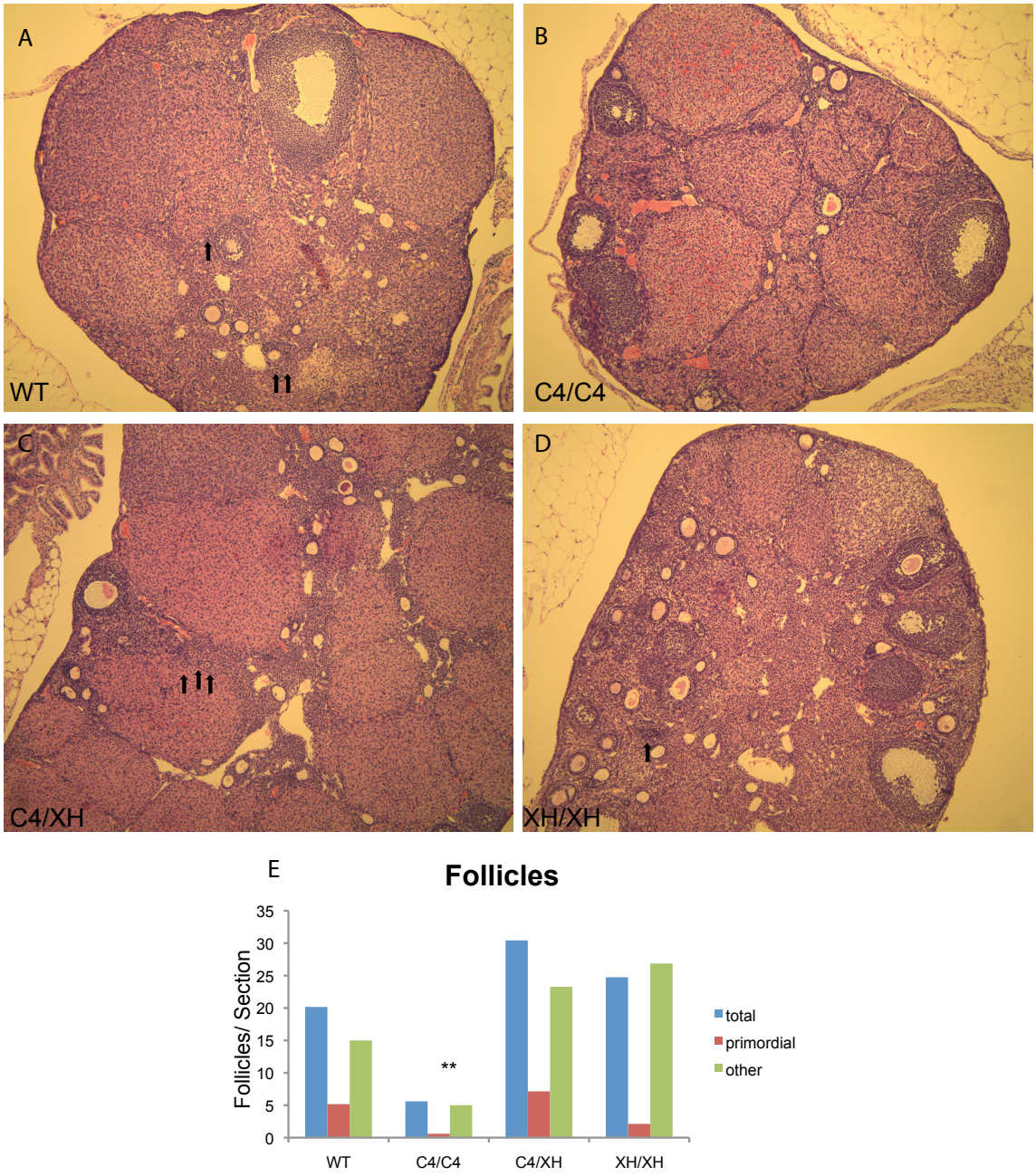

Figure 3-5 Decreased Follicles in *Fancm*$^{C4/C4}$ ovaries.
A-D Representative images of 12-24 wk old ovary at 10x of given genotype (cross-sections may vary). Wild-type (WT), *Fancm*$^{C4/C4}$ (C4/C4), *Fancm*$^{C4/XH}$ (C4/XH), and *Fancm*$^{XH/XH}$ (XH/XH) genotypes**.** ARROWS point to primordial or primary follicle. N. Quantification of follicles per section. n>10 for each genotype.

indicates unrepaired DNA damage, however more animals do need to be evaluated due to a low N-number of 2 animals per genotype.*Fancm*$^{C4/C4}$ ovaries exhibit a significant age-dependent decrease in number of follicles compared to wild-type and the 2 other *Fancm* mutant mouse alleles (TTEST *Fancm*$^{C4/C4}$ p=0.002, *Fancm*$^{C4/XH}$ p=0.29, *Fancm*$^{XH/XH}$ p=0.12) (Figure 3-5.)

Germ cell loss in *Fancm*$^{C4/C4}$ is p53 dependent and *Fancm*^{C4C4} is synthetically lethal with *Atm*$^{-/-}$

With the decreased testes weight and some GCD tubules noted in *Fancm*$^{C4/C4}$ males, we want to see if there is a decrease in the germ cell population at birth before reactivation of proliferation of the gonocytes. In the *Fancm*$^{C4/C4}$ males there was a significant decrease in the number of germ cells per tubule as quantified with MVH (a marker of germ cells) staining (p=0.002), suggesting the loss of germ cells occurred before birth (Figure 3-6A-C). Since germ cell loss could be due to apoptosis during formation, migration, and population of the germ cells in the gonad we conducted genetic crosses with DNA checkpoint and repair mutants. The first double mutant is with *Trp53*, a transcription factor when activated ultimately induces apoptosis when DNA repair is incomplete. *Fancm*$^{C4/C4}$; *Trp53*$^{-/-}$ double mutants rescues the germ cell loss (p=0.005, Figure 3-6F), suggesting that some type of DNA damage is triggering cell death. Consistent with this result, the double mutant with *Cdkn1a,* a downstream target of TRP53 involved in cell cycle arrest, also rescues the germ cell loss (p=0.03, Figure 3-6G).

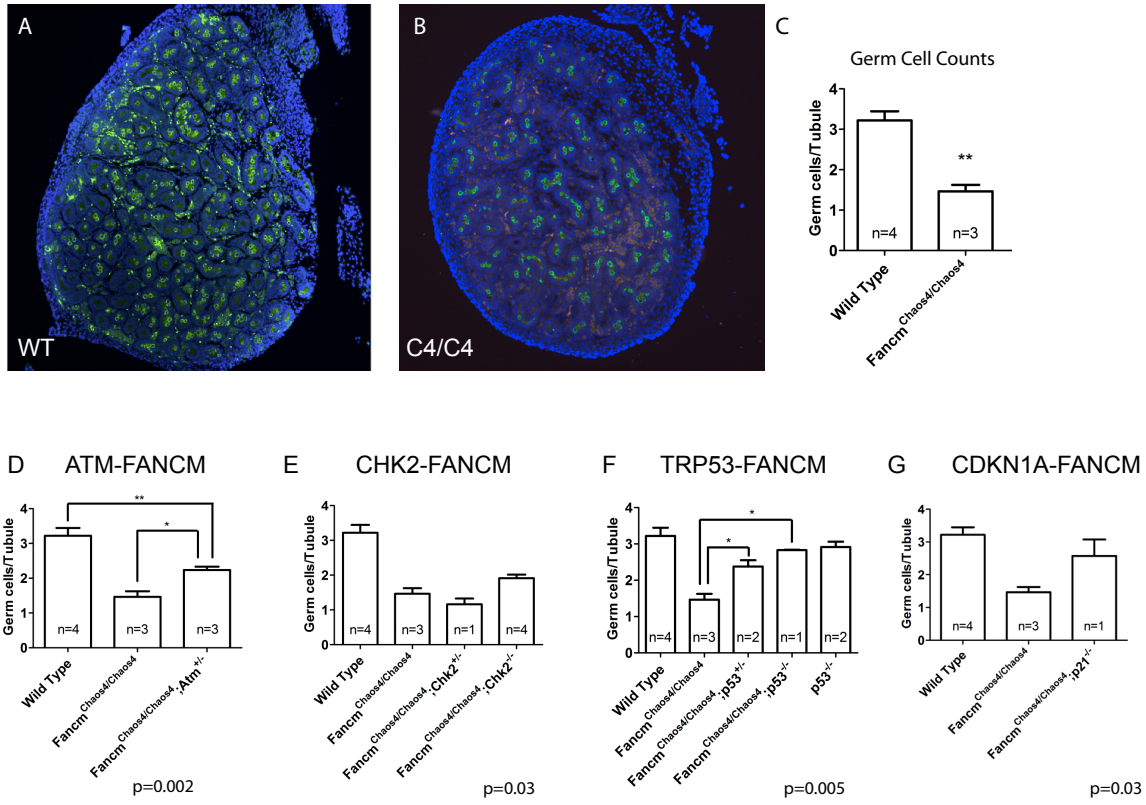

Figure 3-6 Depleted Germ Cells at 1dpp in *Fancm*$^{C4/C4}$, with this loss being dependant on S-phase checkpoint signaling.

A-B 1 day post-partum testes stained with DAPI-blue and VASA (MVH)-green (germ cells) of given genotype. **C** Quantification of germ cells at 1dpp in *Fancm*$^{C4/C4}$ males. **D-G** Genetic crosses of *Fancm*$^{C4/C4}$ with members of the DNA checkpoint proteins germ cell quantifications at 1dpp. **-significant difference. Genetic background of C3Heb/FejA of at least 5 generations.

Table 3-2 *Fancm*$^{C4/C4}$ is lethal with *Atm*$^{-/-}$

	Fancm$^{C4/C4}$:*Atm*$^{+/+}$	*Fancm*$^{C4/C4}$:*Atm*$^{+/-}$	*Fancm*$^{C4/C4}$:*Atm*$^{-/-}$
Observed	21	28	0
Expected	12.25	24.5	12.25

χ^2 p-value 7.49E-05

To find out what type of DNA damage is occurring that leads to apoptosis, we created double mutants that are involved in the double-strand break (DSB) repair pathway. First cross involves *Chk2,* which phosphorylates a number of proteins for activation in the DSB response including TRP53. In these double mutants the germ cell loss was rescued (p=0.03, Figure 3-6E). Upstream of CHK2 is *Atm,* which is activated by DSBs and phosphorylates CHK2 for activation. Mice doubly mutant for *Fancm*$^{C4/C4}$ and *Atm*$^{-/-}$ are synthetic lethal (Table 3-2), however *Fancm*$^{C4/C4}$;*Atm*$^{+/-}$ mice exhibit a partial rescue of germ cell loss (p=0.002 Figure 3-6D). This suggests that some, if not all, of the germ cell loss that is occurring in *Fancm*$^{C4/C4}$ mice is due to DSBs that are unrepaired leading to apoptosis. The synthetic lethality seen with *Atm*$^{-/-}$ is consistent with other mutants in the FA complex (31). This indicates that FANCM functions in a parallel pathway, such as that activated by ATR, which mediates repair of damage that occurs during DNA replication.

Fancm$^{C4/C4}$ and _Fancm_$^{XH/XH}$ primary cell lines exhibit elevated chromosomal abnormalities.

FA cells are known to have elevated DNA breaks and radial chromosomes. This phenotype is exhibited in *Fancm*$^{C4/C4}$ and *Fancm*$^{XH/XH}$ primary mouse embryonic fibroblasts (MEFs) (Figure 3-7B,C,E). The *Fancm*$^{KO/KO}$ cells also have an increase in sister chromatid exchange (SCE), which is the number of exchanges between sister chromatids in order for DNA repair to occur (16). In primary MEFs we observed an elevation in SCE in the

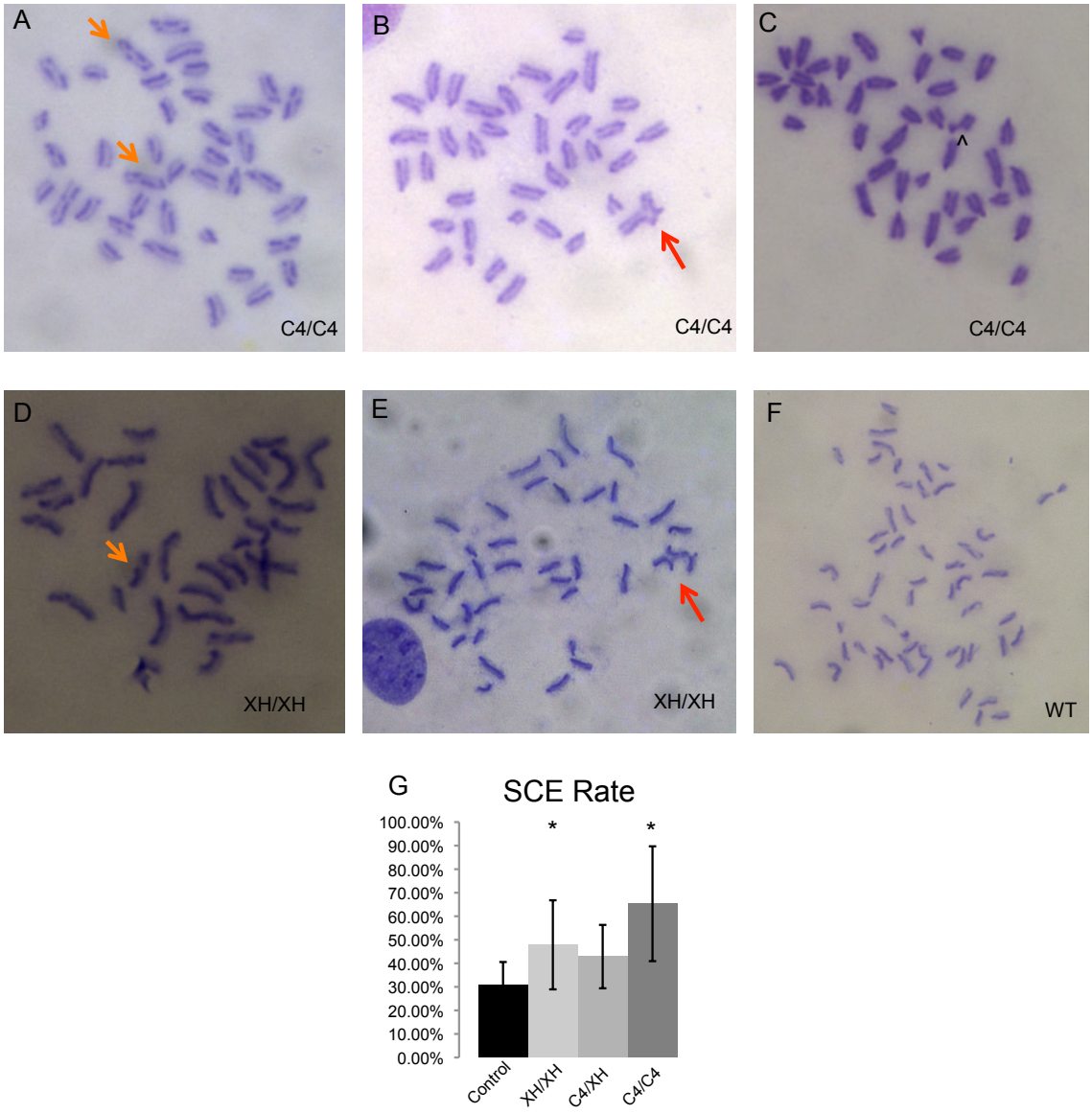

Figure 3-7 Elevated chromosomal instability and sister chromatid exchange. **A-E** Metaphase spreads of primary MEFs of given genotype. SCE assay performed on **A,B,D,E,F** with differential staining of the sister chromatids. When there is increased sister chromatid exchange occurring there is more of a step-ladder effect on the chromosome arms of alternating light/dark staining (orange arrows). **G** The differences are significant in *Fancm*$^{C4/C4}$ and *Fancm*$^{XH/XH}$ MEFS by TTEST $p<0.05$. **B,E** shows examples of radial formations seen in the *Fancm* mutant cells (red arrows). **C** The occasional break that is seen in the *Fancm* mutant cells (arrowhead). Wild-type (WT), *Fancm*$^{C4/C4}$ (C4/C4), *Fancm*$^{C4/XH}$ (C4/XH), and *Fancm*$^{XH/XH}$ (XH/XH).

FancM$^{C4/C4}$ (TTEST p<0.001), and in the *Fancm*$^{XH/XH}$ MEFs (TTEST p=0.01). However, an insufficient number of *Fancm*$^{C4/XH}$ MEFs were analyzed to make a conclusion regarding possible elevation in SCE (Figure 3-7A,D,F).

Fancm$^{C4/C4}$ deficient females are tumor susceptible

Since the mutant animals have genomic instability in the form of micronuclei in peripheral blood, primary MEFs have elevated chromosomal abberations, and the *Fancm*$^{KO/KO}$ animals had an elevated tumor rate (16), our mutant mice were aged up to 1.5yrs to assess possible tumor susceptibility. *Fancm*$^{C4/C4}$ and *Fancm*$^{C4/+}$females had an elevated susceptibility to tumors (Table 3-3 and 3-4). Meanwhile in males only one genotype had an increase in tumor incidence, the 12-48wk old *Fancm*$^{C4/XH}$ males, which had one case of lymphoma (28wks), a lung adenoma (45wks), and a hepatoma(45wks) (Tables 3-3 and 3-4). The earliest tumor onset in wild-type occurred at 52wks (Tables 3-3 and 3-4).

Diminished cell growth, premature senescence, with no drug hypersensitivity observed in mutant cells.

Upon analysis of primary MEFs, cell growth of all mutant lines were diminished from wild-type (Figure 3-8A). We analyzed population doubling and in all mutant MEFs premature senescence occurred (Figure 3-8C). The timing of immortalization of these lines occurred at different passages. *Fancm*$^{C4/C4}$ line

Table 3-3 Tumor Frequency of *Fancm* mutants.

TUMOR Frequency-Females		
WT	0 out of 28 (44-80wks)	0.00%
C4/+	**9 out of 27 (44-80wks)**	**33.33%**
C4/C4	**15 out of 26 (44-80wks)**	**57.69%**
C4/XH	**1 out of 6 (20-54wks)**	**16.67%**
XH/XH	0 out of 5 (28-52wks)	0.00%

TUMOR Frequency-Males		
WT and HETs	19 out of 36 (50-80wks)	55.26%
C4/C4	8 out of 17 (70-80wks)	47.06%
C4/XH	**3 out of 12 (12-48wks)**	**25.00%**
XH/XH	0 out of 8 (12-78wks)	0.00%
WT	4 out of 45 (12-55 wks)	9.00%

Wild-type (WT), *Fancm*$^{C4/C4}$ (C4/C4), *Fancm*$^{C4/XH}$ (C4/XH), and *Fancm*$^{XH/XH}$ (XH/XH) mutant alleles

Table 3-4 Histopathology of *Fancm* mutant mice

Animal	Age (wks)	Genotype		Histopathology	Tumor
17251	54	WT	Female	Ovary - follicular cyst; spleen - red pulp mildly expanded by extramedullary heperplasia (EMH) and abundant hemosiderin laden macrophages, white pulp also mildly hyperplastic; uterus - mild cystic endometrial hyperplasia and dilation of lumen	
13116	45	WT	Female	Follicular cyst	
11125	81	WT	Female	ovary - 2 small follicular cysts	
16096	80	WT	Female	Follicular cyst and hemorrhagic cyst	
2611	106	Chaos4/+	Female	Epithelial Tumor	X
13894	81	chaos4/+	Female	one fluid filled cyst on each ovary	
13896	81	chaos4/+	Female	Follicular cysts	
21225	66	chaos4/+	Female	Ovarian Teratoma	X
21226	66	chaos4/+	Female	uterine edema, adrenal gland tumor?, small spleen, small black tumors on lung	X
404	46	Chaos4/+	Female	uterus - some proteinaceous fluid and neuts in lumen	
11123	81	Chaos4/+	Female	uterus - unilateral hydro/mucometra; cystic endometrial hyperplasia, potential adenomyosis	
13118	45	chaos4/+	Female	ovary - multifocal mineralized follicles unilateral;	
14389	75	Chaos4/+	Female	Liver Tumor	X
14391	75	Chaos4/+	Female	1 fluid cyst on each, fluid filled uterus, but not too enlarged, there ma have been a small mammary tumor.	
14652	83	Chaos4/+	Female	Follicular cyst	
14964	81	Chaos4/+	Female	Hemorrhagic ovarian cyst	X
15364	80	Chaos4/+	Female	ovary - large follicular cyst; uterus - multifocal perivascular lymphoid aggregates; liver - multifocal perivascular lymphoid aggregates; cervical lymph node - paracortex expanded by sheets of lymphocytes, small cell lymphoma	X
15868	50	Chaos4/+	Female	ovary - unilateral follicular cyst; uterus - abundant nondegenerate neutrophils in glands, endometrium, lumen; liver - mild multifocal emh	

16095	80	chaos4/+	Female	liver - hepatocellular carcinoma and hematoma;	X
#154	102	Chaos4/+	Female	adrenal - mild subcapsular cell hyperplasia;liver - mild multifocal EMH and necrotizing hepatitis; mammary gland - mild lymphoid infiltrates; spleen - moderate hemosiderin in white and red pulp	
11108	95	Chaos4/+	Female	Ovary - tubulostroma hyperplasia; liver - large biliary cyst with peripheral inflammatory infiltrates	
11110	95	Chaos4/+	Female	Liver, spleen - histiocytic sarcoma; kidney - mineral in distal collecting ducts, mild multifocal tubular ectasia and proteinosis; adrenal gland - locally extensive moderate subscapsular cell hyperplasia; ovary and uterus - some neoplastic cells in peripheral adipose;brain - multifocal mineralized blood vessels in brainstem and thalamus	X
11118	81	Chaos4/+	Female	ovary - paraovarian cyst; mineralized follicles; mammary gland adenocarcinoma	X
11119	81	Chaos4/+	Female	ovary - follicular cyst;	
17247	54	XH297/+	Female	Uterus - mild hydrometra	
2708	58	Chaos4/Chaos4	Female	Basisquamous carcinoma	X
17817	24	chaos4/chaos4	Female	Uterine Tumor	X
21223	66	chaos4/chaos4	Female	cystic ovary, edema, start of a liver tumor, cyst on kidney, brown hair stripes, intestinal tumors, small lump on tail	X
402	46	Chaos4/Chaos4	Female	endometrial hyperplasia-adenoma based on size(UT), Ov-cavernous sinuses that may have lead to the corpora hemorrhagia	X
3368	85	Chaos4/Chaos4	female	Mammary or epithelial tumor	X
11124	81	Chaos4/Chaos4	Female	ovary - multiple cysts compressing and distorting ovarian architecture, Liver and Lung adenoma	X
13117	45	chaos4/chaos4	Female	Skin Tumor, hemorrhagic ovarian cyst	X
14390	75	Chaos4/Chaos4	female	Uterine Tumor, skin tumor, follicular cysts	X
14650	83	Chaos4/Chaos4	Female	Mammary Tumor	X
14965	81	Chaos4/Chaos4	Female	Mammary Tumor, follicular cysts	X
14967	81	Chaos4/Chaos4	Female	Liver Tumor	X
16097	80	chaos4/chaos4	Female	Uterine Tumor, follicular cysts	X
19169	24	chaos4/chaos4	Female	Follicular cyst	
#155	102	Chaos4/Chaos4	Female	Brain and epithelial tumors	X
11113	99	Chaos4/Chaos4	Female	Multiple small liver tumors, mammary tumor	X
11116	81	Chaos4/Chaos4	Female	caverous hemoraghioma cysts, and paraovarium cyst in second ovary. Tumor-secratory mammary adenocarcinoma	X
11117	81	Chaos4/Chaos4	Female	tubularstromal adenoma/carcinoma low grade, bloody cystic oavary- another potentian tubular stromal carcinoma, UT-polypoid adenoma, endometric hypersplasia, Lung- 2 early adenomas	X
17248	54	Chaos4/XH297	Female	Spleen - mild lymphoid hyperplasia; ovary - large (9 mm) follicular cyst with mineralization	
20397	31	Chaos4/XH297	Female	Spleen - mild lymphoid hyperplasia	
20692	26	Chaos4/XH297	Female	Uterus - some hemosiderin laden macrophages in wall; spleen - mild lymphoid hyperplasia, many hemosiderin laden macrophages in white pul	
20761	21	Chaos4/XH297	Female	Spleen - lymphoid hyperplasia, mild increase in EMH	
21003	21	Chaos4/XH297	female	Bone tumor on Jaw 7X11mm	X
16802	52	WT	Male	Liver Adenoma	X
17877	55	WT	Male	Islet cell tumor	X
13115	85	WT	Male	Liver Tumor	X
13113	85	WT	Male	Liver Tumor	X
13889	72	chaos4/+	Male	Liver Tumor	X

14199	80	chaos4/+	Male	Liver Tumors	X
11307	89	Chaos4/+	Male	liver - focal adenoma	X
11311	89	chaos4/+	Male	preputial gland - keratin filled cyst, focal suppurative and granulomatous inflammation; liver - multifocal areas of mineralization surrounded by fibrous connective tissue	
14388	69	Chaos4/+	Male	Liver Tumors	X
14648	83	Chaos4/+	Male	liver - hepatocellular carcinoma and hematoma	X
14960	81	Chaos4/+	Male	liver - hepatocellular carcinoma	X
14646	83	chaos4/+	Male	liver - hepatocellular carcinoma	X
14200	80	chaos4/chaos4	Male	Lung Tumor	X
11310	89	chaos4/chaos4	Male	liver - hepatocellular carcinoma;	X
13984	80	chaos4/chaos4	Male	kidney - mild multifocal tubular mineralization; liver - multiple adenomas	X
13985	80	chaos4/chaos4	Male	lung - multifocal peribronchiolar and perivascular lymphoid aggregates	
14647	83	Chaos4/Chaos4	Male	liver - hepatocellular carcinoma	X
15359	80	Chaos4/Chaos4	Male	testis - mineralized and sclerotic	
16092	80	chaos4/chaos4	Male	haired skin - focal pyogranulomatous inflammation and sebaceous gland hyperplasia (is this near the ear?; lymph nodes, moderately reactive; liver - adenoma and focus of cellular alteration	X
16094	73	Chaos4/Chaos4	Male	Testis - rare multinucleate cells, <10% of tubules lined by single layer vacuolated Sertoli cells; Spleen - marked myeloid hyperplasia and splenomegaly; haired skin - infundibular keratinizing acanthoma; locally extensive hepatic necrosis; peritonitis and pancreatitis;	
11104	106	Chaos4/Chaos4	Male	Liver - hepatocellular carcinoma; testis - focal hemangioma with fibrin thrombin, mild degeneration	X
11105	106	Chaos4/Chaos4	Male	Testis - severe degeneration, most tubules lined by single layer of vacuolated sertoli cells, focal cavernous hemangioma	
20345	34	Chaos4/XH297	Male	expanded T cell areas in spleen, lymph nodes, thymus	
20346	34	Chaos4/XH297	Male	spleen - mild lymphoid hyperplasia	
20389	29	Chaos4/XH297	Male	Lymph nodes, thymus - lymphoma	X
20393	31	Chaos4/XH297	Male	Subcutis - follicular cyst; lymphoid hyperplasia in spleen	
20689	30	Chaos4/XH297	Male	Spleen - red pulp mildy expanded by extramedullary hyperplasia(EMH)	
20690	26	Chaos4/XH297	Male	liver - multifocal telangiectasia; lymph node - mild expansion of paracortex	
20691	26	Chaos4/XH297	Male	spleen - mild expansion of red pulp (EMH) and white pulp (lymphoid hyperplasia)	
20998	45	Chaos4/XH297	Male	Lung - adenoma; lymph nodes - many hemosiderin laden macrophages in sinuses	X
20999	45	Chaos4/XH297	Male	Liver - adenoma	X
21001	48	Chaos4/XH297	Male	lymph nodes - increased hemosiderin laden macrophages in one node	
20329	33	XH297/XH297	Male	Liver - centrilobular hepatocytes large and vacuolated, multiple foci of necrotizing hepatitis; spleen - lymphoid hyperplasia and increased EMH	

went through crisis and overcame senescence by passage 6. The *FancM*$^{C4/XH}$ crisis occurred between passage 8 and 9, and the *Fancm*$^{XH/XH}$ crisis was after passage 10 along with WT lines (Figure 3-8C). All lines eventually did go on to become immortalized (not shown). With decreased cell growth and premature senescense we went on to observe the cell cycle through FACS analysis. In both the *Fancm*$^{XH/XH}$ and *Fancm*$^{C4/XH}$ cells there was a G2/M delay/arrest, but this was not observed in the *Fancm*$^{C4/C4}$ cells (Figure 3-8B). This difference in immortalization pattern may show the different types of genomic instability that is occurring and how the cell is may be able compensate.

Since a characteristic of Fanconi anemia cells is sensitivity to crosslinking agents (MMC) and FANCM loss also leads to sensitivities to aphidicolin (APH) and camptothecin (CPT) (16), we tested whether our mutant alleles are also susceptible to these agents, which would be expected if relevant biochemical functions of the protein are defective. In cells treated with MMC and APH there was no hypersensitivity, however there appears to be a slight resistance to CPT by *Fancm*$^{XH/XH}$ MEFs in the lower drug concentrations (Figure 3-8D-F). This suggests that these alleles of *Fancm* have retained some function for drug resistance even with the increase in genome instability, and that these alleles are not complete nulls.

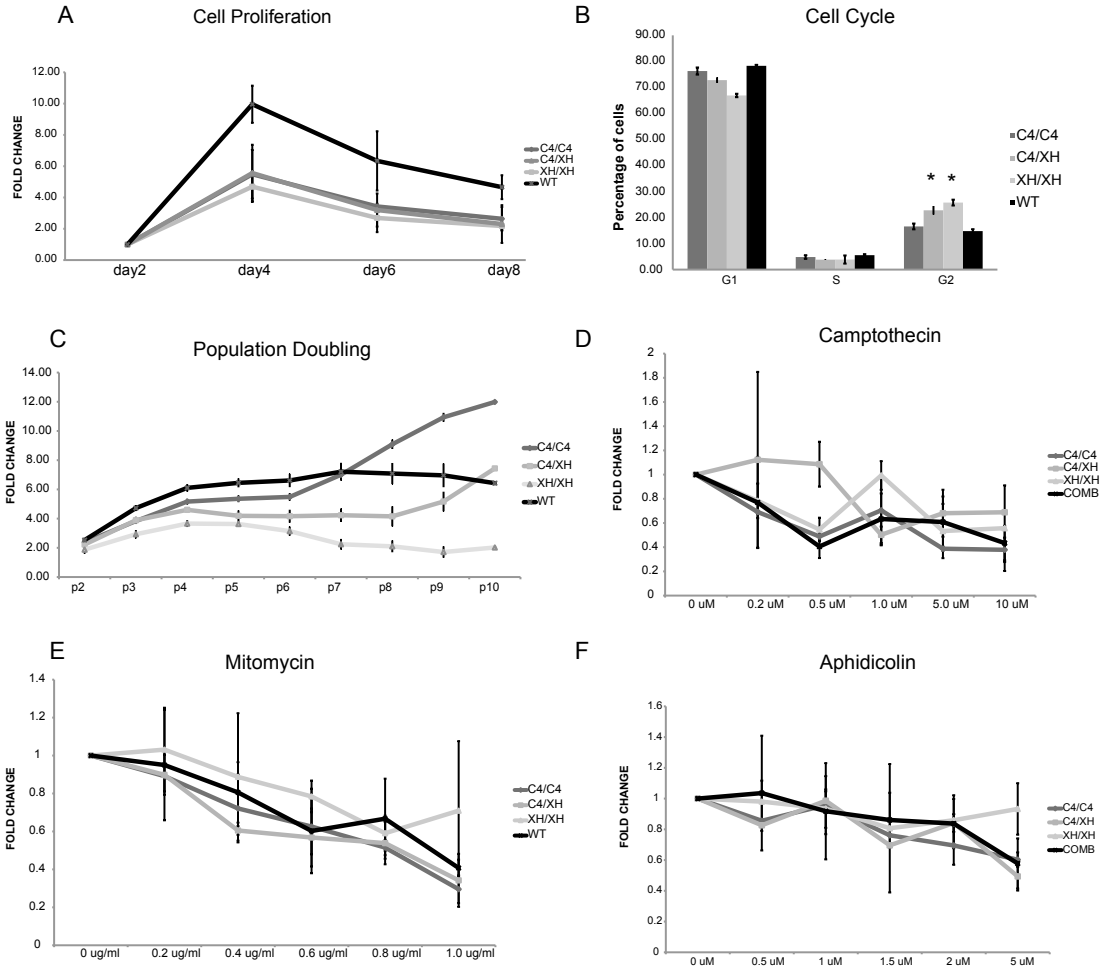

Figure 3-8 Cell cycle defects and premature senescence in *Fancm* mutant cells, but no sensitivity to crosslinking agents or the replication inhibitor Aphidicolin.

A Cell growth curves show a decrease in growth of the mutant cell lines in early passage primary MEFs. **B** Cell cycle of MEFs at day 8 reveal a significant G2/M delay/arrest of *Fancm*$^{XH/XH}$ and *Fancm*$^{C4/XH}$ cell lines. **C** Population doubling in serial passaging reveals premature senescence in mutant cells with early crisis and recovery in *Fancm*$^{C4/C4}$. **D-F** Drug treatments of compounds and indicated concentration on X-axis with remaining cells measured on the Y-axis. Wild-type (WT), *Fancm*$^{C4/C4}$ (C4/C4), *Fancm*$^{C4/XH}$ (C4/XH), and *Fancm*$^{XH/XH}$ (XH/XH) mutant alleles.

3.4 Discussion

In this study I have described two mouse alleles of *Fancm.* These mice have shown similarities and differences to the published knock-out mouse (Table 3-5) (16). The point mutation in the *Fancm*^{C4} allele may affect the translocase activity, the ATPase activity or both. However it may also affect the folding of the protein causing it to have reduced functional activity. Based on the differences of phenotype from the null allele, this protein is hypomorphic and may retain the function of its endonuclease domain as well as most of its binding capabilities. The truncation protein that is presumed to form in the genetrap allele *Fancm*^{XH} may have retained its translocase and ATPase activity. *Fancm*^{XH} may have also retained its ability to bind and anchor the FA proteins and localize to the chromatin.

FANCM has multiple roles in DNA repair processes, from sensing DNA damage to choice and recruitment of repair pathways to facilitating repair. The N-terminal helicase/translocase domain functions in DNA remodeling abilities, such as fork reversal, D-loop dissociation, and Holliday junction resolution. The N-terminal of FANCM also has roles in moving the protein along chromatin to points of DNA damage and stalled forks. The helicase/translocase domain interacts with FA proteins and is partially needed for FANCD2 mono-ubiquitination, however the ATPase activity is not required. This domain is required for resistance to cross-linking agents and UV, but a point mutation that ablates the ATPase activity in DT40 cells but maintains the translocase activity is not sensitive to cross-linking agents (32). This domain is required for suppression of

SCE and is needed for activation of the S-phase checkpoint (33). A subset of these functions may be defective in the *Fancm*$^{C4/C4}$ mutant mouse.

The *Fancm*$^{XH/XH}$ genetrap mouse putatively has a truncated FANCM protein causing a loss of the BLM interacting motif and the endonuclease domain. The endonuclease domain is needed for interaction with FAAP24. Loss of the FANCM C-terminal domain shares some phenotypes with those of cells deficient for FAAP24 (3, 6–8, 27). These include decreased ability to mono-ubiquitinate FANCD2, decreased interaction with FA core complex, and decrease DNA substrate specificity. This domain is partially required for resistance against crosslinking agents, however it is not required for resistance to UV. The C-terminal domain is however required for resistance to CPT (32, 34). This domain is only partially required for suppression of SCEs. In the S-phase checkpoint the C-terminal domain is required, possibly through its ability to stabilize RPA and through its interaction with HCLK (6-7).

The decreased body size of *Fancm*$^{XH/XH}$ mice may be caused by the DNA damage-induced apoptosis at the whole animal level. Decreased body size is seen in other FA mouse mutants and in *Atm* mutants, but was not reported not in the *Fancm*^{KO} (16). The *Fancm*$^{XH/XH}$ mutation is presumably a truncating mutation that leaves some function of FANCM N-terminal domains active, this leaves the possibility that the s-phase checkpoint is intact and allowing removal of damage cells, leading to a smaller body size.

Table 3-5 List of observed phenotypes in *Fancm* mutant mice

Phenotype	*FancM*$^{KO/KO}$	*FancM*$^{C4/C4}$	*FancM*$^{C4/XH}$	*FancM*$^{XH/XH}$
Female Loss	YES	**NO**	**NO**	YES
Decreased Body Size	??	NO	NO	**YES**
Germ Cell Loss	YES	YES	**NO?**	**NO?**
Tumors	YES	YES	MAYBE	**NO?**
Chromosomal Abnormalities	YES	YES	??	YES
Increased SCE	YES	YES	**NO?**	**MAYBE**
MMC sensitivity	YES	**NO?**	**NO?**	**NO?**
Cisplatin Sensitivity	YES	??	??	??
CPT Sensitivity	??	NO?	NO?	**Resistance**?
APH Sensitivity	??	NO	NO	NO
G2/M Arrest	YES?	**NO**	YES	YES
Early Senescence	??	YES	YES	YES
FANCD2 mono-ub	Decreased	??	??	??

Fancm$^{C4/C4}$ mice exhibit germ cell depletion, as do *Fancm*^{KO} mice and other mouse models of Fanconi Anemia. This is very interesting since this allele is the one that has a mutation in the helicase domain that may interfere with one or all three activities associated with it; the translocase/helicase DNA remodeling function, the ATPase activity, or the interaction with HCLK, which is involved in stabilizing ATR and signals the s-phase checkpoint. Without these, the ability to repair damage, this could lead to a loss of germ cells, typically through a p53 dependant pathway. The loss of germ cells in the *Fancm*$^{C4/C4}$ mice appears to be driven by this pathway, based on double mutant studies that showed a rescue of germ cells loss when in combination with *Chk2*$^{-/-}$, *Trp53*$^{-/-}$, or *Cdkn1a*$^{-/-}$. If signaling through the ATR pathway is compromised, such as the case may be in our mutants, than DNA lesions that occur during DNA replication may convert into DSBs. This then activates the ATM pathway to trigger eventual repaired. The double mutant of *Fancm*$^{C4/C4}$ and *Atm*$^{-/-}$ is synthetic lethally showing that FANCM and ATM work in parallel pathways in DNA repair (28, 35, 36).

The giant multinucleated cells seen in mice with these alleles of *Fancm* indicates DNA damage leading to incomplete mitosis and/or failed cytokenesis. Giant multinucleated cells are also seen in mice with reduced levels of TRP53, which implies that an alternative method of removing damaged cells may be invoked by both *Fancm* and *Trp53* mutants (28, 35, 36). This phenotype is not as obvious in the *Fancm*$^{XH/XH}$ testes, which may be due to the fact that the repair mechanism is more functional in this mutant or that an alternative repair is still functional.

The meiotic defects in *Fancm*$^{C4/C4}$ leads to persistent RAD51 and γH2AX in meiotic spreads. As animals age an almost total meiotic-like arrest is observed within the seminiferous tubules as the damage continues to accumulate. Meiotic defects such as unrepaired DNA damage and mispaired chromosomes have been observed in a number of FA mutants (37, 38).

Both *Fancm*$^{C4/C4}$ and *Fancm*$^{XH/XH}$ cells have increased SCE rates, but how the SCEs are forming may be related to 2 different mechanisms. In *Fancm*$^{C4/C4}$ cells, SCEs may be forming due to lack of activity of the helicase/translocase during fork-reversal and D-loop disruption, leading to an increase in DSBs that need to get repaired leading to the activation of SCE. In *Fancm*$^{XH/XH}$, the allele lacks the C-terminus, including the MM2 motif which interacts with RMI1 and TOPOIIIα and acts as a landing pad for BLM (20, 39). If there is a lack of BLM this will result in a loss of HR, the cells then choose to use SCE to repair the damage. This phenotype is seen in BLM mutant cells (39).

The unperturbed G2/M delay/arrest noted in *Fancm*$^{C4/XH}$ and *Fancm*$^{XH/XH}$ but not the *Fancm*$^{C4/C4}$ cells indicates that, while DNA damage is occurring in these mutants of *Fancm,* only *Fancm*$^{C4/C4}$ cells seem to be able to go through both the S-phase checkpoint as well as the mitotic checkpoint without causing any noticeable cell cycle delays. This may be that the amount of DNA damage that has occurred in these cells may be less or that the types of lesions remaining are different. This may indicated the repair function in the *Fancm*$^{C4/C4}$ is able to function better, or there is a lack of checkpoint signaling.

Taken together this repertoire of *Fancm* mouse alleles will allow for further dissection of the roles of FANCM within the S-phase checkpoint, its repair functions within the Fanconi Anemia complementation group, as well as the DNA damage sensing and repair abilities outside of the FA complex.

3.5 Methods

Mice. ENU mutagenesis of mice was performed as previously described (29). Micronuclei assay was performed as previously described (29). Genetic mapping using micronuclei as the phenotype was done as previously described (40). Sequencing of candidate genes was done by using cDNA derived from mutant animal testis RNA using gene specific primers the genes were amplified and then Sanger sequenced. Gene trap-bearing ES cell lines (from 129 substrains) ware obtained from BayGenomics (XH297). Chimeras were generated by microinjection of the ES cells into C57BL/6J blastocysts using standard procedures. Following germ-line transmission, alleles were backcrossed into C3HeB/FeJ^{a} ("C3H"). Exact insertion sites of gene trap vectors were determined by "primer walking" as described (29). Genotyping of these animals were performed either by PCR amplification of the neo gene within the vector, by insertion-specific assay, or utilizing polymorphic flanking microsatellite markers *D12Mit69, D12Mit71* that are polymorphic between 129 and C3H and B6.

Histology and immunohistochemistry. For basic histology, tissues were fixed in 4% paraformaldehyde overnight, paraffin embedded, sectioned, and stained with hematoxylin and eosin (H&E). For germ cell counts, 10μM sections of 1 day old gonads were immunostained as described (41, 42). Antibodies: Rabbit anti-DDX4/MVH (Abcam ab13840, 1:250); goat anti-rabbit Alexa 488 conjugate (Molecular Probes A11008, 1:1000). Germ cells were counted in three sections from the midportion of each gonad and averaged. The data were analyzed using

one-way ANOVA with Bonferroni correction (Prism software package). The resulting *P* values were used to determine significance ($P<0.05$).

MEF growth studies. MEF growth analyses and metaphase spreads were performed as described (43). For senescence assays, cells were counted every 3 days and replated at $5X10^5$ and passaged until they became immortalized.

Drug treatments were performed for 2 hrs at concentrations noted, the drugs were removed and cells were placed in normal with counts of surviving cells after 48 hrs. Sister-chromatid exchange assay were performed as previously described (16).

Acknowledgements This work was supported by grants from the NY Stem Cell Foundation (JS), and the NIH (T32 HD052471 training slot to SAH). We thank R. Munroe for ES cell microinjections

3.6 References:

1. Winter JP de, Joenje H (2009) The genetic and molecular basis of Fanconi anemia. *Mutation research* 668:11-9.
2. Rego MA, Kolling FW, Howlett NG (2009) The Fanconi anemia protein interaction network: casting a wide net. *Mutation research* 668:27-41.
3. Kim JM, Kee Y, Gurtan A, D'Andrea AD (2008) Cell cycle-dependent chromatin loading of the Fanconi anemia core complex by FANCM/FAAP24. *Blood* 111:5215-22.
4. Machida YJ et al. (2006) UBE2T is the E2 in the Fanconi anemia pathway and undergoes negative autoregulation. *Molecular cell* 23:589-96.
5. Meetei AR et al. (2003) A novel ubiquitin ligase is deficient in Fanconi anemia. *Nature genetics* 35:165-70.
6. Collis SJ et al. (2008) FANCM and FAAP24 function in ATR-mediated checkpoint signaling independently of the Fanconi anemia core complex. *Molecular cell* 32:313-24.
7. Horejŝí Z, Collis SJ, Boulton SJ (2009) FANCM-FAAP24 and HCLK2: roles in ATR signalling and the Fanconi anemia pathway. *Cell cycle (Georgetown, Tex.)* 8:1133-7.
8. Huang M et al. (2010) The FANCM/FAAP24 complex is required for the DNA interstrand crosslink-induced checkpoint response. *Molecular cell* 39:259-68.

9. Crossan GP et al. (2011) Disruption of mouse Slx4, a regulator of structure-specific nucleases, phenocopies Fanconi anemia. *Nature Genetics* 43.
10. Wang W (2007) Emergence of a DNA-damage response network consisting of Fanconi anaemia and BRCA proteins. *Nature reviews. Genetics* 8:735-48.
11. Pichierri P, Rosselli F (2004) The DNA crosslink-induced S-phase checkpoint depends on ATR-CHK1 and ATR-NBS1-FANCD2 pathways. *The EMBO journal* 23:1178-87.
12. Andreassen PR, D'Andrea AD, Taniguchi T (2004) ATR couples FANCD2 monoubiquitination to the DNA-damage response. *Genes & development* 18:1958-63.
13. Ishiai M et al. (2008) FANCI phosphorylation functions as a molecular switch to turn on the Fanconi anemia pathway. *Nature structural & molecular biology* 15:1138-46.
14. Collins NB et al. (2009) ATR-dependent phosphorylation of FANCA on serine 1449 after DNA damage is important for FA pathway function. *Blood* 113:2181-90.
15. Tischkowitz M, Winqvist R (2011) Using mouse models to investigate the biological and physiological consequences of defects in the Fanconi anaemia/breast cancer DNA repair signalling pathway. *The Journal of pathology* 224:301-5.

16. Bakker ST et al. (2009) Fancm-deficient mice reveal unique features of Fanconi anemia complementation group M. *Human molecular genetics* 18:3484-95.

17. Meetei AR et al. (2005) A human ortholog of archaeal DNA repair protein Hef is defective in Fanconi anemia complementation group M. *Nature genetics* 37:958-63.

18. Singh TR et al. (2010) MHF1-MHF2, a histone-fold-containing protein complex, participates in the Fanconi anemia pathway via FANCM. *Molecular cell* 37:879-86.

19. Yan Z et al. (2010) A histone-fold complex and FANCM form a conserved DNA-remodeling complex to maintain genome stability. *Molecular cell* 37:865-78.

20. Deans AJ, West SC (2009) FANCM connects the genome instability disorders Bloom's Syndrome and Fanconi Anemia. *Molecular cell* 36:943-53.

21. Gari K, Décaillet C, Delannoy M, Wu L, Constantinou A (2008) Remodeling of DNA replication structures by the branch point translocase FANCM. *Proceedings of the National Academy of Sciences of the United States of America* 105:16107-12.

22. Gari K, Décaillet C, Stasiak AZ, Stasiak A, Constantinou A (2008) The Fanconi anemia protein FANCM can promote branch migration of Holliday junctions and replication forks. *Molecular cell* 29:141-8.

23. Zheng X-F et al. (2011) Processing of DNA structures via DNA unwinding and branch migration by the S. cerevisiae Mph1 protein. *DNA repair*.

24. Xue Y, Li Y, Guo R, Ling C, Wang W (2008) FANCM of the Fanconi anemia core complex is required for both monoubiquitination and DNA repair. *Human molecular genetics* 17:1641-52.

25. Mosedale G et al. (2005) The vertebrate Hef ortholog is a component of the Fanconi anemia tumor-suppressor pathway. *Nature structural & molecular biology* 12:763-71.

26. Schwab R a, Blackford AN, Niedzwiedz W (2010) ATR activation and replication fork restart are defective in FANCM-deficient cells. *The EMBO journal* 29:806-18.

27. Ciccia A et al. (2007) Identification of FAAP24, a Fanconi anemia core complex protein that interacts with FANCM. *Molecular cell* 25:331-43.

28. Huang M et al. (2011) Human MutS and FANCM complexes function as redundant DNA damage sensors in the Fanconi Anemia pathway. *DNA repair*:1-10.

29. Shima N et al. (2003) Phenotype-based identification of mouse chromosome instability mutants. *Genetics* 163:1031-40.

30. Moran JL et al. (2006) Utilization of a whole genome SNP panel for efficient genetic mapping in the mouse. *Genome research* 16:436-40.

31. Kennedy RD et al. (2007) Fanconi anemia pathway-deficient tumor cells are hypersensitive to inhibition of ataxia telangiectasia mutated. *The Journal of clinical investigation* 117:1440-9.

32. Rosado IV, Niedzwiedz W, Alpi AF, Patel KJ (2009) The Walker B motif in avian FANCM is required to limit sister chromatid exchanges but is dispensable for DNA crosslink repair. *Nucleic acids research* 37:4360-70.

33. Whitby MC (2010) The FANCM family of DNA helicases/translocases. *DNA repair* 9:224-36.

34. Singh TR et al. (2009) Impaired FANCD2 monoubiquitination and hypersensitivity to camptothecin uniquely characterize Fanconi anemia complementation group M. *Blood* 114:174-80.

35. Modrich P (2006) Mechanisms in eukaryotic mismatch repair. *The Journal of biological chemistry* 281:30305-9.

36. Kennedy RD, D'Andrea AD (2005) The Fanconi Anemia/BRCA pathway: new faces in the crowd. *Genes & development* 19:2925-40.

37. Houghtaling S et al. (2003) Epithelial cancer in Fanconi anemia complementation group D2 (Fancd2) knockout mice. *Genes & development* 17:2021-35.

38. Wong JCY (2003) Targeted disruption of exons 1 to 6 of the Fanconi Anemia group A gene leads to growth retardation, strain-specific microphthalmia, meiotic defects and primordial germ cell hypoplasia. *Human Molecular Genetics* 12:2063-2076.

39. Vinciguerra P, D'Andrea AD (2009) FANCM: A landing pad for the Fanconi Anemia and Bloom's Syndrome complexes. *Molecular cell* 36:916-7.

40. Reinholdt L, Ashley T, Schimenti J, Shima N (2004) Forward genetic screens for meiotic and mitotic recombination-defective mutants in mice. *Methods in molecular biology (Clifton, N.J.)* 262:87-107.

41. Reinholdt LG, Munroe RJ, Kamdar S, Schimenti JC (2006) The mouse gcd2 mutation causes primordial germ cell depletion. *Mechanisms of development* 123:559-69.

42. Hartford SA et al. (2011) Minichromosome maintenance helicase paralog MCM9 is dispensible for DNA replication but functions in germ-line stem cells and tumor suppression. *Proceedings of the National Academy of Sciences of the United States of America*.

43. Shima N et al. (2007) A viable allele of Mcm4 causes chromosome instability and mammary adenocarcinomas in mice. *Nature genetics* 39:93-8.

Chapter 4: Meeting at the Fork, MCM9 and FANCM.

The MCM2-7 DNA replicative helicase paralog, MCM9, is not essential for DNA replication (1). This is contrary to the *in vitro* data from *Xenopus* extracts where loss of MCM9 results in loss of DNA replication (2). As described in Chapter 2, mice lacking MCM9 display germ cell depletion, loss of spermatogonial stem cells as males age, and increased tumor formation. MCM9 mutant MEFs undergo premature senescence, exhibit increased chromatid breaks, and have a delayed release into S-phase following aphidicolin (APH) treatment. The pleotropic phenotypes in *Mcm9* mutants share commonalities with mice ablated for Fanconi anemia (FA) genes, which raises the intriguing possibility that MCM9 may function in concert with the FA complementation group during DNA replication.

The FA complementation group is involved in stabilizing collapsed and/or arrested replication forks, appears to work in concert with translesion synthesis and homologous recombination proteins to repair damage during DNA replication, and promotes ATR-mediated checkpoint signaling (3–11). All of the FA complementation group members that have been mutated in mice result in subfertility and germ cell depletion, and some FA mouse mutants also show cancer susceptibility at relatively older ages (12).

The other mouse mutants I have described in Chapter 3, are members of the Fanconi Anemia complementation group, containing separation of function mutations in *Fancm*. The *Fancm* mutants exhibit genomic instability, but lack

hypersensitivity to DNA damaging agents, and only one mutant allele exhibits germ cell depletion. Since both the MCM2-7 DNA replicative helicase and the Fanconi Anemia complementation group function at the DNA replication fork, I'll speculate about the precise role MCM9 in DNA replication and/or DNA repair and how it may interact with the Fanconi Anemia proteins.

4.1 Origin specification.

In order for DNA replication to occur, origins of replication need to be specified. First the origin is bound by the origin recognition complex (ORC), followed by binding of CDC6 and CDT1 which then proceeds to load the MCM2-7 heterohexameric helicase. This collection of proteins composes the pre-replication complex (pre-RC), and the origin is now "licensed" (Figure 4-1) (13). In order to become active, CDC7 and CDK remove CDC6 and recruit MCM10. MCM10 with MCM2-7 recruits CDC45, followed by the rest of the replisome (13). There are two other MCM paralogs, MCM8 and MCM9, which have not yet been shown to interact with MCM2-7. These two genes have arisen or were lost together during evolution (14), and both have been shown to interact with different pre-RC factors. MCM8 physically interacts with CDC6 (15), and MCM9 was shown to interact with CDT1 (2). What are their roles, if any, in pre-RC function and do they function together or independently?

MCM9 does not appear to be involved in origin loading, as indicated by the equal amounts of loaded MCM2-7 and CDT1 in MCM9 mutant cells when

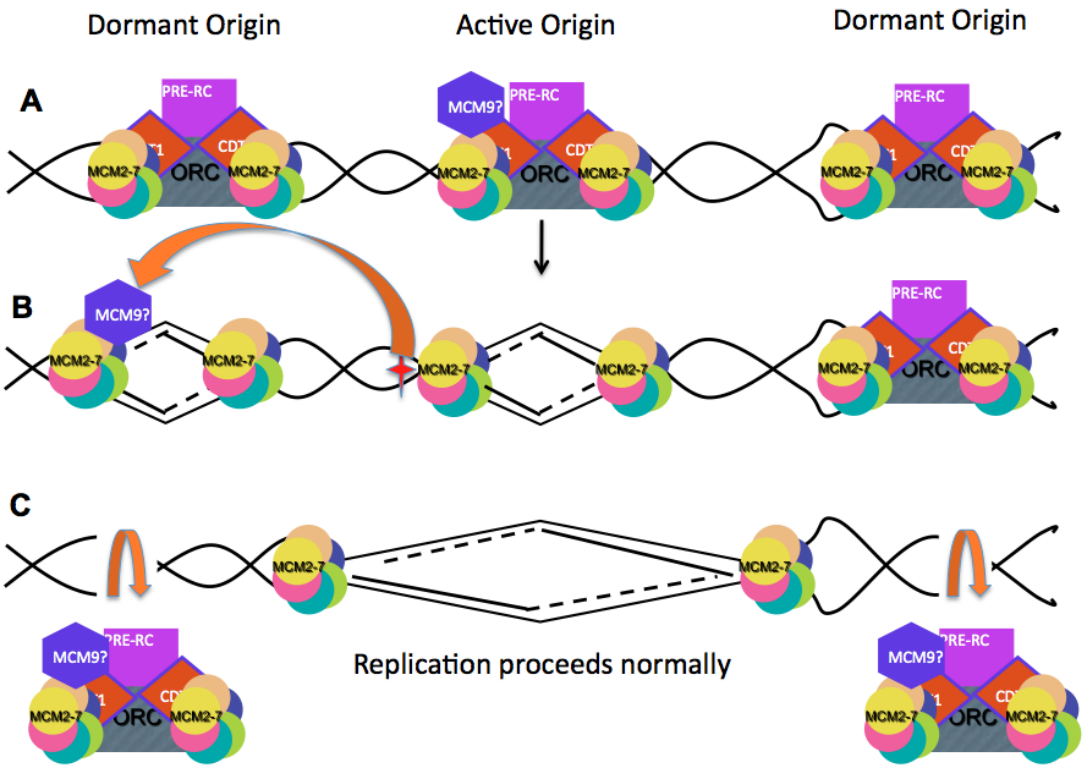

Figure 4-1 Origin Specification

A. During G1 phase of the cell cycle, a number of origins of replication are licensed with the factors needed to initiate DNA replication. At the start of S-phase only a subset of these origins are activated. Does MCM9 have a role in determining the active origin? **B.** As the DNA replication fork elongates it may encounter DNA lesions (red star),that may inhibit the fork from progressing. Is MCM9 involved in activating dormant origins during replication stress? **C.** If the replication fork progresses normally the other dormant origins need to be removed so replication can proceed past them. Is MCM9 involved in removal of proteins from dormant origins?

compared to wild-type (1). We have also shown that a decrease in the number of active origins, through the *Mcm4*$^{Chaos3/Chaos3}$*:Mcm2*$^{GT/+}$ males (16), does not lead to germ cell loss (1). However, this does not exclude a role for MCM9 at the DNA replication origin. MCM9 may have a role in selecting the active origin (Figure 4-1A). Cells lacking MCM9 may show a change in the commonly activated origins, or have a difference in intra-origin distances. If MCM9 is involved in offloading of dormant origins then there should be a delay in S-phase progression as the active replication machinery attempts to proceed (Figure 4-1).

There are more origins licensed than what become active origins of replication (17–20). The remaining "dormant" origins are there as back-up in case an active origin is no longer able to proceed (Figure 4-1). One theory on origin selection and activation of dormant origins involves origin "factories", where replication factors act locally to select one active origin within a certain chromatin domain. When a replication fork is compromised, the DNA damage checkpoint protein CHK1 prevents distant late origins from firing while nearby dormant origins fire within the origin factory. However, the mechanism that regulates specific origin firing is not clearly understood (21–23). What is the determining factor that decides which pre-RC gets activated? How do origins remain dormant until a fork is stressed? How is a dormant origin removed when the replication fork needs to proceed?

4.2 Replication Stress

MCM9 may be involved in activating dormant origins at times of replication stress (Figure 4-1B). Aphidicolin (APH) is a DNA polymerase inhibitor causing ssDNA to accumulate and become bound by RPA, which acts as a signal for S-phase checkpoints activation and halting of replication. It has been shown that ATR and ATM are not responsible for the APH-induced origin refiring, suggesting that another factor signals when replication is ready to proceed (24). When cells are released from APH there is a staggered delay of origin re-start and new origin firing (24). What signals this firing? In *Mcm9* mutant MEFs, we see a delay of restart from APH block into S-phase. Is this due to lack of signal of which origins should be fired? Is this due to lack of restart of stalled replication forks? Delayed choice of dormant origin to be activated?

4.3 ICL, MCM9, and similarity to Fanconi Anemia

DNA breaks, DNA adducts, and DNA interstrand crosslinks at the replication fork interfere with its progression. When the replisome encounters lesions, such as DNA breaks and DNA adducts, DNA synthesis is unable to continue. This leaves long stretches of ssDNA onto which RPA binds (Figure 4-2A). RPA then allows the ATR-Chk1 signaling pathway to be activated which stops the MCM2-7 helicase from progressing and dormant origins are prevented from firing until needed (25). However, when the MCM2-7 DNA helicase encounters an interstrand crosslink, the replisome is still able to progress to the point where MCM2-7 has stalled (Figure 4-2B). This leaves no long stretch of

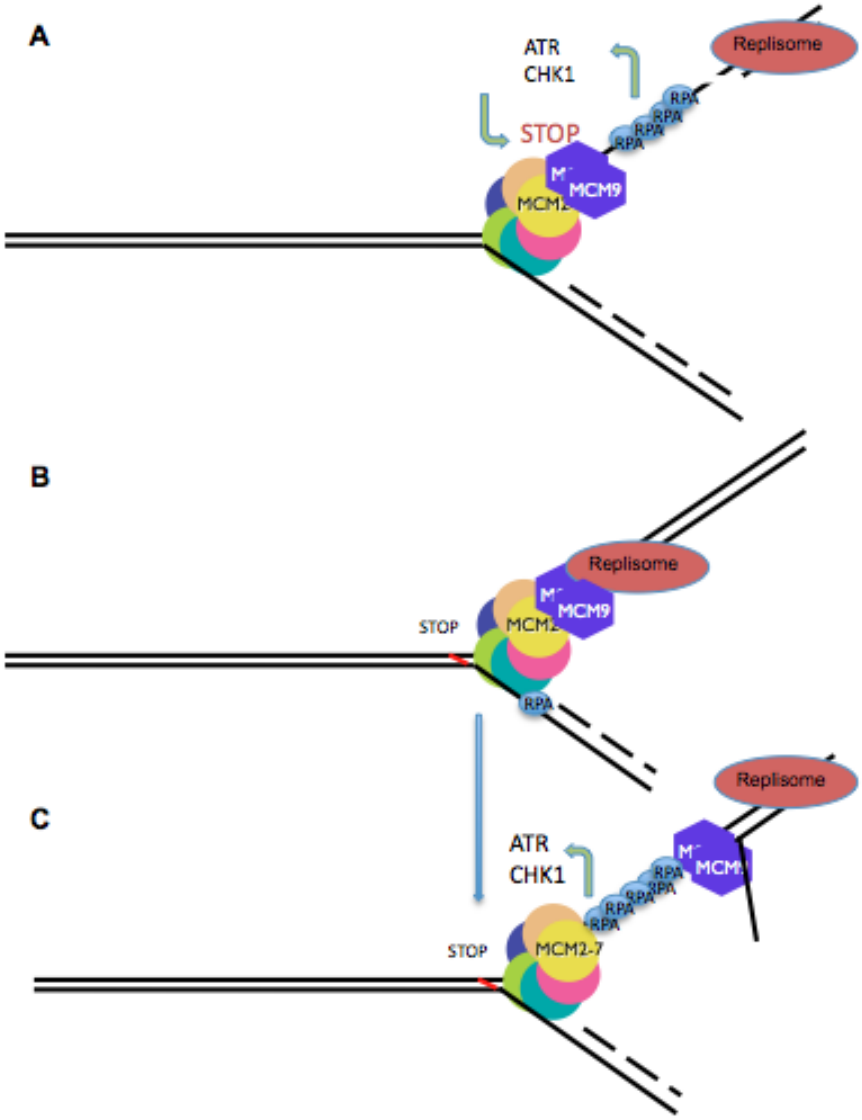

Figure 4-2 Replication Stress.

A. During DNA replication, DNA lesions such as DNA breaks and bulky lesions may cause the replisome to stop synthesizing DNA while the helicase continues on leaving long stretches of ssDNA. This ssDNA is coated by RPA which signals through the ATR pathway to the MCM2-7 helicase to stop progressing. Is MCM9 involved in this step to stop DNA replication during stress? **B.** If the MCM2-7 helicase encounters an interstrand crosslink there is no long stretch of ssDNA since the replisome is able to keep up with the DNA helicase. **C.** How is the ssDNA formed, is MCM9 responsible for unwinding the newly synthesized DNA to allow RPA to bind and signal the repair factors?

ssDNA for RPA to bind to facilitate DNA damage repair signaling. The MCM2-7 helicase has been shown to have a role in RPA loading and CHK1 phosphorylation to signal repair when the fork encounters a lesion (26). What causes ssDNA for RPA to bind when the MCM2-7 helicase encounters an interstrand crosslink? Is it possible that MCM9 is involved in these functions (Figure 4-2)?

As MCM2-7 elongates DNA for replication, MCM9 may travel with the elongating replication fork. MCM9 may signal when the fork stops progressing and allow accumulation of RPA, either by inhibiting the polymerase, or by unwinding the newly formed DNA that is behind the fork to allow for RPA accumulation (Figure 4-2B,C). MCM9 may be involved in signaling when the fork has stopped progressing, and if this is true, there should be alteration of ATR-Chk1 signaling.

Recent studies reported that unreplicated regions flanked by two stalled forks that persist into M-phase are marked with sister foci of FANCD2, a Fanconi Anemia protein that presumably directs the resolution of such structures through homologous recombination (27). These FANCD2 foci have also been shown to form on the incompletely replication regions in *Mcm4*^{Chaos3} cells (28). In these cells, there was also persistence of RAD51 and BLM foci.

The connection between the DNA replicative helicase and the Fanconi Anemia pathway needs to be explored, as these protein families both function at the DNA replication fork. MCM9 may be working as part of a sensor that travels with the MCM2-7 helicase and may signal a repair pathway when the fork has

stopped progressing at an interstrand crosslink (Figure 4-2&3). MCM9 may be involved in the restart of the replication fork after the repair is complete at the stalled fork (Figure 4-3), either as the DNA helicase or by reloading, recruiting, or activating MCM2-7. If the damage has been repaired, but the fork has failed to restart, this could lead to unreplicated DNA or slowed DNA replication.

FANCM has been show through multiple biochemical assays to be involved in many stages of DNA repair, from sensing damage, to activating S-phase checkpoint, to repair pathway choice, and actually facilitating repair by remodeling the replication fork (29). FANCM loss enhances sensitivity to the DNA damaging agents UV (activates nucleotide excision repair) and camptothecin (CPT, activates double stranded break repair) in addition to MMC. FANCM may have a role in sensing or bringing in repair factors for these different types of DNA lesions that interfere with the progression of the DNA replication fork. Loss of FANCM allows the replication fork to proceed at a faster rate (30). In addition, FANCM loss causes RPA to be destabilized on ssDNA (10) (Figure 4-3). FANCM also has the ability to remodel DNA replication forks into chicken foot structures for fork reversal, to resolve Holliday Junctions, and is involved in D-loop formation (31–36). FANCM also has the ability to activate ATR checkpoint signaling, stabilize RPA formation, and tether FA and BLM for repair (9, 10, 30, 37–41). All of this data suggests that FANCM travels with the DNA replication fork and has multiple roles in DNA repair at the DNA replication fork.

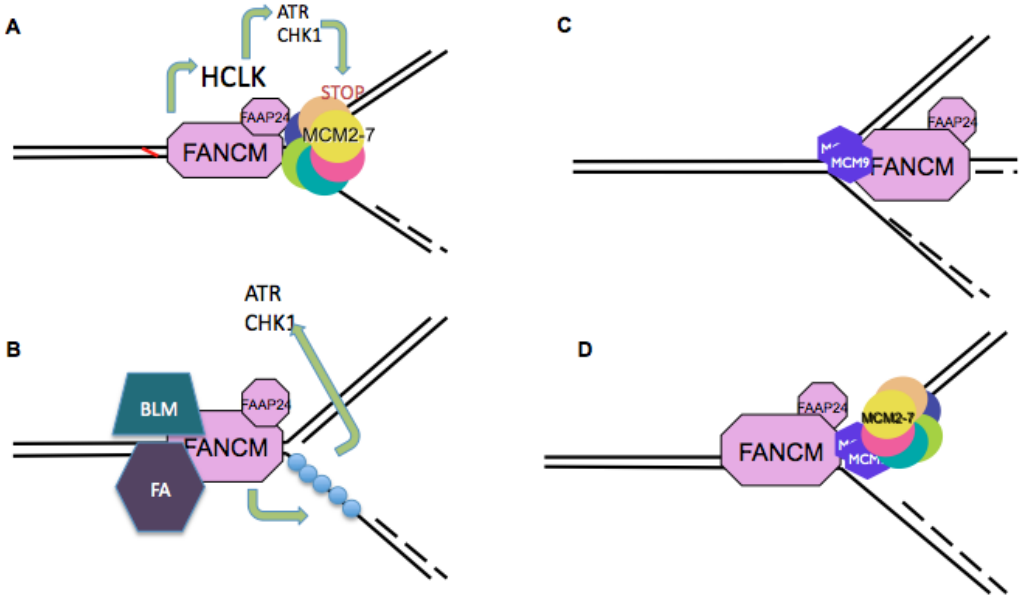

Figure 4-3 The role of FANCM at the replication fork.

A. FANCM may travel along with the DNA replication machinery and act as a sensor for DNA damage. When damage is encountered, FANCM signals to ATR which then stops the progression of the replication fork. **B.** FANCM then goes on to stabilize/load RPA onto ssDNA and then serve as an anchor for the Fanconi Anemia proteins and BLM for repair of some lesions. **C.** FANCM may help restart the fork through fork reversal and allow the DNA helicase, or MCM9, to reload. **D.** DNA replication can proceed again.

4.4 Break-induced Replication

Break-induced replication (BIR) is a homologous recombination repair pathway that acts when double-strand breaks only have one end that shares homology. The end invades into the homologous region utilizing the RAD51 filament and then instead of a short stretch of DNA synthesis, the replication machinery is engaged and replication proceeds to the end of the chromosome (42–44) (Figure 4-4). This mechanism is used to restart forks when the replication machinery has become uncoupled. BIR is also an alternative mechanism (ALT) of maintaining telomeres in the absence of telomerase (42, 45, 46). Telomerase itself is primarily active in the stem and germ cells and is turned off in somatic cells. Telomerase null mice exhibit anemia, bone marrow failure, and defects in the gastrointestinal tract and skin, in addition to germ cell loss due to apoptosis (47).

The replication machinery was shown to be engaged during BIR in budding yeast (42), which lacks MCM8 and MCM9. In eukaryotes that have MCM8/9, it is possible that these proteins are used to activate BIR and ALT (Figure 4-4). MCM8 and/or MCM9 may be facilitating the repair by opening up the DNA so that the repair and replication machinery can access the template DNA. MCM8 and/or MCM9 may be acting as a DNA repair helicase in this type of repair.

Loss of telomere maintenance can lead to premature senescence. The early regulation of telomere length is decided by a telomerase-free system, either through Telomere-sister chromatid exchange or DNA recombination (48). In this

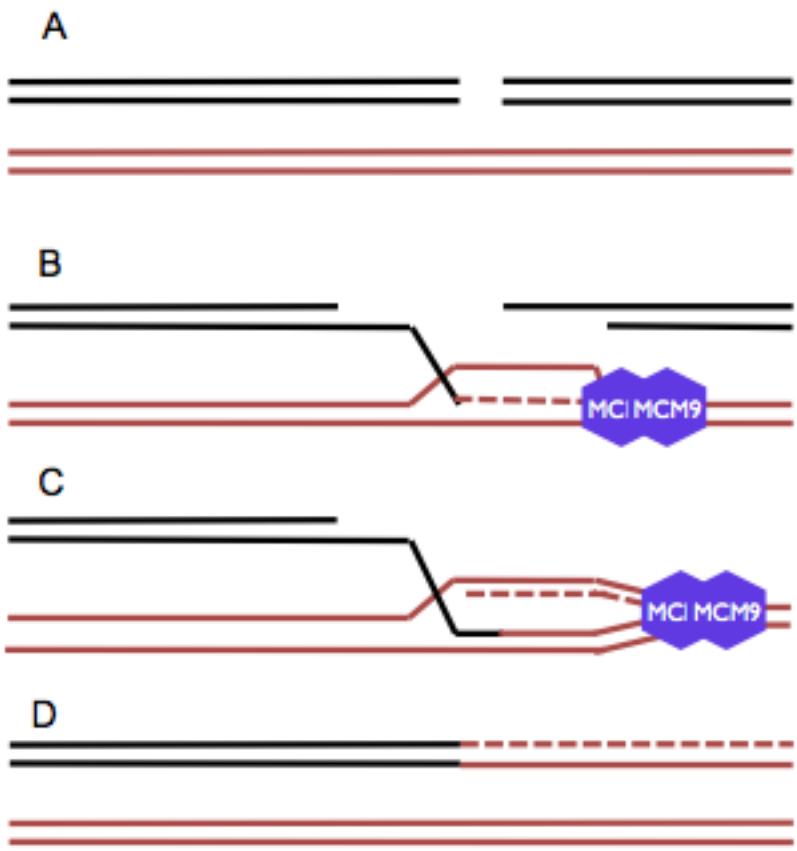

Figure 4-4 Break-induced replication

A. A dsDNA break has formed and the HR repair pathway begins a homology search. **B.** When homology is found strand invasion and DNA synthesis begins, does MCM9 facilitate the opening of the chromatin for DNA synthesis to occur? **C.** If there is homology found for only one end of the break, DNA replication will occur and proceed to the end of the chromosome. Alternative lengthening of telomeres also may take place. Is MCM9 the DNA helicase for this mechanism, or is it involved with loading of the other replicative factors in the absence of an origin of replication? **D.** When replication is completed loss of heterozygosity results.

system the shorten telomeres seen in the zygotes are lengthen from the 1-cell stage through the blastocyst stage (48). Could BIR also have a role in this early telomere lengthening? Could MCM9 help decide replication "age" by maintaining telomere length? Since loss of MCM9 causes premature senescence in primary MEFS, could this be due to premature shortening of telomeres? A premature senescence phenotype could also explain the shortfall of germ cells, as they might have stopped proliferating earlier. This may explain the continued loss of the spermatogonial stem cell compartment as they terminally differentiate.

If MCM9 is involved in the BIR pathway it may allow us a unique look at stem cells and how a replication-linked gene may affect its ability to replicate and divide. This mechanism may control how many cycles of replication a stem cell goes through, and without MCM9 the cell could terminally differentiate.

4.5 Germ cell loss and DNA repair.

Accurate transmission of genetic information is critical to the health and the success of species. Proper specification and maintenance of the germ-line stem cell is a key part of this. During gamete formation genome maintenance is critical to prevent mutation, insertions, and deletions to prevent the offspring from inheriting defects that may be detrimental.

Of the 19 genes reported to cause "decreased primordial germ cell number" in the Mouse Genome Database, only *Fancl,* and *Pin1* have known roles in genome maintenance. The other FA genes also cause primordial germ cell depletion, but these haven't been investigated fully and are not listed.

Numerous other DNA repair genes have been studied in mice, but none have been linked to primordial germ cell depletion. *Pin1* has been implicated in the control of cell cycle progression, telomere maintenance, and DNA damage and replication checkpoints. In primordial germ cells *Pin1* is required for the normal progression of the cell cycle in proliferation during and immediately after migration of the germ cells (49, 50). *Fancl* is specifically required for the proliferation of post-migratory primordial germ cells but not the proliferation of migratory primordial germ cells (51). *Fancl* is an E3 ligase and a member of the Fanconi anemia complementation group.

The FA complementation group mutants are the only set of DNA repair genes that have exhibited primordial germ cell depletion. This suggests that germ cells are hypersensitive to the loss of the ability to repair interstrand crosslinks. Is it because these cells are more prone to ICL during gamete formation? Is it due to specific ICL that affect transcription of certain genes? It has been shown that during epigenetic reprogramming ssDNA is formed that may be resolved through the BER pathway (53). Is FANCM important part of signaling in this pathway? Is it that these germ cells are undergoing rapid proliferation during gametogenesis that the FA repair pathway is the preferred mechanism for screening and repair of genomic damage?

As shown earlier FANCM is involved in sensing or repairing numerous types of DNA damage that can be found during procession of the replication fork. Loss of FANCM results in a quicker procession of the replication fork (30),this suggests that FANCM may travel with the replication machinery. This leaves the

possibility that FANCM is a key part of the mechanism that maintains genomic integrity during the rapid proliferation and expansion of the germ cells.

With the FANCM mutants, we have an opportunity to study separation of function in gametes with one hypomorphic allele, *Fancm*$^{C4/C4}$, that results in germ cell loss, and the *Fancm*$^{XH/XH}$ and *Fancm*$^{C4/XH}$ alleles, do not exhibit germ cell loss. This loss of germ cells in *Fancm*$^{C4/C4}$ suggests FANCM ATPase, translocase or possibly some other function associated within this translocase domain is key in maintaining germ cell genome stability. The N-terminal translocase domain functions in DNA remodeling abilities. The N-terminal of FANCM also has roles in moving the protein along chromatin to points of DNA damage and stalled forks. The translocase domain is required for resistance to cross-linking agents and UV (52). This domain is required for suppression of SCE and is needed for activation of the S-phase checkpoint (29).

The N-terminal translocase/helicase domain functions in DNA remodeling. The loss of this domain has its own consequences, however, is not likely the cause of the germ cell depletion. Since the loss of the endonuclease domain (which has substrate specificity binding activity) does not affect germ cell formation, The activities of the N-terminal DNA remodeling activities of FANCM is an upstream function, suggesting these are not the cause of germ cell loss. This leaves the ability of FANCM to travel along the DNA and sense and signal DNA damage as the most likely cause of germ cell depletion.

4.6 Significance

MCM9 is paralogous to the MCM2-7 DNA replicative helicase subunits, yet it does not appear to have a role in unperturbed DNA replication. MCM9 mutants have defects of the germ-line stem cells and are susceptible to hepatocellular carcinoma. These phenotypes are similar to those mice with mutations in the Fanconi anemia complementation group, which is involved in DNA interstrand crosslink repair at the DNA replication fork. The other mouse mutants described here are members of the Fanconi Anemia complementation group, with separation of function mutations in *Fancm*. The *Fancm* mutants exhibit genomic instability, however lack DNA damaging agent hypersensitivity, and only one allele has germ cell depletion. With this collection of mouse mutants we have a unique opportunity to study DNA replication-link DNA repair pathways. Additionally, we will be able to tease out mechanisms involved in maintaining the genomic integrity of germ-line stem cells.

4.7 References

1. Hartford SA et al. (2011) Minichromosome maintenance helicase paralog MCM9 is dispensible for DNA replication but functions in germ-line stem cells and tumor suppression. *Proceedings of the National Academy of Sciences of the United States of America*.
2. Lutzmann M, Méchali M (2008) MCM9 binds Cdt1 and is required for the assembly of prereplication complexes. *Molecular cell* 31:190-200.
3. Wang W (2007) Emergence of a DNA-damage response network consisting of Fanconi anaemia and BRCA proteins. *Nature reviews. Genetics* 8:735-48.
4. Pichierri P, Rosselli F (2004) The DNA crosslink-induced S-phase checkpoint depends on ATR-CHK1 and ATR-NBS1-FANCD2 pathways. *The EMBO journal* 23:1178-87.
5. Andreassen PR, D'Andrea AD, Taniguchi T (2004) ATR couples FANCD2 monoubiquitination to the DNA-damage response. *Genes & development* 18:1958-63.
6. Ishiai M et al. (2008) FANCI phosphorylation functions as a molecular switch to turn on the Fanconi anemia pathway. *Nature structural & molecular biology* 15:1138-46.
7. Collins NB et al. (2009) ATR-dependent phosphorylation of FANCA on serine 1449 after DNA damage is important for FA pathway function. *Blood* 113:2181-90.

8. Collis SJ et al. (2008) FANCM and FAAP24 function in ATR-mediated checkpoint signaling independently of the Fanconi anemia core complex. *Molecular cell* 32:313-24.
9. Horejŝí Z, Collis SJ, Boulton SJ (2009) FANCM-FAAP24 and HCLK2: roles in ATR signalling and the Fanconi anemia pathway. *Cell cycle (Georgetown, Tex.)* 8:1133-7.
10. Huang M et al. (2010) The FANCM/FAAP24 complex is required for the DNA interstrand crosslink-induced checkpoint response. *Molecular cell* 39:259-68.
11. Crossan GP et al. (2011) Disruption of mouse Slx4, a regulator of structure-specific nucleases, phenocopies Fanconi anemia. *Nature Genetics* 43.
12. Tischkowitz M, Winqvist R (2011) Using mouse models to investigate the biological and physiological consequences of defects in the Fanconi anaemia/breast cancer DNA repair signalling pathway. *The Journal of pathology* 224:301-5.
13. Sun J, Kong D (2010) DNA replication origins, ORC/DNA interaction, and assembly of pre-replication complex in eukaryotes. *Acta biochimica et biophysica Sinica* 42:433-9.
14. Liu Y, Richards TA, Aves SJ (2009) Ancient diversification of eukaryotic MCM DNA replication proteins. *BMC evolutionary biology* 9:60.

15. Volkening M, Hoffmann I (2005) Involvement of human MCM8 in prereplication complex assembly by recruiting hcdc6 to chromatin. *Molecular and cellular biology* 25:1560-8.

16. Kawabata T et al. (2011) A reduction of licensed origins reveals strain-specific replication dynamics in mice. *Mammalian genome : official journal of the International Mammalian Genome Society*.

17. Burkhart R et al. (1995) Interactions of human nuclear proteins P1Mcm3 and P1Cdc46. *European journal of biochemistry / FEBS* 228:431-8.

18. Mahbubani HM, Chong JP, Chevalier S, Thömmes P, Blow JJ (1997) Cell cycle regulation of the replication licensing system: involvement of a Cdk-dependent inhibitor. *The Journal of cell biology* 136:125-35.

19. Donovan S, Harwood J, Drury LS, Diffley JF (1997) Cdc6p-dependent loading of Mcm proteins onto pre-replicative chromatin in budding yeast. *Proceedings of the National Academy of Sciences of the United States of America* 94:5611-6.

20. Wong PG et al. (2011) Cdc45 limits replicon usage from a low density of preRCs in mammalian cells. *PloS one* 6:e17533.

21. Ge XQ, Blow JJ (2010) Chk1 inhibits replication factory activation but allows dormant origin firing in existing factories. *The Journal of cell biology* 191:1285-97.

22. Blow JJ, Ge XQ, Jackson D a (2011) How dormant origins promote complete genome replication. *Trends in biochemical sciences* 36:405-14.

23. Karnani N, Dutta A (2011) The effect of the intra-S-phase checkpoint on origins of replication in human cells. *Genes & development* 25:621-33.

24. Marheineke K, Hyrien O (2001) Aphidicolin triggers a block to replication origin firing in Xenopus egg extracts. *The Journal of biological chemistry* 276:17092-100.

25. Flynn RL, Zou L (2011) ATR: a master conductor of cellular responses to DNA replication stress. *Trends in biochemical sciences* 36:133-40..

26. Byun TS, Pacek M, Yee M-ching, Walter JC, Cimprich KA (2005) Functional uncoupling of MCM helicase and DNA polymerase activities activates the ATR-dependent checkpoint. *Genes & development* 19:1040-52.

27. Naim V, Rosselli F (2009) The FANC pathway and BLM collaborate during mitosis to prevent micro-nucleation and chromosome abnormalities. *Nature cell biology* 11:761-8.

28. Kawabata T et al. (2011) Stalled Fork Rescue via Dormant Replication Origins in Unchallenged S Phase Promotes Proper Chromosome Segregation and Tumor Suppression. *Molecular cell* 41:543-53.

29. Whitby MC (2010) The FANCM family of DNA helicases/translocases. *DNA repair* 9:224-36.

30. Luke-Glaser S, Luke B, Grossi S, Constantinou A (2010) FANCM regulates DNA chain elongation and is stabilized by S-phase checkpoint signalling. *The EMBO journal* 29:795-805.

31. Yan Z et al. (2010) A histone-fold complex and FANCM form a conserved DNA-remodeling complex to maintain genome stability. *Molecular cell* 37:865-78.

32. Collis SJ, Boulton SJ (2010) FANCM: fork pause, rewind and play. *The EMBO journal* 29:703-5.

33. Gari K, Décaillet C, Stasiak AZ, Stasiak A, Constantinou A (2008) The Fanconi anemia protein FANCM can promote branch migration of Holliday junctions and replication forks. *Molecular cell* 29:141-8.

34. Thompson LH, Jones NJ (2010) Stabilizing and remodeling the blocked DNA replication fork: anchoring FANCM and the Fanconi anemia damage response. *Molecular cell* 37:749-51.

35. Gari K, Décaillet C, Delannoy M, Wu L, Constantinou A (2008) Remodeling of DNA replication structures by the branch point translocase FANCM. *Proceedings of the National Academy of Sciences of the United States of America* 105:16107-12.

36. Zheng X-F et al. (2011) Processing of DNA structures via DNA unwinding and branch migration by the S. cerevisiae Mph1 protein. *DNA repair*.

37. Vinciguerra P, D'Andrea AD (2009) FANCM: A landing pad for the Fanconi Anemia and Bloom's Syndrome complexes. *Molecular cell* 36:916-7.

38. Xue Y, Li Y, Guo R, Ling C, Wang W (2008) FANCM of the Fanconi anemia core complex is required for both monoubiquitination and DNA repair. *Human molecular genetics* 17:1641-52.

39. Deans AJ, West SC (2009) FANCM connects the genome instability disorders Bloom's Syndrome and Fanconi Anemia. *Molecular cell* 36:943-53.

40. Schwab R a, Blackford AN, Niedzwiedz W (2010) ATR activation and replication fork restart are defective in FANCM-deficient cells. *The EMBO journal* 29:806-18.

41. Sobeck A, Stone S, Landais I, Graaf B de, Hoatlin ME (2009) The Fanconi anemia protein FANCM is controlled by FANCD2 and the ATR/ATM pathways. *The Journal of biological chemistry* 284:25560-8.

42. Lydeard JR et al. (2010) Break-induced replication requires all essential DNA replication factors except those specific for pre-RC assembly. *Genes & development* 24:1133-44.

43. Llorente B, Smith CE, Symington LS (2008) Break-induced replication: what is it and what is it for? *Cell cycle (Georgetown, Tex.)* 7:859-64.

44. Kasparek TR, Humphrey TC (2011) DNA double-strand break repair pathways, chromosomal rearrangements and cancer. *Seminars in cell & developmental biology* 22:886-897.

45. Nabetani A, Ishikawa F (2011) Alternative lengthening of telomeres pathway: recombination-mediated telomere maintenance mechanism in human cells. *Journal of biochemistry* 149:5-14.

46. O'Hare TH, Delany ME (2011) Molecular and cellular evidence for the alternative lengthening of telomeres (ALT) mechanism in chicken. *Cytogenetic and genome research* 135:65-78.

47. Strong M a et al. (2011) Phenotypes in mTERT^{+}/$^{-}$ and mTERT^{-}/$^{-}$ mice are due to short telomeres, not telomere-independent functions of telomerase reverse transcriptase. *Molecular and cellular biology* 31:2369-79.

48. Liu L et al. (2007) Telomere lengthening early in development. *Nature cell biology* 9:1436-41.

49. Atchison FW, Capel B, Means AR (2003) Pin1 regulates the timing of mammalian primordial germ cell proliferation. *Development (Cambridge, England)* 130:3579-86.

50. Lee TH et al. (2009) Essential role of Pin1 in the regulation of TRF1 stability and telomere maintenance. *Nature cell biology* 11:97-105.

51. Agoulnik AI et al. (2002) A novel gene, Pog, is necessary for primordial germ cell proliferation in the mouse and underlies the germ cell deficient mutation, gcd. *Human molecular genetics* 11:3047-53.

52. Rosado IV, Niedzwiedz W, Alpi AF, Patel KJ (2009) The Walker B motif in avian FANCM is required to limit sister chromatid exchanges but is dispensable for DNA crosslink repair. *Nucleic acids research* 37:4360-70.

53. Hajkova P et al. (2010) Genome-wide reprogramming in the mouse germ line entails the base excision repair pathway. *Science (New York, N.Y.)* 329:78-82.